

1 **Response to Referee #1 (Dr. Kleinen)**

2 We would like to thank Dr. Kleinen for his thoughtful and constructive review. Our responses to  
3 all of the referee's comments (italicized) are presented below.

4 *In their manuscript, the authors present a model study of soil carbon accumulation in Alaska*  
5 *over the last 15000 years with a special focus on peat carbon accumulation. Overall, the*  
6 *manuscript is quite interesting and suitable for publication in biogeosciences. However, a*  
7 *number of minor issues remain before it is ready for publication.*

8 We made all edits and changes following the referee's comments and suggestions. We detailed  
9 our responses below.

10 *Figure 2 shows the vegetation distribution used to drive the model for 5 time slices. However,*  
11 *results are presented in Figs. 7 and 9 for 6 time slices. This is confusing for the reader. At the*  
12 *very least it needs to be clearly marked in the figure caption. The symbols used in Fig. 2 to show*  
13 *peat basal dates are also very difficult to make out. Maybe it is possible for the authors to make*  
14 *this Figure clearer.*

15 We have five vegetation distribution maps for five time slices. In Fig. 2, we present those five  
16 maps. We present six maps of carbon density distribution in Figs. 7 and 8. The reason is that  
17 during 5 ka-1900 AD, there was climate change affecting carbon accumulation rates, although  
18 the vegetation map remains the same during 9ka-1900 AD. Yes, it is indeed confusing for  
19 readers. Thus, in this revision, we made the explanation in the captions of Figs 2, 7, and 8 to  
20 clarify this. Also, we have made all panels in Fig. 2 clearer and changed the symbol size.

21 *Figure 7: Figure caption is unclear. How can you show cumulative SOC density? This would*  
22 *imply only the very last time in the time interval is shown. I assume you actually mean the mean*  
23 *SOC density.*

24 Correct. For non-peatland soils, we wanted to show the mean carbon density during each time  
25 slice. We have made the caption clearer to readers and change the "cumulative" to "average".

26 *Figure 12: Caption also unclear. I assume the late 20th century distribution is shown? Figure*  
27 *caption shows 15ka to 2000AD, implying a mean value over this time frame.*

28 The maps of total SOC density in Alaska are the sums of SOC during all periods, from 15ka,  
29 which is the beginning of the simulation, to the late 20<sup>th</sup>, which is the end. This is the cumulative  
30 carbon density. We have changed the caption of panel (d) to "area-weighted total (peatland plus  
31 non-peatland) SOC density from 15 ka to 2000 AD, and added "total" in the descriptions of other  
32 panels.

33 *Since a large part of the results hinges on the modelled changes in peatland area, it is essential*  
34 *that a description of how area changes are determined is provided. Currently it is only stated*  
35 *that area is prescribed from Matthews & Fung, implying no change is possible.*

36 *Page 15, line 339 – page 16, line 349: how were peatland area changes determined? Completely*  
37 *unclear (see comment #4)*

38 The change of peatland area is determined by the basal ages of the peatland. And from the  
39 distribution of the basal ages in Fig. 2, we link some vegetation types during each time slice to  
40 the ages. For example, during 15-11ka, the peatland area is determined based on the alpine  
41 tundra. However, within each pixel, we assume the inundated area represents the peatland area  
42 and other area represents non-peatland. The inundation area information is from the modern  
43 inundation map and does not change. The number of pixels that have peatland vegetation is  
44 changing through time determined by the basal age distribution. The percentage of peatland area  
45 within each pixel is unchanging. We have made the description clearer in the Method section.  
46 We added the peatland expansion into Results& Discussion section to better describe the link  
47 between basal ages and the peatland area change. We also added the drawbacks of such  
48 assumption.

49 *Page 4, lines 94-95: the Spahni et al. Model has actually been evaluated with respect to the*  
50 *variables listed – see Wania et al. Publications on the LPJ-Why model on which Spahni is based.*

51

52 Thanks for pointing out our wrong statement here. We checked the relevant references and  
53 corrected our statement.

54 *Page 5, line 97: Why do you cite Kleinen et al. 2010? They do not use a processbased peatland*  
55 *model, but rather prescribed peat accumulation. I assume you actually meant to cite Kleinen et*  
56 *al. 2012?*

57 We have cited Kleinen et al. (2012) instead.

58 *Page 7 and 8, lines 159-166: The aboveground vegetation in your calibration site is significantly*  
59 *different from the Mer Bleu site you use for belowground calibration. In addition the climatic*  
60 *situation at the two sites is significantly different. Therefore it seems quite a stretch to argue that*  
61 *belowground processes are basically the same. Please provide more justification for this*  
62 *assumption.*

63 Assuming the belowground carbon in Mer Bleu is the same as that in APEXCON could be  
64 wrong. In this revision, we added another site (Suurisuo mire complex) in southern Finland,  
65 which is a sedge fen dominated by *Carex rostrata*. We compared the ratios of belowground  
66 biomass over total biomass at both sites and applied 70% to APEX site and then estimated the

67 belowground biomass. We added the description in the text and cited the reference in this  
68 revision.

69 *Page 8, line 173: Please correct date for late Holocene time frame*

70 We have corrected the date from “9 ka-1900AD” to “5ka-1900 AD”.

71 *Page 9, lines 194-195: The Shuttle Radar Topography Mission (SRTM) only covered latitudes*  
72 *56S-60N. Therefore there is NO SRTM data for Alaska. You obviously used some other source*  
73 *for topography data – please provide correct reference.*

74 We directly used the data from He et al. (2014). We cited Zhuang et al. (2007) paper instead.

75 *Page 9, lines 197-203: Downscaling / bias correction is unclear. From the text one gets the*  
76 *impression, that ECBILT fields and CRU data may be significantly different for 20th century.*  
77 *However, my reading of the original publications is that bias correction minimised that*  
78 *difference. Please clarify this – it would strongly strengthen the text.*

79 Yes, the climate data were bias-corrected to minimize the difference between ECBILT and CRU.  
80 We made the clarification on this.

81 *Page 12, line 256: References to Figures 2 and 3 mixed up, please correct.*

82 We have made the change.

83

84 *Page 13, lines 279-289: Study sites unclear. Please provide table of site locations.*

85 Below is the table of descriptions of those sites. We cited Wang et al. (2016) in this revision

86

87 Sites used for comparison of carbon accumulation rates between simulation and observation [*Jones and*  
88 *Yu, 2010*]

| Site name      | Location    | Peatland type | Latitude | Longitude | Dating method | No. of dates | Basal age (cal yr BP) | Time-weighted Holocene accumulation rates (g C m <sup>-2</sup> yr <sup>-1</sup> ) |
|----------------|-------------|---------------|----------|-----------|---------------|--------------|-----------------------|---|
| Kenai Gasfield | Alaska, USA | fen           | 60°27'N  | 151°14'W  | AMS           | 12           | 11,408                | 13.1  |
| No Name Creek  | Alaska, USA | fen           | 60°38'N  | 151°04'W  | AMS           | 11           | 11,526                | 12.3  |
| Horsetrail fen | Alaska, USA | rich fen      | 60°25'N  | 150°54'W  | AMS           | 10           | 13,614                | 10.7  |

89

90 *Page 14, lines 314-316 and table 4: table 4 only lists uncertainty ranges for peatland vegetation.*  
91 *How were uncertainty ranges for upland vegetation derived? Certainly not from the ranges in*  
92 *table 4. Please clarify. Page 15, lines 333-334 – see comment #13.*

93 *Thankfully, the authors have used a spellchecker, so there are very few typos. However, there*  
94 *are numerous places in the text, where grammar needs checking: Temporal forms are not always*  
95 *consistent, and some sentences are missing single words or larger parts. Therefore CAREFUL*  
96 *COPY-EDITING is highly important.*

97 The uncertainties of the upland vegetation are from the uncertainties of parameters in previous  
98 study (Tang and Zhuang, 2008; 2009). We used the prior ranges of the parameters based on those  
99 studies. We added this statement in the text in this revision. Following the referee's  
100 recommendation, we have carefully checked the whole text in terms of language.

101

102

103

104

105

106

107

108

109

110

111

112

113

114

115

116 **Response to Referee #2 (Dr. Tupek)**

117 We would like to thank Dr. Tupek for his thoughtful and constructive review, as well as his  
118 detailed comments. Our responses to all of the referee's comments are provided as below.

119 *Authors tested SOC simulations from the modified version of their Terrestrial Ecosystem Model*  
120 *(TEM) for peatlands (P-TEM) for Alaska region for time periods defined by climatic*  
121 *characteristics (solar radiation, temperature, and precipitation levels) and vegetation*  
122 *distribution during last 15 000 years. The model was applied for peatlands and non-peatlands*  
123 *(mineral soil forests). Simulated C distributions, NPP, and peat depths were presented for*  
124 *Alaska at fine scale spatial resolution (maps) and summarized for vegetation types. This can be*  
125 *an interesting study if presented carefully*

126 Thanks for the constructive comments. Following your comments, we made all edits and  
127 changes as detailed below. **The Method, Result, and Discussion sections were totally revised.**  
128 **We also had revisions with respect to grammar and typos in the Abstract, Introduction and**  
129 **Conclusions sections. However, those revisions were not marked. Please see the final**  
130 **manuscript without tracks for a better vision.**

131 *The advances of the model include hydrology, soil thermal, C and N dynamics modules. This*  
132 *looks promising however, the model code is not publicly available and need to be asked from*  
133 *authors. No software details were given. I'd like to see the code and run an example simulation*  
134 *in R to understand the model structure. Description of NPP simulation by the model is missing.*  
135 *Description of Carbon and Nitrogen dynamics of CNDM module is also missing. Add*  
136 *descriptions for clarity. Results largely depended on the adopted distribution of vegetation types.*  
137 *Authors mentioned that distribution of vegetation types and their changes overdriven C*  
138 *accumulation over climate, but also noted that climate had probably driven distribution of*  
139 *vegetation types. Individual parameter values are not listed. It would be interesting to see the*  
140 *changes of key parameters between vegetation types in relation to their prevailing climate.*

141 Response: The descriptions of P-TEM including modules of STM, HM, CNDM, and MDM were  
142 less listed in this manuscript indeed. The main reason is that we have described the model  
143 framework, specific parameters and the parameterization processes, along with the comparison  
144 between simulation and observation regarding soil moisture, methane emissions, water-table  
145 depth, and carbon and nitrogen dynamics in our previous study. Specifically, please find the  
146 paper "**Quantifying Peat Carbon Accumulation in Alaska Using a Process-Based**  
147 **Biogeochemistry Model**" for details ([Wang, S., Q. Zhuang, Z. Yu, S. Bridgham, and J. K. Keller \(2016\), Quantifying peat carbon accumulation in Alaska using a process-based biogeochemistry model, J. Geophys. Res. Biogeosci., 121, doi:10.1002/2016JG003452.](#)).

150 The above paper was under review by JGR-Biogeosciences at that time we submitted this  
151 regional study to Biogeoscience. Now the paper was published, therefore we believe there is no  
152 reason to repeat those model details. We have cited this newly published paper in the text in this  
153 revision.

154 Our model source codes are written in C/C++, not in R. The model has a number of sub-models,  
155 thus its source code is rather lengthy. We appreciate your interests in the model, we are open to  
156 collaborate by using the model to do research so that we have sufficient time to understand the  
157 code.

158

159 *Description of observations of peat depths that were used for model validation is not sufficient.*  
160 *Some description is in section 2.5 but it is not clear and the points on the maps in Fig. 2 are*  
161 *barely visible. Describe clearly.*

162 Response: The peat depths for model validation are from Hugelius et al. (2014). We used the  
163 basal ages to determine the process of peatland expansion from Gorham et al. (2012). We added  
164 our findings of the linkage between basal ages and vegetation distribution in the Result&  
165 Discussion section (sec. 3.3) and discussed the related uncertainties. We also changed the symbol  
166 size in Fig. 2 to make the figure of the basal age distribution much clearer to readers.

167 *Structure of the paper is unclear. Reorder the ideas, avoid using repetitions.*

168 Response: Thanks for the comments. In this revision, we re-ordered the ideas mainly in Result  
169 and Discussion sections and made the structure more logical to readers. We also combined the  
170 Result and Discussion sections to avoid repetitions. We shortened the Sec. 3.1, 3.2 and added the  
171 text describing peat expansion and vegetation changes in Sec. 3.3.

172 *Methods are presented in results. Results are presented in discussion. For example lines 369-370*  
173 *in results describe how peat depth was calculated for the first time. Discussion Section 4.3*  
174 *presents too many numbers without deeper insights on reason behind differences between other*  
175 *studies. At the end of discussion a scatterplot Fig. 14 between observed and modeled peat depths*  
176 *is presented for the 1st time. The Fig. 14 shows that without exceptional agreement of 3 largest*  
177 *values the rest of the scatter is just a gunshot indicating poor performance of the model in most*  
178 *conditions. Authors avoid the explanation. Move results to result section. Present some values in*  
179 *Tables. In discussion interpret the results with a focus on the model and data input.*

180 Response: Thanks for the comments, which helped us significantly improve our presentation of  
181 the study. In this revision, we combined the Result and Discussion sections. Also we have  
182 shortened some sentences, only providing key points. We have moved the statement of the peat  
183 depth calculation into the Method section. In the Result& Discussion section, we added some  
184 contents regarding the reasons behind the vegetation changes through time, e.g., the relationships  
185 between climate and vegetation distribution. Besides, we added some sentences to discuss the  
186 uncertainties of the model and some assumptions in this study. This can represent the reasons  
187 behind the differences between model simulation and observation. For the comparison of peat  
188 depth, we used the peat sample at each site and directly compared the modeled depth with the  
189 observation for that particular pixel. However, as the peat characteristics may differ from site to  
190 site, even several kilometers apart, it is very hard for the model to really capture the true peat  
191 depth. We added this statement at the end of the discussion. The model is suitable for being  
192 applied at regional level and can capture the peat depths features (e.g., the mean values) in a  
193 large area as showed similarity of the spatial peat depth distribution between our model and  
194 observation (see Hugelius et al. (2014) Figure 3 for observed peat depth distribution).

195 *Interesting results as underestimation in uplands, lack of C loss simulation (Fig. 2), reasons*  
196 *behind vegetation controlling C storage, disagreement with observations, assumption that*  
197 *peatlands will remain C sink are brushed away. The agreement with other studies is OK but not*  
198 *enough for discussion. Describe reasons for agreement/disagreements, give insights on*  
199 *function/performance and reason why to use/trust your model. Although the authors claimed that*  
200 *the PTEM includes CN module, nothing can be learned from reading the paper how this or other*  
201 *modules affect the results. Given the SOC underestimation of uplands and large scatter with*  
202 *peatlands, and large-scale climate estimates, could accounting for differences in nutrient status*  
203 *or reevaluating response of C/N ratio be a key for improved estimation of spatial variability of*  
204 *SOC accumulation of P-TEM or TEM model?*

205 Given the complexity of the biogeochemistry of peatlands, we were not able to address and  
206 discuss all processes and mechanisms related to C and N in our simulations. Rather we  
207 dedicated our discussion on 1) how the features of vegetation distribution changes over time  
208 affect carbon accumulation; 2) how different climates in various paleo-periods affect carbon  
209 accumulation rates. We admitted that we have not discussed how N affects C in the model.  
210 However, P-TEM is a version that inherited all processes of C and N interactions in an early  
211 version of TEM (Zhuang et al., 2003, McGuire et al., 1992), which has been extensively  
212 evaluated and applied in numerous applications in northern high latitudes. Here we assume the C  
213 and N interactions will also be valid for the peatland ecosystems. In fact, we have started to use  
214 C and N data collected from SPRUCE (Brain et al., 2016) experiment to evaluate the N  
215 feedbacks to C dynamics. We expect to have a new version of P-TEM to fully account for C and  
216 N feedbacks in peatland ecosystems.

217 *Authors claim that recent climate is warmer and wetter in summers and therefore with future*  
218 *warmer-wetter climate peatland carbon sink will continue. Possibility of increased respiration*  
219 *and C loss due to droughts or warmer winters is not mentioned. For the conclusion on future C*  
220 *sink a simulations with climate scenarios would be useful.*

221 Agreed. We have revised our statement regarding future carbon accumulation. We further stated  
222 that further study is needed to have a better view on the soil carbon dynamic under future climate  
223 scenarios. Given the complexity of peatland dynamics in terms of their areal changes (e.g.,  
224 expansion and shrinkage, and new peatland formation), we feel analyzing how peatland carbon  
225 responds to future climate changes and peatland dynamics is a tremendous work, which is well  
226 beyond this study. In addition, the current paper is already very long. Thus, we decided to  
227 conduct a full analysis on Arctic peatland carbon responses to future climates in a separate study.

228

229 *Increase Figs. 2, 3, 4 and their legends size by 50 or 100%*

230 We have increased the legends size and symbol size to make the figures clearer.

231 Meanwhile, the sequence of some tables and figures has been adjusted to better present the  
232 results.

233 *why are panels b, d, f in Fig. 3 scaled by zero? that makes differences to appear smaller increase*  
234 *legend in Fig. 5*

235 We have decreased the axis scale in Fig. 3 to make the difference appear bigger. We also  
236 increased the legend in Fig. 5.

237 *increase Fig. 7 and 9, why fig. 9 it has 2 legend bars?*

238 We have increased the size of each panel. We mistakenly put extra color bar in panel (f). We  
239 have deleted it.

240 *line 137 “observed water contents drive STM”?, did you mean observed temperatures?*

241 The STM considers soil water content at different depths to simulate the soil temperature. We  
242 used the observed soil water content at particular site to drive the STM when parameterizing the  
243 model in [Wang, S., Q. Zhuang, Z. Yu, S. Bridgham, and J. K. Keller \(2016\), Quantifying peat  
244 carbon accumulation in Alaska using a process-based biogeochemistry model, J. Geophys.  
245 Res. Biogeosci., 121, doi:10.1002/2016JG003452.](#) During the regional simulation, we used the  
246 simulated soil water content at different depths directly from HM to drive the STM.

247 *lines 235-238 reformulate for clarity*

248 We have reformulated the sentences.

249 *line 293 correct value of C storage*

250 We have changed this value to 0.8 kg C m<sup>-2</sup>.

251 *lines 300-302, 309 reformulate for clarity*

252 We have made the reformulation.

253 *line 315 range of what?*

254 The range here is for vegetation carbon storage. We have clarified this.

255 *lines 325 “spots were widely spread” reformulate, “SOC concentration” do you mean SOC  
256 storage?*

257 We have reformulated them.

258 *line 326 reformulate “tundra was taking back area” or similar*

259 We have reformulated it.

260 *line 361 Table 4 is not showing parameters*

261 We have changed the statement to “due to uncertainties of observation” and cited the paper  
262 which has the parameters listed.

263 *lines 375-377 reformulate for clarity*

264 We have reformulated the section.

265 *lines 420 – 460 reformulate for clarity*



266 We have reformulated the discussion part.

267 *line 424 why if  $p < 0.05$  “some certain effects”?*

268 From the result in Wang et al. (2016) that p-value is less than 0.05, we can get the idea that the  
269 interaction factor is one of the significant factors. We reorganized this part.

270 *line 428 “positive effect” of temperature? low temp slowed SOC accumulation, that’s negative*  
271 *effect*

272 Yes, it should be “negative effect” as the cooler condition during the neoglacier period slowed  
273 the carbon accumulation. We reformulated this sentence.

274 *line 437 delete “suggesting the warmest climate during HTM” it comes by definition of HTM*

275 Correct. Repeating the definition of HTM can be awkward. We revised it.

276 *lines 443-448 does not make sense*

277 We deleted this part since it was talking about the uncertainties coming from the climate model  
278 (ECBILT) itself, and has already been discussed in He et al. (2014). In this study, we directly  
279 used the output of the model.

280 *line 452 what is “stored C in overall in the spatial scale”?*

281 We have reformulated the statement.

282 *line 454 “negative accumulation rate” avoid writing nonsense*

283 We have added “(meaning C loss)” right after this statement.

284 *lines 485 – 545 reformulate whole section, move results into results, check for repetitions,*  
285 *highlight only most important trends and insights, shorten discussion if nothing much relevant to*  
286 *say*

287 We have reformulated the result and discussion.

288 *lines 508-519 OK*

289 *References – change into the corresponding format of Biogeosciences*

290 Thanks for pointing this out. We have changed the reference and citation format according to  
291 *Biogeosciences* submission requirement The manuscript has never been submitted to other  
292 journals before.

293

294

295

296

297

298

299

300

301

302

303

304

305

306

307

308

309

310

311

312

313

314

315

316

317

318

319

320

321

322  
323  
324  
325  
326  
327  
328  
329  
330  
331  
332  
333  
334  
335  
336  
337  
338  
339  
340  
341  
342  
343  
344  
345  
346  
347  
348  
349

**Quantifying Soil Carbon Accumulation in Alaskan Terrestrial Ecosystems during the Last 15,000 Years**

Sirui Wang<sup>1</sup>, Qianlai Zhuang<sup>1,2\*</sup>, Zicheng Yu<sup>3</sup>

<sup>1</sup>Department of Earth, Atmospheric, and Planetary Sciences, Purdue University, West Lafayette, Indiana, 47907

<sup>2</sup>Department of Agronomy, Purdue University, West Lafayette, IN 47907

<sup>3</sup>Department of Earth and Environmental Sciences, Lehigh University, Bethlehem, PA 18015

Correspondence to: [qzhuang@purdue.edu](mailto:qzhuang@purdue.edu)

350 **Abstract:** Northern high latitudes contain large amounts of soil organic carbon (SOC), in which  
351 Alaskan terrestrial ecosystems account for a substantial proportion. In this study, the SOC  
352 accumulation in Alaskan terrestrial ecosystems over the last 15,000 years was simulated using a  
353 process-based biogeochemistry model for both peatland and non-peatland terrestrial ecosystems.  
354 Comparable with the previous estimates of 25-70 Pg C in peatland and 13-22 Pg C in non-  
355 peatland soils within 1-m depth in Alaska, our model estimated a total SOC of 36-63 Pg C at  
356 present, including 27-48 Pg C in peatland soils and 9-15 Pg C in non-peatland soils. Vegetation  
357 stored only 2.5-3.7 Pg C in Alaska currently with 0.3-0.6 Pg C in peatlands and 2.2-3.1 Pg C in  
358 non-peatlands. The simulated average rate of peat C sequestration was 2.3 Tg C yr<sup>-1</sup> with a peak  
359 value of 5.1 Tg C yr<sup>-1</sup> during the Holocene Thermal Maximum (HTM) in the early Holocene,  
360 four folds higher than the average rate of 1.4 Tg C yr<sup>-1</sup> over the rest of the Holocene. The SOC  
361 accumulation slowed down, or even ceased, during the neoglacial climate cooling after the mid-  
362 Holocene, but accumulation increased again in the 20<sup>th</sup> century. The model-estimated peat depths  
363 ranged from 1.1 to 2.7 m, similar to the field-based estimate of 2.29 m for the region. We found  
364 that the changes in vegetation types and their distributions due to climate change were the main  
365 factors determining the spatial variations of SOC accumulation during different time periods.  
366 Warmer summer temperature and stronger radiation seasonality, along with higher precipitation  
367 in the HTM and the 20<sup>th</sup> century might have resulted in the extensive peatland expansion and  
368 carbon accumulation, implying that soil C accumulation would continue under future warming  
369 conditions.

370 **Keywords:** Carbon, Peatlands, Alaska, Modelling, Climate

371

372 **1. Introduction**

373 Global surface air temperature has been increasing since the middle of the 19<sup>th</sup> century  
374 (Jones and Mogberg, 2003; Manabe and Wetherald, 1980, 1986). Since 1970, the warming trend  
375 has accelerated at a rate of 0.35 °C per decade in northern high latitudes (Euskirchen et al., 2007;  
376 McGuire et al., 2009). It is predicted that the warming will continue in the next 100 years (Arctic  
377 Climate Impact Assessment 2005; Intergovernmental Panel on Climate Change (IPCC), 2013,  
378 2014). The land surface in northern high latitudes (>45° N) occupies 22% of the global surface  
379 and stores over 40% of the global soil organic carbon (SOC) (McGuire et al., 1995; Melillo et  
380 al., 1995; McGuire and Hobbie, 1997). Specifically, the northern high latitudes were estimated to  
381 store 200-600 Pg C (1 Pg C = 10<sup>15</sup> g C) in peatland soils depending on the depth considered  
382 (Gorham, 1990, 1991; Yu, 2012), 750 Pg C in non-peatland soils (within 3 m) (Schuur et al.,  
383 2008; Tarnocai et al., 2009; Hugelius et al., 2014), and additional 400 Pg C in frozen loess  
384 deposits of Siberia (Zimov et al., 2006a). Peatland area is around 40 million hectares in Alaska  
385 compared with total 350 million hectares in northern high-latitude regions (Kivinen and  
386 Pakarinen, 1981). Alaskan peatlands account for the most vast peatland area in the USA and  
387 cover at least 8% of total land area (Bridgham et al., 2006). To date, the regional soil C and its  
388 responses to the climate change are still with large uncertainty (McGuire et al., 2009; Loisel et  
389 al., 2014).

390 The warming climate could increase C input to soils as litters through stimulating plant  
391 net primary production (NPP) (Loisel et al., 2012). However, it can also decrease the SOC by  
392 increasing soil respiration (Yu et al., 2009). Warming can also draw down the water table in  
393 peatlands by increasing evapotranspiration, resulting in a higher decomposition rate as the  
394 aerobic respiration has a higher rate than anaerobic respiration in general (Hobbie et al., 2000).

395 SOC accumulates where the rate of soil C input is higher than decomposition. The variation of  
396 climate may switch the role of soils between a C sink and a C source (Davidson and Janssens,  
397 2006; Davidson et al., 2000; Jobbagy and Jackson, 2000). Unfortunately, due to the data gaps of  
398 field-measurement and uncertainties in estimating regional C stock (Yu, 2012), with limited  
399 understanding of both peatlands and non-peatlands and their responses to climate change, there is  
400 no consensus on the sink and source activities of these ecosystems (Frolking et al., 2011; Belyea,  
401 2009; McGuire et al., 2009).

402 To date, both observation and model simulation studies have been applied to understand  
403 the long-term peat C accumulation in northern high latitudes. Most field estimations are based on  
404 series of peat-core samples (Turunen et al., 2002; Roulet et al., 2007; Yu et al., 2009; Tarnocai et  
405 al., 2009). However, those core analyses may not be adequate for estimating the regional C  
406 accumulation due to their limited spatial coverage. Model simulations have also been carried out.  
407 For instance, Frolking et al. (2010) developed a peatland model considering the effects of plant  
408 community, hydrological dynamics and peat properties on SOC accumulation. The simulated  
409 results were compared with peat-core data. They further analyzed the contributions of different  
410 plant functional types (PFTs) to the peat C accumulation. However, this 1-D model has not been  
411 used in large spatial-scale simulations by considering other environmental factors (e.g.,  
412 temperature, vapor pressure, and radiation). In contrast, Spahni et al. (2013) used a dynamic  
413 global vegetation and land surface process model (LPX), based on LPJ (Sitch et al., 2003),  
414 imbedded with a peatland module, which considered the nitrogen feedback on plant productivity  
415 (Xu-Ri and Prentice, 2008) and plant biogeography, to simulate the SOC accumulation rates of  
416 northern peatlands. However, these models have not been evaluated with respect to their  
417 simulations of soil moisture, water table depth, methane fluxes, and carbon fluxes presumably

418 due to relatively simple model structures, especially in terms of ecosystem processes (Stocker et  
419 al., 2011, 2014; Kleinen et al., 2010). Furthermore, climatic effects on SOC were not fully  
420 explained. The Terrestrial Ecosystem Model (TEM) has been applied to study C and nitrogen  
421 pools and fluxes in the Arctic (Zhuang et al., 2001, 2002, 2003, 2015; He et al., 2014). However,  
422 the model has not been calibrated and evaluated with peat-core C data, and has not been applied  
423 to investigate the peatland C dynamics. Building upon these efforts, recently we fully evaluated  
424 the peatland version of TEM (P-TEM) including modules of hydrology (HM), soil thermal  
425 (STM), C and nitrogen dynamics (CNDM) for both upland and peatland ecosystems (Wang et  
426 al., 2016).

427 Here we used the peatland-core data for various peatland ecosystems to parameterize and  
428 test P-TEM (Figure 1). The model was then used to quantify soil C accumulation of both  
429 peatland and non-peatland ecosystems across the Alaskan landscape since the last deglaciation.  
430 This study is among the first to examine the current peatlands and non-peatlands C distributions  
431 and peat depths in various ecosystems at the regional scale.

432

## 433 **2. Methods**

### 434 **2.1 Model Description**

435 ~~In P-TEM, peatland soil organic C (SOC) accumulation is determined by the difference~~  
436 ~~between the net primary production (NPP) and aerobic and anaerobic decomposition. Peatlands~~  
437 ~~accumulate C where NPP is greater than decomposition, resulting in positive net ecosystem~~  
438 ~~production (NEP):~~

439 
$$NEP = NPP - R_H - R_{CH_4} - R_{CWM} - R_{CM} - R_{COM} \quad (1)$$

440 P-TEM was developed based on the Terrestrial Ecosystem Model (TEM) at a monthly  
441 step (Zhuang et al., 2003; 2015). It explicitly considers the process of aerobic decomposition  
442 ( $R_H$ ) related to the variability of water table depth; net methane emission after methane oxidation  
443 ( $R_{CH_4}$ );  $CO_2$  emission due to methane oxidation ( $R_{CWM}$ ) (Zhuang et al., 2015);  $CO_2$  release  
444 accompanied with the methanogenesis ( $R_{CM}$ ) (Tang et al., 2010; Conrad, 1999); and  $CO_2$  release  
445 from other anaerobic processes ( $R_{COM}$ , e.g., fermentation, terminal electron acceptor (TEA)  
446 reduction) (Keller and Bridgman, 2007; Keller and Takagi, 2013). For upland soils, we only  
447 considered the heterotrophic respiration under aerobic condition (Raich, 1991). For detailed model  
448 description see Supplement.

449 We model peatland soils as a two-layer system for hydrological module (HM) while  
450 keeping the three-layer system for upland soils (Zhuang et al., 2002). The soil layers above the  
451 lowest water table position are divided into: (1) moss (or litter) organic layer (0-10 cm); and (2)  
452 humic organic layer (10-30 cm) (Wang et al., 2016). Based on the total amount of water content  
453 within those two unsaturated layers, the actual water table depth (WTD) is estimated. The water  
454 content at each 1 cm above the water table can be then determined after solving the water  
455 balance equations (Zhuang et al., 2004).

456 In the STM module, the soil vertical profile is divided into four layers: (1) snowpack in  
457 winter, (2) moss (or litter) organic layer, (3) upper and (4) lower humic organic soil (Wang et al.,  
458 2016). Each of these soil layers is characterized with a distinct soil thermal conductivity and heat  
459 capacity. We used the observed water contents at the particular sites to drive the STM (Zhuang et  
460 al., 2001).



461 The methane dynamics module (MDM) (Zhuang et al., 2004) considers the processes of  
462 methanogenesis, methanotrophy, and the transportation pathways including: (1) diffusion  
463 through the soil profile; (2) plant aided transportation; and (3) ebullition. The soil temperatures  
464 calculated from STM, after interpolation into 1 cm sub layers, are input to the MDM. The water  
465 table depth and soil water content in the unsaturated zone for methane production and emission  
466 are obtained from HM, and the net primary production (NPP) is calculated from the CNDM.  
467 Soil water pH is prescribed from observed data and the root distribution determines the redox  
468 potential (Zhuang et al., 2004).

## 469 **2.2 Model Parameterization**

470 We have parameterized the key parameters of the individual modules including HM,  
471 STM, and MDM (Wang et al., 2016). The parameters in CNDM for upland soils and vegetation  
472 have been optimized in the previous studies (Zhuang et al 2002, 2003; Tang and Zhuang 2008).  
473 The parameters for peatland soils in P TEM were parameterized using a moderate rich  
474 *Sphagnum* spp. open fen (APEXCON) and a *Sphagnum* black spruce (*Picea mariana*) bog  
475 (APEXPER) (Table 3). Both are located in the Alaskan Peatland Experiment site (APEX) study  
476 area, where *Picea mariana* is the only tree species above breast height in APEXPER. Three  
477 water table position manipulations were established in APEX including a control, a lowered, and  
478 a raised water table plots (Chivers et al., 2009; Turetsky et al., 2008; Kane et al., 2010; Churchill  
479 et al., 2011). There were also several internal collapse scars that formed with thaw of surface  
480 permafrost, including a non-, an old, and a new collapse plots. APEXCON represents the control  
481 manipulation and APEXPER represents the non-collapse plot. The annual NPP and aboveground  
482 biomass at both sites have been measured in 2009. There were no belowground observations;  
483 however, at a Canadian peatland, Mer Bleue, which includes *Sphagnum* spp. dominated bog

484 ~~(dominated by shrubs and *Sphagnum*) and pool fen (dominated by sedges and herbs and~~  
485 ~~*Sphagnum*). Assuming the belowground biomass in APEXCON and APEXPER was close to that~~  
486 ~~in Mer Bleue, we used the belowground biomass at Mer Bleue to represent the missing~~  
487 ~~observations at both sites (Table 4). We conducted a set of 100,000 Monte Carlo ensemble~~  
488 ~~simulations for each site level calibration, and parameters with the highest mode in posterior~~  
489 ~~distribution were selected (Tang and Zhuang, 2008, 2009).~~

### 490 **2.3 Regional Vegetation Data**

491 ~~The Alaskan C stock was simulated through the Holocene where the vegetation biome~~  
492 ~~maps were reconstructed at four time periods: a time period encompassing a millennial scale~~  
493 ~~warming event during the last deglaciation known as the Bølling-Allerød at 15–11 ka (1 ka =~~  
494 ~~1000 cal-yr Before Present), HTM during the early Holocene at 11–10 and 10–9 ka as well as the~~  
495 ~~mid- (9–5 ka) and late Holocene (9 ka–1900 AD) (He et al., 2014). We used the modern~~  
496 ~~vegetation distribution for the simulation during the period 1900–2000 AD (Figure 2). We~~  
497 ~~assumed that the vegetation distribution remained static within each corresponding time period.~~  
498 ~~Five vegetation types were classified as upland vegetation: boreal deciduous broadleaf forest,~~  
499 ~~boreal evergreen needleleaf and mixed forest, alpine tundra, wet tundra; and barren (Table 1).~~  
500 ~~Mountain ranges and large water bodies were delineated as ‘Barren’ and data could not be~~  
501 ~~interpolated across them. By using the same vegetation distribution map, we reclassified the~~  
502 ~~upland vegetation into two peatland vegetation types: *Sphagnum* spp. poor fens (SP) generated~~  
503 ~~from tundra ecosystems, and *Sphagnum* spp. black spruce (*Picea mariana*) bog/ peatland (SBP)~~  
504 ~~generated from forest ecosystems (Table 1), both of which dominate the major area of Alaskan~~  
505 ~~peatlands. We used both the upland and peatland vegetation types to simulate the C dynamics in~~  
506 ~~Alaska.~~

507 Upland and peatland distribution for each grid cell was determined using the wetland  
508 inundation data extracted from the NASA/GISS global natural wetland dataset (Matthews and  
509 Fung, 1987). The resolution was resampled to  $0.5^\circ \times 0.5^\circ$  from  $1^\circ \times 1^\circ$ . We postulated that,  
510 given the same topography of Alaska during the Holocene, it was reasonable to assume that the  
511 wetland distribution can be represented by modern inundation map. The inundation fraction was  
512 assumed to be the same within each grid through time and the land grids not covered by  
513 expanded peatland yet were assumed as uplands. We calculated the total area of modern Alaskan  
514 peatlands to be  $302,410 \text{ km}^2$ , which was within the range from  $132,000 \text{ km}^2$  (Bridgham et al.,  
515 2006) to  $596,000 \text{ km}^2$  (Kivinen and Pakarinen, 1991). The soil water pH data were extracted  
516 from Carter and Scholes (2000), and the elevation data were derived from Shuttle Radar  
517 Topography Mission and were resampled to  $0.5^\circ \times 0.5^\circ$  spatial resolution.

#### 518 **2.4 Climate Data**

519 Climate data were downscaled and bias corrected from ECBilt-CLIO model output  
520 (Timm and Timmermann, 2007; He et al., 2014). Climate fields include monthly precipitation,  
521 monthly air temperature, monthly net incoming solar radiation, and monthly vapor pressure  
522 ( $2.5^\circ \times 2.5^\circ$ ). We used the same time dependent forcing atmospheric carbon dioxide  
523 concentration data for model input as were used in ECBilt-CLIO transient simulations from the  
524 Taylor Dome (Timm and Timmermann, 2007). The historical climate data used for the  
525 simulation through the 20<sup>th</sup>-century are monthly CRU2.0 data.

526 The mean annual net incoming solar radiation (NIRR) was  $78 \pm 4.8 \text{ W m}^{-2}$  before the  
527 HTM (15–11 ka). It showed an increase at the early HTM (11–10 ka), reaching  $83.6 \pm 4.5 \text{ W m}^{-2}$   
528 and continued to increase to  $84 \pm 4.7 \text{ W m}^{-2}$  at the late HTM (10–9 ka). NIRR decreased after

529 the HTM through the entire mid-Holocene (9–5 ka) to a minimum of  $79 \pm 5 \text{ W m}^{-2}$  at the end of  
530 the Holocene. It became higher from 1900 to 2000 AD, with annual mean  $82 \pm 5.1 \text{ W m}^{-2}$   
531 (Figure 3b). The mean annual air temperature showed a similar pattern as it rose from  $-7 \pm 1.8 \text{ }^\circ\text{C}$   
532 to  $-5 \pm 1.6 \text{ }^\circ\text{C}$  at the early HTM and reached  $-4.7 \pm 1.5 \text{ }^\circ\text{C}$  at the late HTM, indicating a warmer-  
533 than-present climate. There was also a temperature decrease when HTM ended through the rest  
534 of the Holocene and the temperature increased again from 1900 AD to  $-5.8 \pm 1.5 \text{ }^\circ\text{C}$ , presumably  
535 due to the global warming (Figure 3d). Total annual precipitation increased from  $306 \pm 40 \text{ mm}$  to  
536  $369 \pm 25 \text{ mm}$  at the end of the HTM, suggesting an overall wet climate. A dryer condition  
537 occurred from the mid-Holocene and became driest in the late Holocene (5 ka–1900 AD) (Figure  
538 3f). The monthly values of NIRR followed the same pattern as annual means, except during the  
539 winter. The maximum summer radiation occurred during the late HTM, leading to the highest  
540 radiation seasonality. Large seasonality also appeared in the 20<sup>th</sup> century, however, lower than  
541 that during the HTM (Figure 3a). Temperature seasonality followed the trend of annual  
542 temperature. The days of year with temperature above  $0 \text{ }^\circ\text{C}$  increased 10–15 days at the HTM  
543 compared with that before the HTM, suggesting a longer growing season (Figure 3c).  
544 Precipitations were highest during the summer (July–September) in each time period and lowest  
545 during the winter and early spring (December–April). The periods at 15–11 ka and in the late-  
546 Holocene exhibited less overall, especially summer precipitations than at the HTM. During the  
547 20<sup>th</sup> century, there was less winter precipitation but it was compensated by a higher summer  
548 precipitation compared with the late Holocene (Figure 3e). The orbital-induced maximum  
549 seasonality of insolation and the warmest climate during the HTM as described in Huybers et al.  
550 (2006) and Yu et al. (2010) corresponded well to the simulated trends of air temperature.

551

552 **2.5 Data of Peatland Basal Ages**

553 ~~———— We conducted the simulation from 15 to 5 ka for an Alaskan peatland assuming it started~~  
554 ~~to accumulate C since 15 ka. However, assuming that peatlands in all grids had the same basal~~  
555 ~~age (15 ka) could overestimate the total peat SOC accumulation. Therefore we used the observed~~  
556 ~~basal ages of peat samples from Gorham et al. (2012) and categorized them into different time~~  
557 ~~periods (Figure 2). We found that during each period, the spatial distribution of peatland basal~~  
558 ~~ages was similar to that of the vegetation types (e.g., peatland initiation points were mainly~~  
559 ~~located where was dominated by alpine tundra at south, northwestern, and southeastern coast~~  
560 ~~during 15–11 ka). We thus used the vegetation types to estimate the peatland basal ages at~~  
561 ~~regional scales (Table 2).~~

562 **2.6 Simulations and Sensitivity Test**

563 ~~To verify the model ability to simulate the peat C accumulation rates in the past 15,000~~  
564 ~~years, we conducted a simulation using pixels located on the Kenai Peninsula from 15 to 5 ka~~  
565 ~~after model parameterization. We compared the model simulation results with the peat core data~~  
566 ~~from four peatlands on the Kenai Peninsula, Alaska (Jones and Yu, 2010; Yu et al., 2010) (see~~  
567 ~~Wang et al. (2016) for detail). The observed data include the peat depth, bulk density of both~~  
568 ~~organic and inorganic matters at 1 cm interval, and age determinations. The simulated C~~  
569 ~~accumulation rates represent the actual (“true”) rates at different times in the past. However, the~~  
570 ~~calculated accumulation rates from peat cores are considered as “apparent” accumulation rates,~~  
571 ~~as peat would continue to decompose since the time of formation until present when the~~  
572 ~~measurement was made (Yu, 2012). To facilitate comparison between simulated and observed~~  
573 ~~accumulation rates, we converted the simulated “true” accumulation rates to “apparent” rates;~~

574 following the approach by Spahni et al. (2013). That is, we summed the annual net C  
575 accumulation over each 500-year interval and deducted the total amount of C decomposition  
576 from that time period, then dividing by 500 years.

577 For the study region, we conducted a transient simulation using continuous monthly  
578 meteorology data (Figure 2) from 15 ka to 2000 AD. Five maps (Figure 3) were used to represent  
579 the vegetation distributions of Alaska and were assumed to be static during each time period  
580 (e.g., 15–11 ka, 11–10 ka, 10–9 ka, 9 ka–1900 AD, and 1900–2000 AD). The simulation was  
581 firstly conducted assuming all grid cells were taken up by upland vegetation to get the upland  
582 soil C spatial distributions during different time periods. We then conducted the second  
583 simulation assuming all grid cells were dominated by peatland vegetation by merging upland  
584 types into peatland types following Table 1 to obtain the distributions of peat SOC accumulation.  
585 We used the inundation fraction map to extract both uplands and peatlands from each grid and  
586 estimated the corresponding SOC stocks within each grid, which were then summed up to  
587 represent the Alaskan SOC stock.

588 We conducted a sensitivity test to evaluate the responses of NPP, SOC decomposition  
589 rates (aerobic plus anaerobic respiration), and net SOC balance to the climate variables.  
590 Simulations under three scenarios were conducted to test the temperature effect. We used the  
591 original forcing data as the standard scenario and the warmer (monthly temperature +5°C) and  
592 cooler (–5°C) as other two while keeping the rest forcing data unchanged. Similarly, we used the  
593 original forcing data as the standard scenario and the wetter (monthly precipitation +10 mm) and  
594 drier (–10 mm) to test the effect from precipitation. To further study if vegetation distribution  
595 has stronger effects on SOC sequestration than climate in Alaska, we simply replaced SBP with  
596 SP and simultaneously replaced the upland forests with tundra at the beginning of 15 ka. We also

597 ~~conducted the simulation under “warmer” and “wetter” conditions described before while~~  
598 ~~keeping the vegetation distribution unchanged.~~

## 599 2. Methods

### 600 2.1. Overview

601 To conduct regional simulations of carbon accumulation for both uplands and peatlands,  
602 we first parameterized the P-TEM for representative ecosystems in Alaska. Second, we  
603 organized the regional vegetation and peatland distribution data, spatial basal age data for all  
604 peatland grid cells based on site-level soil core data, and climate data for each period during the  
605 Holocene. Finally, we conducted the regional simulations and sensitivity analysis.

### 606 2.2 Model Description

607 In P-TEM (Wang et al., 2016), peatland soil organic C (SOC) accumulation is determined  
608 by the difference between NPP and aerobic and anaerobic decomposition. Peatlands accumulate  
609 C where NPP is greater than decomposition, resulting in positive net ecosystem production  
610 (NEP):

$$611 \quad NEP = NPP - R_H - R_{CH_4} - R_{CWM} - R_{CM} - R_{COM} \quad (1)$$

612 P-TEM was developed based on the Terrestrial Ecosystem Model (TEM) at a monthly  
613 step (Zhuang et al., 2003; 2015). It explicitly considers the process of aerobic decomposition  
614 ( $R_H$ ) related to the variability of water-table depth; net methane emission after methane oxidation  
615 ( $R_{CH_4}$ );  $CO_2$  emission due to methane oxidation ( $R_{CWM}$ ) (Zhuang et al., 2015);  $CO_2$  release  
616 accompanied with the methanogenesis ( $R_{CM}$ ) (Tang et al., 2010; Conrad, 1999); and  $CO_2$  release  
617 from other anaerobic processes ( $R_{COM}$ , e.g., fermentation, terminal electron acceptor (TEA))

618 reduction) (Keller and Bridgham, 2007; Keller and Takagi, 2013). For upland soils, we only  
619 considered the heterotrophic respiration under aerobic condition (Raich, 1991). For detailed model  
620 description see Wang et al. (2016).

621 We modeled peatland soils as a two-layer system for hydrological module (HM) while  
622 keeping the three-layer system for upland soils (Zhuang et al., 2002). The soil layers above the  
623 lowest water table position are divided into: (1) moss (or litter) organic layer (0-10 cm); and (2)  
624 humic organic layer (10-30 cm) (Wang et al., 2016). Based on the total amount of water content  
625 within those two unsaturated layers, the actual water table depth (WTD) is estimated. The water  
626 content at each 1 cm above the water table can be then determined after solving the water  
627 balance equations (Zhuang et al., 2004).

628 In the STM module, the soil vertical profile is divided into four layers: (1) snowpack in  
629 winter, (2) moss (or litter) organic layer, (3) upper and (4) lower humic organic soil (Wang et al.,  
630 2016). Each of these soil layers is characterized with a distinct soil thermal conductivity and heat  
631 capacity. We used the observed water content to drive the STM (Zhuang et al., 2001).

632 The methane dynamics module (MDM) (Zhuang et al., 2004) considers the processes of  
633 methanogenesis, methanotrophy, and the transportation pathways including: (1) diffusion  
634 through the soil profile; (2) plant-aided transportation; and (3) ebullition. The soil temperatures  
635 calculated from STM, after interpolation into 1-cm sub-layers, are input to the MDM. The water-  
636 table depth and soil water content in the unsaturated zone for methane production and emission  
637 are obtained from HM, and NPP is calculated from the CNDM. Soil-water pH is prescribed from  
638 observed data and the root distribution determines the redox potential (Zhuang et al., 2004).

639



640 **2.3 Model Parameterization**

641 We have parameterized the key parameters of the individual modules including HM,  
642 STM, and MDM in Wang et al. (2016). The parameters in CNDM for upland soils and  
643 vegetation have been optimized in the previous studies (Zhuang et al 2002, 2003; Tang and  
644 Zhuang 2008). Here we parameterized P-TEM for peatland ecosystems using data from a  
645 moderate rich *Sphagnum* spp. open fen (APEXCON) and a *Sphagnum*-black spruce (*Picea*  
646 *mariana*) bog (APEXPER) (Table 1). Both are located in the Alaskan Peatland Experiment  
647 (APEX) study area, where *Picea mariana* is the only tree species above breast height in  
648 APEXPER. Three water table position manipulations were established in APEX including a  
649 control, a lowered, and a raised water table plots (Chivers et al., 2009; Turetsky et al., 2008;  
650 Kane et al., 2010; Churchill et al., 2011). There were also several internal collapse scars that  
651 formed with thaw of surface permafrost, including a non-, an old, and a new collapse plots.  
652 APEXCON represents the control manipulation and APEXPER represents the non-collapse plot.  
653 The annual NPP and aboveground biomass at both sites have been measured in 2009. There were  
654 no belowground observations at APEX, however at a Canadian peatland, Mer Bleue, which  
655 includes *Sphagnum* spp. dominated bog (dominated by shrubs and *Sphagnum*) and pool fen  
656 (dominated by sedges and herbs and *Sphagnum*). The belowground biomass was also observed at  
657 Suurisuo mire complex, southern Finland, a sedge fen site dominated by *Carex rostrate*. We  
658 used the ratio (70%) of belowground biomass to total biomass from these two study sites to  
659 calculate the missing belowground biomass values at APEXCON and APEXPER (Table 2). We  
660 conducted 100,000 Monte Carlo ensemble simulations to calibrate the model for each site using  
661 a Bayesian approach and parameter values with the modes in their posterior distributions were  
662 selected (Tang and Zhuang, 2008, 2009).

663

## 664 **2.4 Regional Model Input Data**

665 The Alaskan C stock was simulated through the Holocene driven with vegetation data  
666 reconstructed for four time periods including a time period encompassing a millennial-scale  
667 warming event during the last deglaciation known as the Bølling-Allerød at 15-11 ka (1 ka =  
668 1000 cal yr Before Present), HTM during the early Holocene at 11-10 and 10-9 ka, and the mid-  
669 (9-5 ka) and late- Holocene (5 ka-1900 AD) (He et al., 2014). We used the modern vegetation  
670 distribution for the simulation during the period 1900-2000 AD (Figure 2). We assumed that the  
671 vegetation distribution remained static within each corresponding time period. Upland  
672 ecosystems were classified into boreal deciduous broadleaf forest, boreal evergreen needleleaf  
673 and mixed forest, alpine tundra, wet tundra; and barren lands (Table 3). By using the same  
674 vegetation distribution map, we reclassified the upland ecosystems into two peatland types  
675 including *Sphagnum* spp. poor fens (SP) dominated by tundra and *Sphagnum* spp.-black spruce  
676 (*Picea mariana*) bog/ peatland (SBP) dominated by forest ecosystems (Table 3).

677 Upland and peatland ecosystem distribution for each grid cell was determined using the  
678 wetland inundation data extracted from the NASA/ GISS global natural wetland dataset  
679 (Matthews and Fung, 1987). The resolution was resampled to  $0.5^\circ \times 0.5^\circ$  from  $1^\circ \times 1^\circ$ . Given  
680 the same topography of Alaska during the Holocene, we assumed that the wetland distribution  
681 kept the same throughout the Holocene. The inundation fraction was assumed to be the same  
682 within each grid through time and the land grids not covered by peatland were treated as uplands.  
683 We calculated the total area of modern Alaskan peatlands to be 302,410 km<sup>2</sup>, which was within  
684 the range from 132,000 km<sup>2</sup> (Bridgman et al., 2006) to 596,000 km<sup>2</sup> (Kivinen and Pakarinen,

685 1991). The soil water pH data were extracted from Carter and Scholes (2000), and the elevation  
686 data were derived from Zhuang et al. (2007).

687 Our regional simulations considered the effects of basal ages on carbon accumulation. To  
688 obtain the spatially explicit basal age data for all peatlands grid cells, we first categorized the  
689 observed basal ages of peat samples from Gorham et al. (2012) into different time periods  
690 (Figure 2). During each period, the spatial distribution of peatland basal ages was correlated with  
691 the dominated vegetation types. For instance, peatland initiations during 15-11 ka occurred in the  
692 pixels that were dominated by alpine tundra at south, northwestern, and southeastern coast. We  
693 thus used the vegetation types to estimate the peatland basal ages for all grid cells at regional  
694 scales (Table 4).

695 Climate data were bias-corrected from ECBilt-CLIO model output (Timm and  
696 Timmermann, 2007) to minimize the difference from CRU data (He et al., 2014). Climate fields  
697 include monthly precipitation, monthly air temperature, monthly net incoming solar radiation,  
698 and monthly vapor pressure at resolution of  $2.5^\circ \times 2.5^\circ$ . We used the same time-dependent  
699 forcing atmospheric carbon dioxide concentration data for model input as were used in ECBilt-  
700 CLIO transient simulations from the Taylor Dome (Timm and Timmermann, 2007). The  
701 historical climate data used for the simulation through the 20<sup>th</sup> century were monthly CRU2.0  
702 data (Mitchell et al., 2004).

## 703 **2.5 Simulations and Sensitivity Test**

704 Simulations for pixels located on the Kenai Peninsula from 15 to 5 ka were first  
705 conducted with the parameterized model. The peat-core data from four peatlands on the Kenai  
706 Peninsula, Alaska (Jones and Yu, 2010; Yu et al., 2010) (see Wang et al. (2016) Table 3) were

707 used to compare with the simulations. The observed data include the peat depth, bulk density of  
708 both organic and inorganic matters at 1-cm interval, and age determinations. The simulated C  
709 accumulation rates represent the actual (“true”) rates at different times in the past. However, the  
710 calculated accumulation rates from peat cores are considered as “apparent” accumulation rates,  
711 as peat would continue to decompose since the time of formation until present when the  
712 measurement was made (Yu, 2012). To facilitate comparison between simulated and observed  
713 accumulation rates, we converted the simulated “true” accumulation rates to “apparent” rates,  
714 following the approach by Spahni et al. (2013). That is, we summed the annual net C  
715 accumulation over each 500-year interval and deducted the total amount of C decomposition  
716 from that time period, then dividing by 500 years.

717 Second, we conducted a transient regional simulation driven with monthly climatic data  
718 (Figure 3) from 15 ka to 2000 AD. The simulation was conducted assuming all grid cells were  
719 taken up by upland ecosystems to get the upland soil C spatial distributions during different time  
720 periods. We then conducted the second simulation assuming all grid cells were dominated by  
721 peatland ecosystems following Table 3 to obtain the distributions of peat SOC accumulation.  
722 Finally, we used the inundation fraction map to extract both uplands and peatlands and estimated  
723 the corresponding SOC stocks within each grid, which were then summed up to represent the  
724 Alaskan SOC stock. We also used the observed mean C content of 46.8% in peat mass and bulk  
725 density of  $166 \pm 76 \text{ kg m}^{-3}$  in Alaska (Loisel et al., 2014) to estimate peat depth distribution from  
726 the simulated peat SOC density ( $\text{kg C m}^{-2}$ ).

727 Third, we conducted a series of extra simulations to further examine how uncertain  
728 climates and vegetation distribution affect our results. We used the original forcing data as the  
729 standard scenario and the warmer (monthly temperature  $+5^\circ\text{C}$ ) and cooler ( $-5^\circ\text{C}$ ) as other two

730 scenarios while keeping the rest forcing data unchanged. Similarly, we used the original forcing  
731 data as the standard scenario and the wetter (monthly precipitation +10 mm) and drier (-10  
732 mm) to test the effect from precipitation. To further study if vegetation distribution has stronger  
733 effects on SOC accumulation than climate in Alaska, we simply replaced SBP with SP and  
734 replaced the upland forests with tundra at the beginning of 15 ka. We then conducted the  
735 simulation under “warmer” and “wetter” conditions simultaneously as described before while  
736 keeping the vegetation distribution unchanged.

737

Formatted: Indent: First line: 0"

### 738 **3. Results**

#### 739 **3.1 Simulated Peatland Carbon Accumulation Rates at Site Level**

740 Our paleo simulation showed a large peak of peat C accumulation rates at 11.9 ka during  
741 the HTM (Figure 4). The simulated “true” and “apparent” rates captured this primary feature in  
742 peat core data at almost all sites (Jones and Yu, 2010). The simulated magnitude of this peak was  
743 similar to observations at No Name Creek and Horse Trail Fen, but overestimated at Kenai  
744 Gasfield and Swanson Fen at 10.9 ka (late HTM). The secondary peak of C accumulation rates  
745 appeared at 6.5 ka in the mid Holocene. The simulation successfully estimated both peaks at  
746 Swanson Fen, No Name Creek, and Kenai Gasfield, but with overestimated magnitude at  
747 Swanson Fen. The comparison between simulation and observation using averages in 500-year  
748 bins revealed a high correlation ( $R^2 = 0.90, 0.88, \text{ and } 0.39$ ), especially at No Name Creek and  
749 Horse Trail Fen. The simulated SOC accumulation rates corresponded well to the synthesis  
750 curves at four sites (Figure 4b).

#### 751 **3.2 Vegetation Carbon Storage**

752 ——— Model simulations showed an overall low mean annual vegetation C storage before the  
753 HTM (15–11 ka) (Figure 5a), paralleled to the relatively low annual NPP (Figure 5b). The  
754 *Sphagnum* dominated peatland represented the lowest vegetation C storage ( $2.5 \text{ kg C m}^{-2}$ ),  
755 much lower than the *Sphagnum* black spruce peatland ( $1 \text{ kg C m}^{-2}$ ). Upland vegetation showed a  
756 generally higher C storage, with the highest amount of C stored in boreal evergreen needleleaf  
757 forests ( $2 \text{ kg C m}^{-2}$ ). The upland forests also showed a higher rate of annual NPP ( $0.31\text{--}0.35$   
758  $\text{kg C m}^{-2}\text{yr}^{-1}$ ). C storage of alpine and moist tundra was higher than peatlands, while the annual  
759 NPP were lower ( $0.08\text{--}0.1 \text{ kg C m}^{-2}\text{yr}^{-1}$ ). Higher NPP were shown in almost all vegetation  
760 types during the early Holocene. There were no significant changes of vegetation C storage in  
761 peatlands and tundra compared with boreal forests. All vegetation showed a higher NPP and  
762 vegetation C during the late HTM. Mean annual vegetation C exceeded  $0.5 \text{ g C m}^{-2}$  and  $1.3$   
763  $\text{g C m}^{-2}$  for *Sphagnum* and black spruce peatlands. Evergreen forest stored over  $4.7 \text{ kg C m}^{-2}$ .  
764 During the mid Holocene, almost all vegetation types represented a decrease in both NPP and  
765 vegetation C. The plant productivity along with the vegetation C began to slightly increase at  
766 late Holocene and became stable, possibly resulted from the rising temperature.

767         Approximately  $2 \text{ Pg C}$  was stored in both upland and peatland vegetation in Alaska  
768 before the HTM (Figure 6). Upland moist tundra accounted for the most amount of C due to its  
769 large area. At the early HTM, evergreen needleleaf forest area became the largest, and about  $1.9$   
770  $\text{Pg C}$  was stored in boreal forests. More C was stored in black spruce peatland also because of  
771 the forest formation. Boreal forest accounted for  $3.5 \text{ Pg C}$  at the late HTM. Decrease of  
772 vegetation C occurred at mid Holocene. The simulation through the Holocene to present  
773 indicated that the lowest amount C was stored in vegetation before the HTM, while vegetation  
774 assimilated the largest amount of C during the late Holocene. We estimated a total  $2.9 \text{ Pg C}$

775 stored in modern Alaskan vegetation, with 0.4 Pg in peatlands and 2.5 Pg in non-peatlands. The  
776 uncertainties of the parameters during the model calibration (Table 4) resulted in a range of 0.3–  
777 0.6 Pg C and 2.2–3.1 Pg C in peatlands and non-peatlands, respectively.

778

779

### 780 **3.3 Soil Carbon Stocks**

781 — Carbon storage in Alaskan non-peatland soils varied spatially (Figure 7). Generally,  
782 deciduous broadleaf forests had a higher SOC ( $8\text{--}13\text{ kg C m}^{-2}$ ) than evergreen needleleaf forests  
783 ( $3\text{--}8\text{ kg C m}^{-2}$ ), while moist tundra had the highest SOC ( $12\text{--}25\text{ kg C m}^{-2}$ ). The SOC showed an  
784 overall increase in both boreal forests and moist tundra during the early HTM (11–10 ka)  
785 (Figures 7a, b). With the continued expansion of the boreal forests during the late HTM (10–9  
786 ka) (Figure 4c), the spots of low SOC concentration were widely spread (Figure 7c). During the  
787 mid- (9–5 ka) and late-Holocene (5 ka–1900 AD), although the wet tundra took back the most  
788 area, the SOC decreased (Figure 7d) presumably due to the cooler and drier conditions, which  
789 was consistent with the decline in mean annual NPP and vegetation C (Figure 5). An increase  
790 occurred again in the last century with mean SOC comparable to the late HTM (Figure 7f). An  
791 average of 3.1 Pg C was simulated before the HTM (Figure 8). The SOC increased sharply  
792 during the early HTM (to 11.5 Pg C) across Alaska and slightly decreased to 9 Pg C at the end of  
793 HTM. There was little variation during the mid- and late-Holocene (10.7 Pg C) and the amount  
794 increased to 11.2 Pg C at the end of the 20<sup>th</sup>-century. Due to model parameterization (Table 4),  
795 the regional soil C estimates ranged from 9 to 15 Pg C at present.

796 ——— The peatland SOC showed a different pattern compared to upland soils. Peatlands started  
797 to accumulate C at 15 ka mainly in northwestern, southeastern, and south coastal regions of  
798 Alaska (Figure 9a). Much less C ( $<10 \text{ kg C m}^{-2}$ ) was accumulated in the southeastern coast in  
799 comparison to other coastal parts ( $>15 \text{ kg C m}^{-2}$ ). Initially, only *Sphagnum* open peatland (SP)  
800 existed, with no *Sphagnum* black spruce forested peatland (SBP). At the beginning of the HTM,  
801 there was a peatland area of  $\sim 4.5 \times 10^5 \text{ km}^2$  (Figure 10). During the early HTM, the SP formed  
802 in the north coast and the SBP rapidly expanded in south coast and east central regions,  
803 becoming the dominant peatland type in Alaska (Figure 9b). Meanwhile the peatlands area  
804 increased to  $\sim 13 \times 10^5 \text{ km}^2$  (Figure 10). The SBP continued to expand to the central Alaska  
805 during the late HTM (Figure 9c). Although peatlands continued to form towards west in the mid-  
806 Holocene (Figures 9d, 10), some areas that were dominated by SBP in interior Alaska stopped  
807 accumulating SOC. By the end of the mid Holocene, almost all the peatlands have formed  
808 (Figure 10) and some grids showed negative accumulation in the late Holocene (Figure 9e).  
809 However, as the global warming began in the 20<sup>th</sup> century, SOC accumulation increased rapidly  
810 again (Figure 9f).

811 The mean annual SOC accumulation rates increased from  $0.9$  to  $28.7 \text{ g C m}^{-2} \text{ yr}^{-1}$  and  
812 from  $0$  to  $57.1 \text{ g C m}^{-2} \text{ yr}^{-1}$  in the early HTM (11–10 ka) for SP and SBP, respectively, with an  
813 area weighted rate of  $41.6 \text{ g C m}^{-2} \text{ yr}^{-1}$  (Figure 11). The accumulation rate of the SP increased to  
814  $48.6 \text{ g C m}^{-2} \text{ yr}^{-1}$  while the rate of SBP slightly decreased to  $56.7 \text{ g C m}^{-2} \text{ yr}^{-1}$  with an overall  
815 rate  $54.7 \text{ g C m}^{-2} \text{ yr}^{-1}$  in the late HTM (10–9 ka) (Figure 11), followed by a drop to  $22.7$  and  $13.1$   
816  $\text{g C m}^{-2} \text{ yr}^{-1}$  in the mid Holocene (Figure 11). Late Holocene rates ranged from  $9.8$  to  $8.0$   
817  $\text{g C m}^{-2} \text{ yr}^{-1}$  for SP and SBP. The rates of SP and SBP reached  $42.5$  and  $33.2 \text{ g C m}^{-2} \text{ yr}^{-1}$   
818 respectively in the 20<sup>th</sup> century.



819 ——— The change in total SOC stock corresponded well to the mean annual accumulation rates  
820 during the last 15,000 years (Figures 8, 11). A total of 37.4 Pg C was estimated to accumulate in  
821 Alaskan peatlands, with 23.9 Pg C in SP and 13.5 Pg C in SBP, from 15 ka to 2000 AD. The  
822 total peat C stock had an uncertainty range of 27–48 Pg C depending on model parameters (Table  
823 4). The peatlands in the northern and southern coastal regions showed the highest SOC densities  
824 ( $>150 \text{ kg C m}^{-2}$ ), while some central regions had the lowest ( $<20 \text{ kg C m}^{-2}$ ) (Figure 12a). For  
825 newly formed peatlands in west central part and west coast,  $<100 \text{ kg C m}^{-2}$  SOC was  
826 accumulated. The non-peatland SOC distribution was mainly decided by the vegetation types,  
827 with high densities ( $>15 \text{ kg C m}^{-2}$ ) in west and north coast where tundra dominated and low  
828 densities ( $<10 \text{ kg C m}^{-2}$ ) in central and east parts where boreal forests dominated (Figure 12b).

829 We used the observed mean C content of 46.8% in peat mass and bulk density of  $166 \pm 76$   
830  $\text{kg m}^{-2}$  in Alaska (Loisel et al., 2014) to estimate peat depth at each peat grid cell from the  
831 simulated peat SOC density ( $\text{kg C m}^{-2}$ ). The spatial pattern of peat depth is identical to the SOC  
832 distribution, with most regions having peat depths of  $<2.5 \text{ m}$  (Figure 12c). Based on the modern  
833 land area in each TEM grid cell and the inundation map, we estimated a weighted average depth  
834 of 1.9 m (ranging from 1.1 to 2.7 m, considering uncertainty in bulk density values) for Alaska  
835 peatlands. We also combined the SOC in both peatlands and non-peatlands results together to  
836 generate the total SOC distribution (Figure 12d). Soils at northern coast had the highest densities,  
837 many grids had  $\text{SOC} > 40 \text{ kg C m}^{-2}$ . Southwestern coast and eastern central Alaska also showed  
838 a high total SOC accumulation ( $>40 \text{ kg C m}^{-2}$ ). Central, eastern parts and west coast had the  
839 lowest SOC densities ( $<20 \text{ kg C m}^{-2}$ ).

### 840 **3.4 Sensitivity Test**

841 We found that NPP and decomposition rates changed simultaneously, but NPP had the  
842 dominant effect as the net SOC accumulation rate of Alaska increased and decreased under  
843 warmer and cooler conditions, respectively (Figures 13a, c, e). The net SOC accumulation rate  
844 increased as the condition became wetter and vice versa (Figures 13b, d, f). We also found an  
845 increase of SOC from 11.2 to 14.6 Pg C for upland mineral soils and 37.5 to 71 Pg C for  
846 peatlands after replacing the SP to SBP and upland forest systems with tundra. Meanwhile, under  
847 “warmer” and “wetter” conditions, the upland and peatland SOC increased by 13.8 Pg C and 35  
848 Pg C, respectively.

#### 849 **4. Discussion**

##### 850 **4.1 Effects of Climate on Ecosystem Carbon Accumulation**

851 — The simulated climate by ECBilt CLIO model showed that among the six time periods, the  
852 coolest temperature appeared at 15–11 ka, followed by the late Holocene (5 ka–1900 AD). Those  
853 two periods were also generally dry (Figure 3f). The former represented colder and drier climate  
854 before the onset of the Holocene and the HTM (Barber and Finney, 2000; Edwards et al., 2001).  
855 The latter represented post-HTM neoglacial cooling, which caused permafrost aggradation  
856 across northern high latitudes (Oksanen et al., 2001; Zoltai, 1995).

857 The simulated NPP, vegetation C density and storage were highest during the HTM  
858 (Figures 5, 6). The highest C accumulation rates in both peatlands and non-peatlands occurred at  
859 the time (Figures 7–11). ECBilt CLIO simulated an increase of temperature in the growing  
860 season (Figure 3c), also leading to a stronger seasonality of temperature during the HTM  
861 (Kaufman et al., 2004, 2016), caused by the maximum summer insolation (Berger and Loutre,  
862 1991; Renssen et al., 2009). The highest mean annual and highest summer precipitations were

863 also simulated during the 10–9 ka period. The highest vegetation C uptake and SOC  
864 accumulation rates coincided with the warmest summer and the wetter than before conditions,  
865 suggesting a strong link between those climate variables and C dynamics in Alaska. Enhanced  
866 climate seasonality characterized by warmer summer, enhanced summer precipitation and  
867 possibly earlier snow melt during the HTM increased NPP, as shown in our sensitivity test.  
868 Annual NPP increased by 40 and 20  $\text{g C m}^{-2} \text{yr}^{-1}$  under the warmer and wetter scenarios,  
869 respectively (Figures 13a, b), indicating summer temperature and precipitation were the primary  
870 controls over NPP. Warmer condition could positively affect the SOC decomposition (Nobrega  
871 et al., 2007). Furthermore, hydrological effect can also be significant as higher precipitation  
872 could raise the water table position, allowing less space for aerobic respiration. As shown in the  
873 sensitivity test, warmer and wetter could lead to an increase of decomposition up to 35 and 15  
874  $\text{g C m}^{-2} \text{yr}^{-1}$ , respectively (Figures 13c, d). Such climatic effects on ecosystem productivity  
875 were consistent with modern studies (Tucker et al., 2001; Kimball et al., 2004; Linderholm,  
876 2006). Our results did not show a decrease in total heterotrophic respiration throughout Alaska  
877 from the higher precipitation, presumably due to a much larger area of upland soils ( $1.3 \times 10^6$   
878  $\text{km}^2$ ) than peatland soils ( $0.26 \times 10^6 \text{ km}^2$ ), as higher precipitation would cause higher aerobic  
879 respiration in the unsaturated zone of upland soils. The relatively low vegetation NPP and C  
880 density, along with the low total vegetation and soil C stocks during 15–11 ka period and late-  
881 Holocene were consistent with the unfavorable cool and dry climate conditions (Figures 5, 6, 8,  
882 11). Our previous simulations at four peatland sites in Alaska (Wang et al., 2016) suggested that  
883 temperature had the most significant effect on peat accumulation rate, followed by the  
884 seasonality of net solar radiation and temperature. Precipitation and the interactive effect from  
885 temperature and precipitation had some certain effects ( $p < 0.05$ ). The period from 15 to 11 ka

886 experienced lower snowfall than the HTM. The combination of decreased snowfall and lower  
887 temperature could result in deeper frost depth due to the decreased insulative effects of the  
888 snowpack, and therefore shortening the period for active photosynthetic C uptake, leading to an  
889 overall low productivity (McGuire et al., 2000; Stieglitz et al., 2003). The positive effect of  
890 temperature on SOC accumulation as shown in this study, may help explain the coincidence  
891 between low SOC accumulation rates across the northern peatland domain and the cooler  
892 condition during the neoglacial period (Marcott et al., 2013; Vitt et al., 2000; Peteet et al., 1998;  
893 Yu et al. 2010). The stimulation of SOC accumulation from the warming and the rapid SOC  
894 accumulation rates during the 20<sup>th</sup> century in our study suggested a continue C sink will exist  
895 under the warmer and wetter climate conditions in the 21<sup>st</sup> century, as also concluded in Spahni  
896 et al. (2013).

897 The 20<sup>th</sup> century represented a temperature rise induced by global warming. It was still  
898 1.1 °C lower than the late HTM, suggesting the warmest climate during the HTM, which agreed  
899 with the previous study (Stafford et al., 2000). It was also lower than the mid-Holocene, which  
900 compared favorably with other estimates (Anderson and Brubaker, 1993; Kaufman et al., 2004).  
901 However, the annual precipitation during modern time estimated from other studies was higher  
902 than the HTM and mid-Holocene (Barber and Finney, 2000). The model output we used may  
903 overestimate the precipitation in the HTM, which could subsequently overestimate the water-  
904 table position and thus, the annual C accumulation rates. As studied, regional precipitation varies  
905 largely depending on the local topography (Stafford et al., 2000), thus the estimates with large-  
906 scale climate models have a large uncertainty. Great heterogeneity is produced from using large  
907 climatic controls (e.g., insolation and sea-ice extent), which casts limits for accurately simulating

908 the location and topographic specific climate data, especially precipitation (Whitlock and  
909 Bartlein, 1993; Mock and Bartlein, 1995).

#### 910 ~~4.2 Effects of Vegetation Distribution on Ecosystem Carbon Accumulation~~

911 ~~Different vegetation distributions during various periods led to clear step changes,  
912 suggesting vegetation composition is likely to be the primary control on C dynamics. Similarly,  
913 SBP areas stored lower C than SP in overall at the spatial scale during each time period (Figure  
914 9). Under cooler and drier climates, forested peatlands generally stopped accumulating SOC  
915 during the mid and late Holocene with some areas accompanied by a negative accumulation rate  
916 (Figures 9d,e), suggesting that such type of peatland could be more vulnerable to climate change  
917 due to its low C storage.~~

918 ~~As key parameters controlling C dynamics in the model (e.g., maximum rate of  
919 photosynthesis, litter fall C) are ecosystem type specific, vegetation distribution change may  
920 have a dominant effect on simulated regional plant productivity and C storage. Our sensitivity  
921 test indicated that by replacing all vegetation types with forest systems, there was a total increase  
922 of 36.9 Pg in upland and peatland soils. There was also an increase of 48.8 Pg C under warmer  
923 and wetter conditions. These tests indicated that both climate and vegetation distribution have  
924 significant effects on C storage.~~

925 ~~However, the high correlation between climate and ecosystem C dynamics as discussed  
926 above indicated that climate was probably the fundamental driver for vegetation composition  
927 changes over time. The vegetation changes as reconstructed from fossil pollen data during  
928 different time periods followed the general climate history during the last 15,000 years (He et al.,  
929 2014). Upland alpine and moist tundra stored the largest amounts of C due to their large areas~~

930 among all vegetation types, as forests areas were limited before the HTM (Figure 6). On the  
931 basis of the observed relationship between the distributions of basal ages of peat samples and  
932 vegetation types (Table 2, Figure 2), alpine and moist tundra were favorable for peatlands  
933 initiation under a cooler climate. No forested peatlands formed before the HTM. Under the warm  
934 condition in the HTM, boreal evergreen needleleaf and deciduous broadleaf forests expanded  
935 (Figures 2b, c) as indicated by other studies (Bartlein et al., 2011; Edwards et al., 2005; Williams  
936 et al., 2001). Meanwhile, large areas were taken up by forested peatlands, characterized by the  
937 sharp increase of SOC storage in such ecosystems. The cooler temperature during the mid-  
938 Holocene limited the productivity of tree plants, leading to the retreat of trees. This is broadly  
939 consistent with other studies (Prentice et al., 1996; Edwards et al., 2000; Williams et al., 2001;  
940 Bigelow et al., 2003). Large proportion of forested peatlands thus changed back into *Sphagnum*  
941 spp. peatlands. The retreat of treeline on the Seward Peninsula in the cooler mid-Holocene likely  
942 reflects much shorter and cooler growing seasons, influenced by an expansion of sea ice in the  
943 Bering Sea (Crockford and Frederick, 2007) and the onset of the cooler Neoglacial climate.  
944 Forested peatlands ceased accumulating SOC in central Alaska with an overall low accumulation  
945 rates through the whole mid- to late Holocene (Figures 8, 9, 11).

#### 946 **4.3 Comparison between Simulated Carbon Dynamics and Other Estimates**

947 A large variation of “true” peat C accumulation rates was simulated on the Kenai  
948 Peninsula (Figure 4a), ranging from -4 (that is, peat C loss) to  $50 \text{ C m}^{-2} \text{ yr}^{-1}$ . We simulated an  
949 average of peat SOC “apparent” accumulation rate of  $11.4 \text{ g C m}^{-2} \text{ yr}^{-1}$  from 15 to 5 ka (Figure  
950 4b), which was slightly higher than the observed average rate from four sites ( $10.45$   
951  $\text{ g C m}^{-2} \text{ yr}^{-1}$ ). The simulated rate during the HTM was  $26.5 \text{ g C m}^{-2} \text{ yr}^{-1}$ , up to five times  
952 higher than the rest of the Holocene ( $5.04 \text{ g C m}^{-2} \text{ yr}^{-1}$ ). The simulation results corresponded to

953 the observations, in which an average rate of  $20 \text{ g C m}^{-2} \text{ yr}^{-1}$  from 11.5 to 8.6 ka was observed,  
954 four times higher than  $5 \text{ g C m}^{-2} \text{ yr}^{-1}$  over the rest of the Holocene.

955 We estimated an average peat SOC “apparent” accumulation rate of  $13 \text{ g C m}^{-2} \text{ yr}^{-1}$  ( $2.3$   
956  $\text{Tg C yr}^{-1}$  for the entire Alaska) from 15 ka to 2000 AD, lower than the value of  $18.6$   
957  $\text{g C m}^{-2} \text{ yr}^{-1}$  as estimated from peat cores for northern peatlands (Yu et al., 2010), and slightly  
958 higher than the observed rate of  $13.2 \text{ g C m}^{-2} \text{ yr}^{-1}$  from four peatlands in Alaska (Jones and Yu,  
959 2010). A simulated peak occurred during the HTM with the rate  $29.1 \text{ g C m}^{-2} \text{ yr}^{-1}$  ( $5.1 \text{ Tg C}$   
960  $\text{yr}^{-1}$ ), which was slightly higher than the observed  $25 \text{ g C m}^{-2} \text{ yr}^{-1}$  for northern peatlands and  
961  $20 \text{ g C m}^{-2} \text{ yr}^{-1}$  for Alaska (Yu et al., 2010). It was almost four times higher than the rate  $6.9$   
962  $\text{g C m}^{-2} \text{ yr}^{-1}$  ( $1.4 \text{ Tg C yr}^{-1}$ ) over the rest of the Holocene, which corresponded to the peat core-  
963 based observations of  $5 \text{ g C m}^{-2} \text{ yr}^{-1}$ . The mid- and late Holocene showed much slower C  
964 accumulation at a rate approximately five folds lower than during the HTM. This corresponded  
965 to the observation of a six-fold decrease in the rate of new peatland formation after 8.6 ka (Jones  
966 and Yu 2010). The C accumulation rates increased abruptly to  $39.2 \text{ g C m}^{-2} \text{ yr}^{-1}$  during the last  
967 century, within the field-measured average apparent rate range of  $20\text{--}50 \text{ g C m}^{-2} \text{ yr}^{-1}$  over the  
968 last 2000 years (Yu et al., 2010).

969 The SOC stock of northern peatlands has been estimated in many studies, ranging from  
970 210 to 621 Pg (Oechel 1989; Gorham 1991; Armentano and Menges, 1986; Turunen et al., 2002;  
971 Yu et al., 2010; see Yu 2012 for a review). Assuming Alaskan peatlands were representative of  
972 northern peatlands and using the area of Alaskan peatlands ( $0.45 \times 10^6 \text{ km}^2$ ; Kivinen and  
973 Pakarinen, 1981) divided by the total area of northern peatlands ( $\sim 4 \times 10^6 \text{ km}^2$ ; Maltby and  
974 Immirzi 1993), we estimated a SOC stock of 23.6–69.9 Pg C for Alaskan peatlands. Our model

975 estimated 27–48 Pg C had been accumulated from 15 ka to 2000 AD. The uncertainty may be  
976 resulted from peat basal age distributions and the peatland area, as we used modern inundation  
977 data to estimate an area of  $0.26 \times 10^6 \text{ km}^2$ . By incorporating the observed basal age distribution,  
978 we estimated that approximately 68% of Alaskan peatlands had formed by the end of the HTM,  
979 similar to the estimation from observed basal peat ages that 75% peatlands have formed by 8.6  
980 ka (Jones and Yu 2010).

981 The northern circumpolar soils were estimated to cover approximately  $18.78 \times 10^6 \text{ km}^2$   
982 (Tarnocai et al., 2009). The non-peatland soil C stock was estimated to be in the range of 150–  
983 191 Pg C for boreal forests (Apps et al., 1993; Jobbagy and Jackson, 2000), and 60–144 Pg C for  
984 tundra (Apps et al., 1993; Gilmanov and Oechel, 1995; Oechel et al., 1993) in the 0–100 cm  
985 depth. Using the difference between Alaskan total land area ( $1.69 \times 10^6 \text{ km}^2$ ) and peatland area  
986 ( $0.45 \times 10^6 \text{ km}^2$ ), we estimated that the non-peatland area in Alaska was  $1.24 \times 10^6 \text{ km}^2$ .  
987 Therefore, Alaska non-peatland area contained 17–27 Pg C by using the ratio of Alaskan non-  
988 peatland over northern non-peatland. In comparison, our estimate of 9–15 Pg C within 1 meter  
989 depth suggested that our model might have underestimated the C stock for non-peatland soils.  
990 Meanwhile, our estimated 2.5–3.7 Pg C stored in the Alaskan vegetation was lower than the  
991 previous estimate of 5 Pg (Balshi et al., 2007; McGuire et al., 2009). The underestimation could  
992 be resulted from the uncertainties in both peatland area fraction within each grid and the model  
993 parameterization.

994 The simulated modern SOC distribution (Figure 12c) was largely consistent with the  
995 study of Hugelius et al. (2014) (see Figure 3 in the paper). The model captured the high peat  
996 SOC density areas on northern and southwestern coasts of Alaska, where observational data  
997 showed some locations with  $\text{SOC} > 75 \text{ kg C m}^{-2}$ . This corresponded to our model simulation that



998 many grids had the SOC  $>75 \text{ kg C m}^{-2}$  in those areas. The observed overall average SOC  
999 density of  $>40 \text{ kg C m}^{-2}$  was also consistent with our simulation. Eastern part and west coast had  
1000 the lowest SOC densities, corresponding to the model result that most grids in those areas had  
1001 SOC values between 20 and  $40 \text{ kg C m}^{-2}$ . Our estimated average peat depth of 1.9 m ranging  
1002 from 1.1 to 2.7 m from simulated peat SOC density was similar to the observed mean depth of  
1003 2.29 m for Alaskan peatlands (Gorham et al., 1991, 2012). Our estimates (Figure 12d) showed a  
1004 high correlation with the 64 observed peat samples (Figure 14) ( $R^2 = 0.45$ ). The large intercept  
1005 of the regression line (101 cm) suggested that the model may not perform well in estimating the  
1006 grids with low peat depths ( $<50 \text{ cm}$ ).

### 1007 **3. Results and Discussion**

#### 1008 **3.1 Simulated Peatland Carbon Accumulation Rates at Site Level**

1009 Our paleo simulations showed a large peak of peat C accumulation rates at 11-9 ka  
1010 during the HTM (Figure 4). The simulated “true” and “apparent” rates captured this primary  
1011 feature in peat-core data at almost all sites (Jones and Yu, 2010; See Wang et al. (2016) Table 3  
1012 for sites details). We simulated an average of peat SOC “apparent” accumulation rate of  $11.4$   
1013  $\text{g C m}^{-2} \text{ yr}^{-1}$  from 15 to 5 ka, which was slightly higher than the observations at four sites  
1014 ( $10.45 \text{ g C m}^{-2} \text{ yr}^{-1}$ ). The simulated rate during the HTM was  $26.5 \text{ g C m}^{-2} \text{ yr}^{-1}$ , up to five  
1015 times higher than the rest of the Holocene ( $5.04 \text{ g C m}^{-2} \text{ yr}^{-1}$ ). This corresponded to the  
1016 observed average rate of  $20 \text{ g C m}^{-2} \text{ yr}^{-1}$  from 11.5 to 8.6 ka, which is, four times higher than  $5$   
1017  $\text{g C m}^{-2} \text{ yr}^{-1}$  over the rest of the Holocene.

1018

1019 **3.2 Vegetation Carbon**

1020 Model simulations showed an overall low vegetation C before the HTM (15-11 ka)  
1021 (Figure 5a), paralleled to the relatively low annual NPP (Figure 5b). The lowest amount of C  
1022 (~0.8 kg C m<sup>-2</sup>) was stored in *Sphagnum*-dominated peatland. *Sphagnum*-black spruce peatland  
1023 also had low vegetation C density (~1 kg C m<sup>-2</sup>). Upland vegetation showed a generally higher  
1024 C storage, among which boreal evergreen needleleaf forest ranked the first (~2 kg C m<sup>-2</sup>).  
1025 Highest NPP accompanied by highest vegetation carbon appeared during the HTM (11-9 ka)  
1026 (Figures 5a and b). Lower annual C uptake along with lower C was found during mid- and late-  
1027 Holocene (9 ka-19<sup>th</sup>), where peatland ecosystems exhibited the most obvious drops (Figures 5a  
1028 and b).

1029 In general, vegetation held about 2 Pg C before the HTM (Figure 6). Upland tundra  
1030 ecosystems accounted for the most amount of C. During the HTM, Boreal evergreen needleleaf  
1031 forest reached its highest and had an overwhelming proportion over total C. Similarly, a peak of  
1032 total vegetation C appeared at the same time, averaging around 4.3 Pg C. Large decrease  
1033 occurred at the mid-Holocene and a slight decline continued till the late-Holocene. We estimated  
1034 a total 2.9 Pg C stored in modern Alaskan vegetation, with 0.4 Pg in peatlands and 2.5 Pg in non-  
1035 peatlands. The uncertainties during the model calibration (Table 4) resulted in 0.3-0.6 Pg C and  
1036 2.2-3.1 Pg C in peatlands (see Wang et al. (2016) for model parameters) and non-peatland  
1037 vegetation (see Tang and Zhuang (2008) for uncertainty analyses for upland vegetation),  
1038 respectively. Our estimation of 2.5-3.7 Pg C stored in the Alaskan vegetation was lower than the  
1039 previous estimate of 5 Pg (Balshi et al., 2007; McGuire et al., 2009), presumably due to the prior  
1040 ranges of model parameters used from Tang and Zhuang (2008). Our overestimation of peatland  
1041 area may also lead to a reduction of Alaskan non-peatland area.

1042

### 1043 **3.3 Soil Carbon**

1044 Carbon storage in Alaskan non-peatland soils varied spatially (Figure 7). Moist tundra  
1045 had the highest SOC density (12-25 kg C m<sup>-2</sup>), followed by deciduous broadleaf forest (8-13  
1046 kg C m<sup>-2</sup>) and evergreen needleleaf forest (3-8 kg C m<sup>-2</sup>) through all time slices between 15 ka  
1047 and 2000 AD. Dramatic changes of vegetation types have occurred in Alaska during different  
1048 periods (Figure 2). Before the HTM (15-11 ka), the terrestrial ecosystem was dominated by  
1049 tundra. Northwestern coast and eastern interior was covered by moist tundra. Southwestern  
1050 Alaska and the interior south of the Brooks Range were dominated by alpine tundra (Figure 2a).  
1051 The basal ages of peat samples from Gorham et al. (2012) suggested that peatlands were likely to  
1052 form from the (alpine) tundra ecosystems, although patches of boreal deciduous broadleaf forest  
1053 and boreal evergreen needleleaf and mixed forest appeared at the north of the Alaska Range.  
1054 Initially, only *Sphagnum* open peatland (SP) existed, with less C (<10 kg C m<sup>-2</sup>) sequestered in  
1055 the southeastern Brooks Range in comparison with southwestern and northwestern coastal parts  
1056 (>15 kg C m<sup>-2</sup>) (Figure 8a). Approximately 4.5 × 10<sup>5</sup> km<sup>2</sup> area was covered by peatlands at the  
1057 beginning of the HTM (~11 ka) (Figure 9). During the HTM (11-9 ka), boreal deciduous  
1058 broadleaf and boreal evergreen needleleaf and mixed forests expanded (Figures 8b and c).  
1059 Coastal tundra (moist wet tundra) covered north of the Brooks Range between 11 and 10 ka,  
1060 where SP continued its expansion (Figure 8b). *Sphagnum*-black spruce forested peatland began  
1061 forming in southwestern coast and eastern interior regions, with a rapid increase of total peatland  
1062 area to about 13 × 10<sup>5</sup> km<sup>2</sup> (Figure 9). At 10-9 ka, boreal deciduous forest expanded to north of  
1063 the Brooks Range, making forest the dominant biome in Alaska (Figure 2c). Prevailing forest  
1064 ecosystems indicated a large expansion of peatland, with SBP covering the interior Alaska

1065 (Figure 8c). During the mid-Holocene (9-5 ka), the terrestrial landscape generally resembled  
1066 present-day ecosystems (Bigelow et al., 2003). Boreal evergreen needleleaf and mixed forest  
1067 prevailed in southern and interior Alaska with tundra returned to north of the Brooks Range and  
1068 western Alaska (Figures 2d and e). Although SP kept forming towards west, some areas  
1069 dominated by SBP in interior Alaska ceased accumulating C (Figure 8d). At 5k-19<sup>th</sup>, almost all  
1070 the peatlands have formed, with some interior regions exhibiting a C loss (Figure 8e). C  
1071 accumulation increased again in the last century, averaging about 20 kg C m<sup>-2</sup> kyr<sup>-1</sup> (Figure 8f).  
1072 We found that the distribution of SOC densities of both upland and peatland varied greatly  
1073 depending on the vegetation distribution within each time slice, indicating that vegetation  
1074 composition might be a major factor controlling regional C dynamics.

1075 An average peat SOC “apparent” accumulation rate of 13 g C m<sup>-2</sup>yr<sup>-1</sup> (2.3 Tg C yr<sup>-1</sup>  
1076 for the entire Alaska) was estimated from 15 ka to 2000 AD (Figure 10), lower than 18.6  
1077 g C m<sup>-2</sup>yr<sup>-1</sup> as estimated from peat cores for northern peatlands (Yu et al., 2010), and slightly  
1078 higher than the observed rate of 13.2 g C m<sup>-2</sup>yr<sup>-1</sup> from four peatlands in Alaska (Jones and Yu,  
1079 2010). A simulated peak occurred during the HTM with the rate 29.1 g C m<sup>-2</sup>yr<sup>-1</sup> (5.1 Tg C  
1080 yr<sup>-1</sup>), which was slightly higher than the observed 25 g C m<sup>-2</sup>yr<sup>-1</sup> for northern peatlands and  
1081 ~20 g C m<sup>-2</sup>yr<sup>-1</sup> for Alaska (Yu et al., 2010). It was almost four times higher than the rate 6.9  
1082 g C m<sup>-2</sup>yr<sup>-1</sup> (1.4 Tg C yr<sup>-1</sup>) over the rest of the Holocene, which corresponded to the peat core-  
1083 based observations of ~5 g C m<sup>-2</sup>yr<sup>-1</sup>. The mid- and late Holocene showed much slower C  
1084 accumulation at a rate approximately five folds lower than during the HTM. This corresponded  
1085 to the observation of a six-fold decrease in the rate of new peatland formation after 8.6 ka (Jones  
1086 and Yu 2010). The C accumulation rates increased abruptly to 39.2 g C m<sup>-2</sup>yr<sup>-1</sup> during the last

1087 century, within the field-measured average apparent rate range of 20-50 g C m<sup>-2</sup>yr<sup>-1</sup> over the  
1088 last 2000 years (Yu et al., 2010).

1089 The SOC stock of northern peatlands has been estimated in many studies, ranging from  
1090 210 to 621 Pg (Oechel 1989; Gorham 1991; Armentano and Menges, 1986; Turunen et al., 2002;  
1091 Yu et al., 2010; see Yu 2012 for a review). Assuming Alaskan peatlands were representative of  
1092 northern peatlands and using the area of Alaskan peatlands (0.45 × 10<sup>6</sup> km<sup>2</sup>; Kivinen and  
1093 Pakarinen, 1981) divided by the total area of northern peatlands (~4 × 10<sup>6</sup> km<sup>2</sup>; Maltby and  
1094 Immirzi 1993), we estimated a SOC stock of 23.6-69.9 Pg C for Alaskan peatlands. Our model  
1095 estimated 27-48 Pg C (23.9 Pg C in SP and 13.5 Pg C in SBP) had been accumulated from 15 ka  
1096 to 2000 AD (Figure 11), due to uncertain parameters (Table 4, see Wang et al. (2016) for model  
1097 parameters). The uncertainty can also be resulted from peat basal age distributions and the  
1098 estimation of total peatland area using modern inundation data as discussed above. By  
1099 incorporating the observed basal age distribution to determine the expansion of peatland through  
1100 time, we estimated that approximately 68% of Alaskan peatlands had formed by the end of the  
1101 HTM, similar to the estimation from observed basal peat ages that 75% peatlands have formed  
1102 by 8.6 ka (Jones and Yu 2010).

1103 The northern circumpolar soils were estimated to cover approximately 18.78 × 10<sup>6</sup> km<sup>2</sup>  
1104 (Tarnocai et al., 2009). The non-peatland soil C stock was estimated to be in the range of 150-  
1105 191 Pg C for boreal forests (Apps et al., 1993; Jobbagy and Jackson, 2000), and 60-144 Pg C for  
1106 tundra in the 0-100 cm depth (Apps et al., 1993; Gilmanov and Oechel, 1995; Oechel et al.,  
1107 1993). 1.24 × 10<sup>6</sup> km<sup>2</sup> non-peatland area was estimated from the total land area of Alaska  
1108 (1.69 × 10<sup>6</sup> km<sup>2</sup>). Therefore, Alaska non-peatland soil contained 17-27 Pg C by using the ratio

1109 of Alaskan over northern non-peatland. In comparison, we modeled 9-15 Pg C (within 1-meter  
1110 depth), depending on the prior ranges of model parameters from Tang and Zhuang (2008).

1111 The simulated modern SOC distribution (Figure 12c) was largely consistent with the  
1112 study of Hugelius et al. (2014) (see Figure 3 in the paper). The model captured the SOC density  
1113 on northern and southwestern coasts of Alaska with most grids  $>40 \text{ kg C m}^{-2}$  on average. Those  
1114 regions also showed high SOC density ( $>75 \text{ kg C m}^{-2}$ ), which was also exhibited in our result.  
1115 East part and west coast had the lowest SOC densities, corresponding to the simulation result that  
1116 most grids had SOC values between 20 and 40  $\text{kg C m}^{-2}$ . We estimated an average peat depth of  
1117 1.9 $\pm$ 0.8 m considering the uncertainties within dry bulk densities. It was similar to the observed  
1118 mean depth of 2.29 m for Alaskan peatlands (Gorham et al., 1991, 2012). Our estimates (Figure  
1119 12d) showed a relatively high correlation with the 64 observed peat samples, especially with  
1120 higher depths (Figure 13) ( $R^2 = 0.45$ ). The large intercept of the regression line (101 cm)  
1121 suggested that the model might have not performed well in estimating the grids with low peat  
1122 depths ( $<50$  cm). The peat characteristics (e.g., bulk density) from location to location may differ  
1123 largely, even if within the same small region. Thus, it is difficult to capture the observed  
1124 variations of peat depths as we used the averaged bulk density of whole Alaska.

### 1125 **3.4 Effects of Climate on Ecosystem Carbon Accumulation**

1126 The simulated climate by ECBilt-CLIO model showed that among the six time periods, the  
1127 coolest temperature appeared at 15-11 ka, followed by the mid- and late- Holocene (5 ka-1900  
1128 AD). Those two periods were also generally dry (Figure 3f). The former represented colder and  
1129 drier climate before the onset of the Holocene and the HTM (Barber and Finney, 2000; Edwards

1130 et al., 2001). The latter represented post-HTM neoglacial cooling, which has caused permafrost  
1131 aggradation across northern high latitudes (Oksanen et al., 2001; Zoltai, 1995).

1132 The simulated NPP, vegetation C density and storage were highest during the HTM.  
1133 Annual C accumulation rates also reached the highest (Figures 5-11). The variation of NPP has a  
1134 similar pattern of the climate (see Figure 3 for climate variables), where higher NPP, along with  
1135 higher vegetation C coincided with warmer temperatures and enhanced precipitation during the  
1136 HTM, compared to other time periods. ECBilt-CLIO simulated a warmest summer and a  
1137 prolonged growing season, leading to a stronger seasonality of temperature during the HTM  
1138 (Kaufman et al., 2004, 2016), in line with the orbitally-induced maximum summer insolation  
1139 (Berger and Loutre, 1991; Renssen et al., 2009). The coincidence between the highest vegetation  
1140 C uptake and SOC accumulation rates and the warmest summer and the wetter-than-before  
1141 conditions indicated a strong link between those climate variables and C dynamics in Alaska.  
1142 Enhanced climate seasonality characterized by warmer summer, enhanced summer precipitation  
1143 and possibly earlier snow melt during the HTM accelerated the photosynthesis and subsequently  
1144 increased NPP (Tucker et al., 2001; Kimball et al., 2004; Linderholm, 2006). As shown in our  
1145 sensitivity test, annual NPP was increased by 40 and 20 g C m<sup>-2</sup> yr<sup>-1</sup> under the warmer and  
1146 wetter scenarios, respectively (Figures 14a, b). Meanwhile, warmer condition could positively  
1147 affect the SOC decomposition (Nobrega et al., 2007). However, it could be offset to a certain  
1148 extent via the hydrological effect, as higher precipitation could raise the water-table position,  
1149 allowing less space for aerobic heterotrophic respiration. Our sensitivity test results indicated  
1150 that warmer and wetter conditions could lead to an increase of decomposition up to 35 and 15  
1151 g C m<sup>-2</sup> yr<sup>-1</sup>, respectively (Figures 14c, d). We did not find a decrease in total heterotrophic  
1152 respiration throughout Alaska from the higher precipitation. It was presumably due to a much

1153 larger area of upland soils ( $1.3 \times 10^6$  km<sup>2</sup>) than peatland soils ( $0.26 \times 10^6$  km<sup>2</sup>), as higher  
1154 precipitation would cause higher aerobic respiration in the unsaturated zone of upland soils, and  
1155 consequently stimulated the SOC decomposition. The relatively low NPP and vegetation C  
1156 density, along with the lower total soil C stocks were consistent with the unfavorable cool and  
1157 dry climate conditions at 15-11 ka and during the mid- and late- Holocene. Statistical analysis  
1158 indicated that temperature had the most significant effect on peat SOC accumulation rate,  
1159 followed by the seasonality of NIRR (Wang et al., 2016). The seasonality of temperature, the  
1160 interaction of temperature and precipitation, and precipitation alone also showed significance.  
1161 The strong link between climate factors and C dynamics may explain the lower SOC  
1162 accumulation during the neoglacier cooling period (Marcott et al., 2013; Vitt et al., 2000; Peteet  
1163 et al., 1998; Yu et al. 2010). The rapid peat SOC accumulation during the 20<sup>th</sup> century under  
1164 warming and wetter climate may suggest a continuous C sink in this century, as concluded in  
1165 Spahni et al. (2013). However, the rising temperature in the future may have positive effects on  
1166 heterotrophic respiration and simultaneously increase evapotranspiration and lower water table.  
1167 This could increase aerobic decomposition and thus switch the Alaskan peatland from a C sink  
1168 into a C source. Moreover, the increasing anthropogenic activities including land use will  
1169 probably increase drought and subsequently enhance the risk of fire, releasing carbon to the  
1170 atmosphere. The fate of Alaskan SOC stock and the biogeochemical cycling of the terrestrial  
1171 ecosystems under future scenarios need further investigation.

1172

### 1173 3.5 Effects of Vegetation Distribution on Ecosystem Carbon Accumulation



1174 Climate variables significantly affect C dynamics within each time slice. However,  
1175 different vegetation distributions during various periods led to clear step changes, suggesting  
1176 vegetation composition was likely to be another primary factor (Figures 6, 7, 8, and 11). As key  
1177 parameters controlling C dynamics in the model (e.g., maximum rate of photosynthesis, litter fall  
1178 C, maximum rate of monthly NPP) are ecosystem type specific, vegetation distribution changes  
1179 may drastically affect regional plant productivity and C storage. Our sensitivity test indicated  
1180 that by replacing all vegetation types with forests, there was a total increase of 36.9 Pg in upland  
1181 plus peatland soils. There was also an increase of 48.8 Pg C under warmer and wetter conditions,  
1182 suggesting that both climate and vegetation distribution may have played important roles in  
1183 carbon accumulation.

1184 The vegetation changes reconstructed from fossil pollen data during different time  
1185 periods followed the general climate history during the last 15,000 years. For instance, the  
1186 migration of dark boreal forests over snow-covered tundra during the HTM was probably  
1187 induced by the warmer and wetter climate resulted from the insolation changes (He et al., 2014).  
1188 The cooler and drier climate after the mid-Holocene limited the growth of boreal broadleaf  
1189 conifers (Prentice et al., 1992), and therefore resulted in the replacement of broadleaf forest with  
1190 needleleaf forest and tundra ecosystems. Since the parameters of our model for individual  
1191 vegetation type were static, parameterizing the model using modern site-level observations might  
1192 have introduced uncertainty to parameters, which may result in regional simulation uncertainties.  
1193 Assuming each parameter as constant (e.g. the lowest water-table boundary, see Wang et al.  
1194 (2016) for details) over time may also weaken the model's response to different climate  
1195 scenarios. Furthermore, applying static vegetation maps at millennial scales and using modern  
1196 elevation and pH data may simplify the complicated changes of landscape and terrestrial

1197 ecosystems, as vegetation can shift within hundreds of years (Ager and Brubake, 1985; see He et  
1198 al. (2014) discussion section). Relatively coarse spatial resolution ( $0.5^\circ \times 0.5^\circ$ ) in P-TEM  
1199 simulations may also introduce uncertainties. In addition, because we used the modern  
1200 inundation map to delineate the peatland and upland within each grid cell, we might have  
1201 overestimated the total peatland area since not all inundated areas are peatlands. Linking field-  
1202 estimated basal ages of peat cores to the vegetation types during each period involves large  
1203 uncertainties due to the limitation of the peat classification and insufficient peat samples. Thus,  
1204 the estimated spatially explicit basal age data shall also introduce a large uncertainty to our  
1205 regional quantification of carbon accumulation.

1206

## 1207 **5. Conclusions**

1208 We used a biogeochemistry model for both peatland and non-peatland ecosystems to  
1209 quantify the C stock and its changes over time in terrestrial ecosystems of Alaska during the last  
1210 15,000 years. The simulated peat SOC accumulation rates were compared with peat-core data  
1211 from four peatlands on the Kenai Peninsula in southern Alaska. The model well estimated the  
1212 peat SOC accumulation rates trajectory throughout the Holocene, indicating the model's  
1213 suitability for simulating peat C dynamics. Our regional simulation showed that 36-63 Pg C had  
1214 been accumulated in Alaskan land ecosystems since 15,000 years ago, including 27-48 Pg C in  
1215 peatlands and 9-15 Pg C in non-peatlands (within 1 m depth). We also estimated that 2.5-3.7 Pg  
1216 C was stored in contemporary Alaskan vegetation, with 0.3-0.6 Pg C in peatlands and 2.2-3.1 Pg  
1217 C in non-peatlands. The estimated average rate of peat C accumulation was  $2.3 \text{ Tg C yr}^{-1}$  with a  
1218 peak ( $5.1 \text{ Pg C yr}^{-1}$ ) in the Holocene Thermal Maximum (HTM), four folds higher than the rate

1219 of 1.4 Pg C yr<sup>-1</sup> over the rest of the Holocene. The 20<sup>th</sup> century represented another high SOC  
1220 accumulation period after the much lowered accumulation rate in the late Holocene. We  
1221 estimated an average depth of 1.9 m of peat in Alaskan peatlands, similar to the observed mean  
1222 depth. We found that the changes of vegetation distribution due to the climatic change were the  
1223 key factors to the spatial variations of SOC accumulation in different time periods. The warming  
1224 in the HTM characterized by the increased summer temperature and increased seasonality of  
1225 solar radiation, along with the higher precipitation might have played an important role in  
1226 causing the high C accumulation rates. Under warming climate conditions, Alaskan peatlands  
1227 may continue acting as C sink in the future.

1228 **6. Acknowledgment.** We acknowledge the funding support from a NSF project IIS-1027955  
1229 and a DOE project DE-SC0008092. We also acknowledge the SPRUCE project to allow us use  
1230 its data. Data presented in this paper are publicly accessible: ECBilt-CLIO Paleosimulation  
1231 (<http://apdrc.soest.hawaii.edu/datadoc/sim2bl.php>), CRU2.0 (<http://www.cru.uea.ac.uk/data>).  
1232 Model parameter data and model evaluation process are in Wang et al. (2016). Other simulation  
1233 data including model codes are available upon request from the corresponding author  
1234 (qzhuang@purdue.edu).

## 1235 7. References

- 1236 *Anderson, P. M., & Brubaker, L. B. (1993). Holocene vegetation and climate histories of*  
1237 *Alaska. Global climates since the last glacial maximum, 385-400.*
- 1238 *Apps, M. J., Kurz, W. A., Luxmoore, R. J., Nilsson, L. O., Sedjo, R. A., Schmidt, R., ... &*  
1239 *Vinson, T. S. (1993). Boreal forests and tundra. Water, Air, and Soil Pollution, 70(1-4), 39-53.*
- 1240 *Armentano, T. V., & Menges, E. S. (1986). Patterns of change in the carbon balance of organic*  
1241 *soil wetlands of the temperate zone. The Journal of Ecology, 755-774.*
- 1242 *Assessment, A. C. I. (2005). Forests, land management and agriculture. Arctic Climate Impact*  
1243 *Assessment, 781-862.*

1244 Balshi, M. S., McGuire, A. D., Zhuang, Q., Melillo, J., Kicklighter, D. W., Kasisehke, E., ... &  
1245 Burnside, T. J. (2007). The role of historical fire disturbance in the carbon dynamics of the pan-  
1246 boreal region: A process-based analysis. *Journal of Geophysical Research: Biogeosciences*, *112*(G2).

1248 Barber, V. A., & Finney, B. P. (2000). Late Quaternary paleoclimatic reconstructions for interior  
1249 Alaska based on paleolake level data and hydrologic models. *Journal of Paleolimnology*, *24*(1),  
1250 29-41.

1251 Bartlein, P. J., Harrison, S. P., Brewer, S., Connor, S., Davis, B. A. S., Gajewski, K., ... &  
1252 Prentice, I. C. (2011). Pollen-based continental climate reconstructions at 6 and 21 ka: a global  
1253 synthesis. *Climate Dynamics*, *37*(3-4), 775-802.

1254 Belyea, L. R. (2009). Nonlinear dynamics of peatlands and potential feedbacks on the climate  
1255 system. *Carbon cycling in northern peatlands*, 5-18.

1256 Berger, A., & Loutre, M. F. (1991). Insolation values for the climate of the last 10 million  
1257 years. *Quaternary Science Reviews*, *10*(4), 297-317.

1258 Bigelow, N. H., Brubaker, L. B., Edwards, M. E., Harrison, S. P., Prentice, I. C., Anderson, P.  
1259 M., ... & Kaplan, J. O. (2003). Climate change and Arctic ecosystems: 1. Vegetation changes  
1260 north of 55°N between the last glacial maximum, mid-Holocene, and present. *Journal of*  
1261 *Geophysical Research: Atmospheres*, *108*(D19).

1262 Bridgman, S. D., Megonigal, J. P., Keller, J. K., Bliss, N. B., & Trettin, C. (2006). The carbon  
1263 balance of North American wetlands. *Wetlands*, *26*(4), 889-916.

1264 Carter, A. J., & Scholes, R. J. (2000). SoilData v2.0: generating a global database of soil  
1265 properties. *Environmentek CSIR, Pretoria, South Africa*.

1266 Change, I. C. (2013). The Physical Science Basis: Working Group I Contribution to the Fifth  
1267 Assessment Report of the Intergovernmental Panel on Climate Change. *New York: Cambridge*  
1268 *University Press*, *1*, 535-1.

1269 Change, I. C. (2014). Mitigation of Climate Change. Contribution of Working Group III to the  
1270 Fifth Assessment Report of the Intergovernmental Panel on Climate Change. *Cambridge*  
1271 *University Press, Cambridge, UK and New York, NY*.

1272 Chivers, M. R., Turetsky, M. R., Waddington, J. M., Harden, J. W., & McGuire, A. D. (2009).  
1273 Effects of experimental water table and temperature manipulations on ecosystem CO<sub>2</sub> fluxes in  
1274 an Alaskan rich fen. *Ecosystems*, *12*(8), 1329-1342.

1275 Churchill, A. (2011). The response of plant community structure and productivity to changes in  
1276 hydrology in Alaskan boreal peatlands. *Master Thesis*, University of Alaska, Fairbanks, AK,  
1277 USA. 119 pp.

1278 Conrad, R. (1999). Contribution of hydrogen to methane production and control of hydrogen  
1279 concentrations in methanogenic soils and sediments. *FEMS Microbiology Ecology*, *28*(3), 193-  
1280 202.

1281 Crockford, S. J., & Frederick, S. G. (2007). Sea ice expansion in the Bering Sea during the  
1282 Neoglacial: Evidence from archaeozoology. *The Holocene*, *17*(6), 699-706.

1283 Davidson, E. A., Trumbore, S. E., & Amundson, R. (2000). Biogeochemistry: soil warming and  
1284 organic carbon content. *Nature*, *408*(6814), 789-790.

1285 Davidson, E. A., & Janssens, I. A. (2006). Temperature sensitivity of soil carbon decomposition  
1286 and feedbacks to climate change. *Nature*, 440(7081), 165-173.

1287 Edwards, M. E., Anderson, P. M., Brubaker, L. B., Ager, T. A., Andreev, A. A., Bigelow, N. H.,  
1288 ... & Jolly, D. (2000). Pollen-based biomes for Beringia 18,000, 6000 and 0-14C yr bp. *Journal*  
1289 *of Biogeography*, 27(3), 521-554.

1290 Edwards, M. E., Mock, C. J., Finney, B. P., Barber, V. A., & Bartlein, P. J. (2001). Potential  
1291 analogues for paleoclimatic variations in eastern interior Alaska during the past 14,000 yr:  
1292 atmospheric circulation controls of regional temperature and moisture responses. *Quaternary*  
1293 *Science Reviews*, 20(1), 189-202.

1294 Edwards, M. E., Brubaker, L. B., Lozhkin, A. V., & Anderson, P. M. (2005). Structurally novel  
1295 biomes: a response to past warming in Beringia. *Ecology*, 86(7), 1696-1703.

1296 Euskirchen, E. S., McGuire, A. D., & Chapin, F. S. (2007). Energy feedbacks of northern high-  
1297 latitude ecosystems to the climate system due to reduced snow cover during 20th century  
1298 warming. *Global Change Biology*, 13(11), 2425-2438.

1299 Frohking, S., Roulet, N. T., Tuittila, E., Bubier, J. L., Quillet, A., Talbot, J., & Richard, P. J. H.  
1300 (2010). A new model of Holocene peatland net primary production, decomposition, water  
1301 balance, and peat accumulation. *Earth System Dynamics*, 1(1), 1-21.

1302 Frohking, S., Talbot, J., Jones, M. C., Treat, C. C., Kauffman, J. B., Tuittila, E. S., & Roulet, N.  
1303 (2011). Peatlands in the Earth's 21st century climate system. *Environmental Reviews*, 19(NA),  
1304 371-396.

1305 Gilmanov, T. G., & Oechel, W. C. (1995). New estimates of organic matter reserves and net  
1306 primary productivity of the North American tundra ecosystems. *Journal of Biogeography*, 723-  
1307 741.

1308 Gorham, E. V. I. L. L. E. (1990). Biotic impoverishment in northern peatlands. *The earth in*  
1309 *transition: patterns and processes of biotic impoverishment*. Cambridge University Press,  
1310 Cambridge, UK, 65-98.

1311 Gorham, E. (1991). Northern peatlands: role in the carbon cycle and probable responses to  
1312 climatic warming. *Ecological applications*, 1(2), 182-195.

1313 Gorham, E., Lehman, C., Dyke, A., Clymo, D., & Janssens, J. (2012). Long-term carbon  
1314 sequestration in North American peatlands. *Quaternary Science Reviews*, 58, 77-82.

1315 He, Y., Jones, M. C., Zhuang, Q., Bochiechio, C., Felzer, B. S., Mason, E., & Yu, Z. (2014).  
1316 Evaluating CO<sub>2</sub> and CH<sub>4</sub> dynamics of Alaskan ecosystems during the Holocene Thermal  
1317 Maximum. *Quaternary Science Reviews*, 86, 63-77.

1318 Hinzman, L. D., Viereck, L. A., Adams, P. C., Romanovsky, V. E., & Yoshikawa, K. (2006).  
1319 Climate and permafrost dynamics of the Alaskan boreal forest. *Alaska's Changing Boreal*  
1320 *Forest*, 39-61.

1321 Hobbie, S. E. (2000). Interactions between litter lignin and nitrogen litter lignin and soil nitrogen  
1322 availability during leaf litter decomposition in a Hawaiian montane forest. *Ecosystems*, 3(5),  
1323 484-494.

1324 Hugelius, G., Strauss, J., Zubrzycki, S., Harden, J. W., Schuur, E., Ping, C. L., ... & O'Donnell, J.  
1325 A. (2014). Estimated stocks of circumpolar permafrost carbon with quantified uncertainty ranges  
1326 and identified data gaps. *Biogeosciences*, *11*(23), 6573–6593.

1327 Huybers, P. (2006). Early Pleistocene glacial cycles and the integrated summer insolation  
1328 forcing. *Science*, *313*(5786), 508–511.

1329 Jobbágy, E. G., & Jackson, R. B. (2000). The vertical distribution of soil organic carbon and its  
1330 relation to climate and vegetation. *Ecological applications*, *10*(2), 423–436.

1331 Jones, M. C., & Yu, Z. (2010). Rapid deglacial and early Holocene expansion of peatlands in  
1332 Alaska. *Proceedings of the National Academy of Sciences*, *107*(16), 7347–7352.

1333 Jones, P. D., & Moberg, A. (2003). Hemispheric and large scale surface air temperature  
1334 variations: An extensive revision and an update to 2001. *Journal of Climate*, *16*(2), 206–223.

1335 Kane, E. S., Turetsky, M. R., Harden, J. W., McGuire, A. D., & Waddington, J. M. (2010).  
1336 Seasonal ice and hydrologic controls on dissolved organic carbon and nitrogen concentrations in  
1337 a boreal rich fen. *Journal of Geophysical Research: Biogeosciences*, *115*(G4).

1338 Kaufman, D. S., Ager, T. A., Anderson, N. J., Anderson, P. M., Andrews, J. T., Bartlein, P. J., ...  
1339 & Dyke, A. S. (2004). Holocene thermal maximum in the western Arctic (0–180°W). *Quaternary  
1340 Science Reviews*, *23*(5), 529–560.

1341 Kaufman, D.S., Axford, Y.L., Heneron, A., McKay, N.P., Oswald, W.W., Saenger, C.,  
1342 Anderson, R.S., Bailey, H.L., Clegg, B., Gajewski, K., Hu, F.S., Jones, M.C., Massa, C.,  
1343 Routson, C.C., Werner, A., Wooller, M.J., Yu, Z., 2016. Holocene climate changes in eastern  
1344 Beringia (NW North America) e a systemic review of multi proxy evidence. *Quaternary Science  
1345 Reviews*, this volume. <http://dx.doi.org/10.1016/j.quascirev.2015.10.021>.

1346 Keller, J. K., & Bridgman, S. D. (2007). Pathways of anaerobic carbon cycling across an  
1347 ombrotrophic–minerotrophic peatland gradient.

1348 Keller, J. K., & Takagi, K. K. (2013). Solid-phase organic matter reduction regulates anaerobic  
1349 decomposition in bog soil. *Ecosphere*, *4*(5), 1–12.

1350 Kimball, J. S., McDonald, K. C., Running, S. W., & Frolking, S. E. (2004). Satellite radar remote  
1351 sensing of seasonal growing seasons for boreal and subalpine evergreen forests. *Remote Sensing  
1352 of Environment*, *90*(2), 243–258.

1353 Kivinen, E., and P. Pakarinen. (1981). Geographical distribution of peat resources and major  
1354 peatland complex types in the world. *Annales Academiae Scientiarum Fennicae, Series A,  
1355 Number 132*.

1356 Kleinen, T., Brovkin, V., von Bloh, W., Archer, D., & Munhoven, G. (2010). Holocene carbon  
1357 cycle dynamics. *Geophysical Research Letters*, *37*(2).

1358 Kuhry, P., & Vitt, D. H. (1996). Fossil carbon/nitrogen ratios as a measure of peat  
1359 decomposition. *Ecology*, *77*(1), 271–275.

1360 Linderholm, H. W. (2006). Growing season changes in the last century. *Agricultural and Forest  
1361 Meteorology*, *137*(1), 1–14.

1362 Loisel, J., Gallego-Sala, A. V., & Yu, Z. (2012). Global scale pattern of peatland-Sphagnum  
1363 growth driven by photosynthetically active radiation and growing season  
1364 length. *Biogeosciences*, *9*(7), 2737–2746.

1365 Loisel, J., Yu, Z., Beilman, D. W., Camill, P., Alm, J., Amesbury, M. J., ... & Belyea, L. R.  
1366 (2014). A database and synthesis of northern peatland soil properties and Holocene carbon and  
1367 nitrogen accumulation. *the Holocene*, 0959683614538073.

1368 Maltby, E., & Immirzi, P. (1993). Carbon dynamics in peatlands and other wetland soils regional  
1369 and global perspectives. *Chemosphere*, 27(6), 999-1023.

1370 Manabe, S., & Wetherald, R. T. (1980). On the distribution of climate change resulting from an  
1371 increase in CO<sub>2</sub> content of the atmosphere. *Journal of the Atmospheric Sciences*, 37(1), 99-118.

1372 Manabe, S., & Wetherald, R. T. (1986). Reduction in summer soil wetness induced by an  
1373 increase in atmospheric carbon dioxide. *Science*, 232(4750), 626-628.

1374 Marcott, S. A., Shakun, J. D., Clark, P. U., & Mix, A. C. (2013). A reconstruction of regional  
1375 and global temperature for the past 11,300 years. *science*, 339(6124), 1198-1201.

1376 Matthews, E., & Fung, I. (1987). Methane emission from natural wetlands: Global distribution,  
1377 area, and environmental characteristics of sources. *Global biogeochemical cycles*, 1(1), 61-86.

1378 McGuire, A. D., Melillo, J. M., Kicklighter, D. W., & Joyce, L. A. (1995). Equilibrium  
1379 responses of soil carbon to climate change: empirical and process-based estimates. *Journal of*  
1380 *Biogeography*, 785-796.

1381 McGuire, A. D., & Hobbie, J. E. (1997). Global climate change and the equilibrium responses of  
1382 carbon storage in arctic and subarctic regions. In *Modeling the Arctic system: A workshop report*  
1383 *on the state of modeling in the Arctic System Science program* (pp. 53-54).

1384 McGuire, A. D., Melillo, J. M., Randerson, J. T., Parton, W. J., Heimann, M., Meier, R. A., ... &  
1385 Sauf, W. (2000). Modeling the effects of snowpack on heterotrophic respiration across northern  
1386 temperate and high latitude regions: Comparison with measurements of atmospheric carbon  
1387 dioxide in high latitudes. *Biogeochemistry*, 48(1), 91-114.

1388 McGuire, A. D., Anderson, L. G., Christensen, T. R., Dallimore, S., Guo, L., Hayes, D. J., ... &  
1389 Roulet, N. (2009). Sensitivity of the carbon cycle in the Arctic to climate change. *Ecological*  
1390 *Monographs*, 79(4), 523-555.

1391 Melillo, J. M., Kicklighter, D. W., McGuire, A. D., Peterjohn, W. T., & Newkirk, K. (1995,  
1392 July). Global change and its effects on soil organic carbon stocks. In *Dahlem Conference*  
1393 *Proceedings*, John Wiley and Sons, New York, John Wiley & Sons, Ltd., Chichester (pp. 175-189).

1394 Moek, C. J., & Bartlein, P. J. (1995). Spatial variability of late Quaternary paleoclimates in the  
1395 western United States. *Quaternary Research*, 44(3), 425-433.

1396 Moore, T. R., Bubier, J. L., Frolking, S. E., Lafleur, P. M., & Roulet, N. T. (2002). Plant biomass  
1397 and production and CO<sub>2</sub> exchange in an ombrotrophic bog. *Journal of Ecology*, 90(1), 25-36.

1398 Nobrega, S., & Grogan, P. (2007). Deeper snow enhances winter respiration from both plant-  
1399 associated and bulk soil carbon pools in birch hummock tundra. *Ecosystems*, 10(3), 419-431.

1400 Oechel, W. C. (1989). Nutrient and water flux in a small arctic watershed: an  
1401 overview. *Holarctic Ecology*, 229-237.

1402 Oechel, W. C., Hastings, S. J., Vourlitis, G., Jenkins, M., Riechers, G., & Grulke, N. (1993).  
1403 Recent change of Arctic tundra ecosystems from a net carbon dioxide sink to a  
1404 source. *Nature*, 361(6412), 520-523.

1405 Oksanen, P. O., Kuhry, P., & Alekseeva, R. N. (2001). Holocene development of the Rogovaya  
1406 river peat plateau, European Russian Arctic. *The Holocene*, 11(1), 25–40.

1407 Peteet, D., Andreev, A., Bardeen, W., & Mistretta, F. (1998). Long-term Arctic peatland  
1408 dynamics, vegetation and climate history of the Pur-Taz region, western Siberia. *Boreas*, 27(2),  
1409 115–126.

1410 Prentice, C., Guiot, J., Huntley, B., Jolly, D., & Cheddadi, R. (1996). Reconstructing biomes  
1411 from palaeoecological data: a general method and its application to European pollen data at 0  
1412 and 6 ka. *Climate Dynamics*, 12(3), 185–194.

1413 Prentice, I. C. (2008). Terrestrial nitrogen cycle simulation with a dynamic global vegetation  
1414 model. *Global Change Biology*, 14(8), 1745–1764.

1415 Raich, J. W., Rastetter, E. B., Melillo, J. M., Kicklighter, D. W., Steudler, P. A., Peterson, B. J.,  
1416 ... & Vorosmarty, C. J. (1991). Potential net primary productivity in South America: application  
1417 of a global model. *Ecological Applications*, 1(4), 399–429.

1418 Renssen, H., Seppä, H., Heiri, O., Roche, D. M., Goosse, H., & Fichefet, T. (2009). The spatial  
1419 and temporal complexity of the Holocene thermal maximum. *Nature Geoscience*, 2(6), 411–414.

1420 Roulet, N. T., Lafleur, P. M., Richard, P. J., Moore, T. R., Humphreys, E. R., & Bubier, J. I. L.  
1421 L. (2007). Contemporary carbon balance and late Holocene carbon accumulation in a northern  
1422 peatland. *Global Change Biology*, 13(2), 397–411.

1423 Schuur, E. A., Bockheim, J., Canadell, J. G., Euskirchen, E., Field, C. B., Goryachkin, S. V., ...  
1424 & Mazhitova, G. (2008). Vulnerability of permafrost carbon to climate change: implications for  
1425 the global carbon cycle. *BioScience*, 58(8), 701–714.

1426 Sitch, S., Smith, B., Prentice, I. C., Arneeth, A., Bondeau, A., Cramer, W., ... & Thonicke, K.  
1427 (2003). Evaluation of ecosystem dynamics, plant geography and terrestrial carbon cycling in the  
1428 LPJ dynamic global vegetation model. *Global Change Biology*, 9(2), 161–185.

1429 Spahni, R., Joos, F., Stocker, B. D., Steinacher, M., & Yu, Z. C. (2013). Transient simulations of  
1430 the carbon and nitrogen dynamics in northern peatlands: from the Last Glacial Maximum to the  
1431 21st century. *Climate of the Past*, 9(3), 1287–1308.

1432 Stafford, J. M., Wendler, G., & Curtis, J. (2000). Temperature and precipitation of Alaska: 50  
1433 year trend analysis. *Theoretical and Applied Climatology*, 67(1–2), 33–44.

1434 Stieglitz, M., Déry, S. J., Romanovsky, V. E., & Osterkamp, T. E. (2003). The role of snow  
1435 cover in the warming of arctic permafrost. *Geophysical Research Letters*, 30(13).

1436 Stocker, B. D., Strassmann, K., & Joos, F. (2011). Sensitivity of Holocene atmospheric CO<sub>2</sub> and  
1437 the modern carbon budget to early human land use: analyses with a process-based  
1438 model. *Biogeosciences*, 8(1), 69–88.

1439 Stocker, B. D., Spahni, R., & Joos, F. (2014). DYPTOP: a cost efficient TOPMODEL  
1440 implementation to simulate sub-grid spatio-temporal dynamics of global wetlands and  
1441 peatlands. *Geoscientific Model Development*, 7(6), 3089–3110.

1442 Tang, J., & Zhuang, Q. (2008). Equifinality in parameterization of process-based  
1443 biogeochemistry models: A significant uncertainty source to the estimation of regional carbon  
1444 dynamics. *Journal of Geophysical Research: Biogeosciences*, 113(G4).



1445 Tang, J., & Zhuang, Q. (2009). A global sensitivity analysis and Bayesian inference framework  
1446 for improving the parameter estimation and prediction of a process-based Terrestrial Ecosystem  
1447 Model. *Journal of Geophysical Research: Atmospheres*, 114(D15).

1448 Tang, J., Zhuang, Q., Shannon, R. D., & White, J. R. (2010). Quantifying wetland methane  
1449 emissions with process-based models of different complexities. *Biogeosciences*, 7(11), 3817-  
1450 3837.

1451 Tarnocai, C., Canadell, J. G., Schuur, E. A. G., Kuhry, P., Mazhitova, G., & Zimov, S. (2009).  
1452 Soil organic carbon pools in the northern circumpolar permafrost region. *Global biogeochemical  
1453 cycles*, 23(2).

1454 Timmermann, A., Timm, O., Stott, L., & Menviel, L. (2009). The roles of CO<sub>2</sub> and orbital  
1455 forcing in driving southern hemispheric temperature variations during the last 21 000  
1456 Yr\*. *Journal of Climate*, 22(7), 1626-1640.

1457 Tucker, C. J., Slayback, D. A., Pinzon, J. E., Los, S. O., Myneni, R. B., & Taylor, M. G. (2001).  
1458 Higher northern latitude normalized difference vegetation index and growing season trends from  
1459 1982 to 1999. *International journal of biometeorology*, 45(4), 184-190.

1460 Turetsky, M. R., Treat, C. C., Waldrop, M. P., Waddington, J. M., Harden, J. W., & McGuire, A.  
1461 D. (2008). Short-term response of methane fluxes and methanogen activity to water table and  
1462 soil-warming manipulations in an Alaskan peatland. *Journal of Geophysical Research:  
1463 Biogeosciences*, 113(G3).

1464 Turunen, J., Tomppo, E., Tolonen, K., & Reinikainen, A. (2002). Estimating carbon  
1465 accumulation rates of undrained mires in Finland—application to boreal and subarctic  
1466 regions. *The Holocene*, 12(1), 69-80.

1467 Vitt, D. H., Halsey, L. A., Bauer, I. E., & Campbell, C. (2000). Spatial and temporal trends in  
1468 carbon storage of peatlands of continental western Canada through the Holocene. *Canadian  
1469 Journal of Earth Sciences*, 37(5), 683-693.

1470 Wang, S., Zhuang, Q., Yu, Z., Bridgham, S., & Keller, J. (2016). Quantifying peat carbon  
1471 accumulation in Alaska using a process-based biogeochemistry model. *Journal of Geophysical  
1472 Research: Biogeosciences* (Under revision).

1473 Whitlock, C., & Bartlein, P. J. (1993). Spatial variations of Holocene climatic change in the  
1474 Yellowstone region. *Quaternary Research*, 39(2), 231-238.

1475 Williams, J. W., Webb, T., Richard, P. H., & Newby, P. (2000). Late Quaternary biomes of  
1476 Canada and the eastern United States. *Journal of Biogeography*, 27(3), 585-607.

1477 Yu, Z., Beilman, D. W., & Jones, M. C. (2009). Sensitivity of northern peatland carbon  
1478 dynamics to Holocene climate change. *Carbon cycling in northern peatlands*, 55-69.

1479 Yu, Z., Loisel, J., Brosseau, D. P., Beilman, D. W., & Hunt, S. J. (2010). Global peatland  
1480 dynamics since the Last Glacial Maximum. *Geophysical Research Letters*, 37(13).

1481 Yu, Z. C. (2012). Northern peatland carbon stocks and dynamics: a  
1482 review. *Biogeosciences*, 9(10), 4071-4085.

1483 Zhuang, Q., Romanovsky, V. E., & McGuire, A. D. (2001). Incorporation of a permafrost model  
1484 into a large-scale ecosystem model: Evaluation of temporal and spatial scaling issues in

1485 [simulating soil thermal dynamics. \*Journal of Geophysical Research: Atmospheres\*, 106\(D24\),](#)  
1486 [33649-33670.](#)

1487 [Zhuang, Q., McGuire, A. D., O'Neill, K. P., Harden, J. W., Romanovsky, V. E., & Yarie, J.](#)  
1488 [\(2002\). Modeling soil thermal and carbon dynamics of a fire chronosequence in interior](#)  
1489 [Alaska. \*Journal of Geophysical Research: Atmospheres\*, 107\(D1\).](#)

1490 [Zhuang, Q., McGuire, A. D., Melillo, J. M., Clein, J. S., Dargaville, R. J., Kicklighter, D. W., ...](#)  
1491 [& Hobbie, J. E. \(2003\). Carbon cycling in extratropical terrestrial ecosystems of the Northern](#)  
1492 [Hemisphere during the 20th century: a modeling analysis of the influences of soil thermal](#)  
1493 [dynamics. \*Tellus B\*, 55\(3\), 751-776.](#)

1494 [Zhuang, Q., Melillo, J. M., Kicklighter, D. W., Prinn, R. G., McGuire, A. D., Steudler, P. A., ...](#)  
1495 [& Hu, S. \(2004\). Methane fluxes between terrestrial ecosystems and the atmosphere at northern](#)  
1496 [high latitudes during the past century: A retrospective analysis with a process-based](#)  
1497 [biogeochemistry model. \*Global Biogeochemical Cycles\*, 18\(3\).](#)

1498 [Zhuang, Q., Zhu, X., He, Y., Prigent, C., Melillo, J. M., McGuire, A. D., ... & Kicklighter, D. W.](#)  
1499 [\(2015\). Influence of changes in wetland inundation extent on net fluxes of carbon dioxide and](#)  
1500 [methane in northern high latitudes from 1993 to 2004. \*Environmental Research Letters\*, 10\(9\),](#)  
1501 [095009.](#)

1502 [Zimov, S. A., Schuur, E. A., & Chapin III, F. S. \(2006\). Permafrost and the global carbon](#)  
1503 [budget. \*Science\(Washington\)\*, 312\(5780\), 1612-1613.](#)

1504 [Zoltai, S. C. \(1995\). Permafrost distribution in peatlands of west central Canada during the](#)  
1505 [Holocene warm period 6000 years BP. \*Géographie physique et Quaternaire\*, 49\(1\), 45-54.](#)

1506 [Ager, T. A., & Brubaker, L.: Quaternary palynology and vegetational history of Alaska. \*Pollen\*](#)  
1507 [\*Records of Late Quaternary North American Sediments\*, 353-384, 1985.](#)

1508 [Apps, M. J., Kurz, W. A., Luxmoore, R. J., Nilsson, L. O., Sedjo, R. A., Schmidt, R., ... &](#)  
1509 [Vinson, T. S.: \*Boreal forests and tundra. Water, Air, and Soil Pollution\*, 70\(1-4\), 39-53, 1993.](#)

1510 [Armentano, T. V., & Menges, E. S.: Patterns of change in the carbon balance of organic soil-](#)  
1511 [wetlands of the temperate zone. \*The Journal of Ecology\*, 755-774, 1986.](#)

1512 [Assessment, A. C. I.: \*Forests, land management and agriculture. Arctic Climate Impact\*](#)  
1513 [\*Assessment\*, 781-862, 2005.](#)

1514 [Balshi, M. S., McGuire, A. D., Zhuang, Q., Melillo, J., Kicklighter, D. W., Kasischke, E., ... &](#)  
1515 [Burnside, T. J.: The role of historical fire disturbance in the carbon dynamics of the pan-boreal](#)  
1516 [region: A process-based analysis. \*Journal of Geophysical Research: Biogeosciences\*, 112\(G2\),](#)  
1517 [2007.](#)

1518 [Barber, V. A., & Finney, B. P.: Late Quaternary paleoclimatic reconstructions for interior Alaska](#)  
1519 [based on paleolake-level data and hydrologic models. \*Journal of Paleolimnology\*, 24\(1\), 29-41,](#)  
1520 [2000.](#)

1521 [Belyea, L. R.: Nonlinear dynamics of peatlands and potential feedbacks on the climate](#)  
1522 [system. \*Carbon cycling in northern peatlands\*, 5-18, 2009.](#)

1523 [Berger, A., & Loutre, M. F.: Insolation values for the climate of the last 10 million](#)  
1524 [years. \*Quaternary Science Reviews\*, 10\(4\), 297-317, 1991.](#)

1525 [Bigelow, N. H., Brubaker, L. B., Edwards, M. E., Harrison, S. P., Prentice, I. C., Anderson, P.](#)  
1526 [M., ... & Kaplan, J. O.: Climate change and Arctic ecosystems: 1. Vegetation changes north of](#)  
1527 [55 N between the last glacial maximum, mid-Holocene, and present. Journal of Geophysical](#)  
1528 [Research: Atmospheres, 108\(D19\), 2003.](#)

1529 [Bridgham, S. D., Megonigal, J. P., Keller, J. K., Bliss, N. B., & Trettin, C.: The carbon balance](#)  
1530 [of North American wetlands. Wetlands, 26\(4\), 889-916, 2006.](#)

1531 [Carter, A. J., & Scholes, R. J.: SoilData v2. 0: generating a global database of soil](#)  
1532 [properties. Environmentek CSIR, Pretoria, South Africa, 2000.](#)

1533 [Change, I. C.: Mitigation of Climate Change. Contribution of Working Group III to the Fifth](#)  
1534 [Assessment Report of the Intergovernmental Panel on Climate Change. Cambridge University](#)  
1535 [Press, Cambridge, UK and New York, NY, 2014.](#)

1536 [Change, I. C.: The Physical Science Basis: Working Group I Contribution to the Fifth](#)  
1537 [Assessment Report of the Intergovernmental Panel on Climate Change. New York: Cambridge](#)  
1538 [University Press, 1, 535-1, 2013.](#)

1539 [Chivers, M. R., Turetsky, M. R., Waddington, J. M., Harden, J. W., & McGuire, A. D.: Effects](#)  
1540 [of experimental water table and temperature manipulations on ecosystem CO<sub>2</sub> fluxes in an](#)  
1541 [Alaskan rich fen.Ecosystems, 12\(8\), 1329-1342, 2009.](#)

1542 [Churchill, A.: The response of plant community structure and productivity to changes in](#)  
1543 [hydrology in Alaskan boreal peatlands. Master Thesis, University of Alaska, Fairbanks, AK,](#)  
1544 [USA. 119 pp, 2011.](#)

1545 [Conrad, R.: Contribution of hydrogen to methane production and control of hydrogen](#)  
1546 [concentrations in methanogenic soils and sediments.FEMS Microbiology Ecology, 28\(3\), 193-](#)  
1547 [202, 1999.](#)

1548 [Davidson, E. A., & Janssens, I. A.: Temperature sensitivity of soil carbon decomposition and](#)  
1549 [feedbacks to climate change. Nature, 440\(7081\), 165-173, 2006.](#)

1550 [Davidson, E. A., Trumbore, S. E., & Amundson, R.: Biogeochemistry: soil warming and organic](#)  
1551 [carbon content. Nature, 408\(6814\), 789-790, 2000.](#)

1552 [Edwards, M. E., Mock, C. J., Finney, B. P., Barber, V. A., & Bartlein, P. J.: Potential analogues](#)  
1553 [for paleoclimatic variations in eastern interior Alaska during the past 14,000 yr: atmospheric-](#)  
1554 [circulation controls of regional temperature and moisture responses. Quaternary Science](#)  
1555 [Reviews, 20\(1\), 189-202, 2001.](#)

1556 [Euskirchen, E. S., McGuire, A. D., & Chapin, F. S.: Energy feedbacks of northern high-latitude](#)  
1557 [ecosystems to the climate system due to reduced snow cover during 20th century](#)  
1558 [warming. Global Change Biology,13\(11\), 2425-2438, 2007.](#)

1559 [Frolking, S., Roulet, N. T., Tuittila, E., Bubier, J. L., Quillet, A., Talbot, J., & Richard, P. J. H.:](#)  
1560 [A new model of Holocene peatland net primary production, decomposition, water balance, and](#)  
1561 [peat accumulation. Earth System Dynamics, 1\(1\), 1-21, 2010.](#)

1562 [Frolking, S., Talbot, J., Jones, M. C., Treat, C. C., Kauffman, J. B., Tuittila, E. S., & Roulet, N.:](#)  
1563 [Peatlands in the Earth's 21st century climate system. Environmental Reviews, 19\(NA\), 371-396,](#)  
1564 [2011.](#)

1565 [Gilmanov, T. G., & Oechel, W. C.: New estimates of organic matter reserves and net primary](#)  
1566 [productivity of the North American tundra ecosystems. \*Journal of Biogeography\*, 723-741, 1995.](#)

1567 [Gorham, E. V. I. L. E.: Biotic impoverishment in northern peatlands. \*The earth in transition:\*](#)  
1568 [patterns and processes of biotic impoverishment. Cambridge University Press, Cambridge, UK,](#)  
1569 [65-98, 1990.](#)

1570 [Gorham, E., Lehman, C., Dyke, A., Clymo, D., & Janssens, J.: Long-term carbon sequestration](#)  
1571 [in North American peatlands. \*Quaternary Science Reviews\*, 58, 77-82, 2012.](#)

1572 [Gorham, E.: Northern peatlands: role in the carbon cycle and probable responses to climatic](#)  
1573 [warming. \*Ecological applications\*, 1\(2\), 182-195, 1991.](#)

1574 [He, Y., Jones, M. C., Zhuang, Q., Bochicchio, C., Felzer, B. S., Mason, E., & Yu, Z.: Evaluating](#)  
1575 [CO<sub>2</sub> and CH<sub>4</sub> dynamics of Alaskan ecosystems during the Holocene Thermal](#)  
1576 [Maximum. \*Quaternary Science Reviews\*, 86, 63-77, 2014.](#)

1577 [Hinzman, L. D., Viereck, L. A., Adams, P. C., Romanovsky, V. E., & Yoshikawa, K.: Climate](#)  
1578 [and permafrost dynamics of the Alaskan boreal forest. \*Alaska's Changing Boreal Forest\*, 39-61,](#)  
1579 [2006.](#)

1580 [Hobbie, S. E.: Interactions between litter lignin and nitrogen litter lignin and soil nitrogen](#)  
1581 [availability during leaf litter decomposition in a Hawaiian montane forest. \*Ecosystems\*, 3\(5\),](#)  
1582 [484-494, 2000.](#)

1583 [Hugelius, G., Strauss, J., Zubrzycki, S., Harden, J. W., Schuur, E., Ping, C. L., ... & O'Donnell, J.](#)  
1584 [A.: Estimated stocks of circumpolar permafrost carbon with quantified uncertainty ranges and](#)  
1585 [identified data gaps. \*Biogeosciences\*, 11\(23\), 6573-6593, 2014.](#)

1586 [Jobbágy, E. G., & Jackson, R. B.: The vertical distribution of soil organic carbon and its relation](#)  
1587 [to climate and vegetation. \*Ecological applications\*, 10\(2\), 423-436, 2000.](#)

1588 [Jones, M. C., & Yu, Z.: Rapid deglacial and early Holocene expansion of peatlands in](#)  
1589 [Alaska. \*Proceedings of the National Academy of Sciences\*, 107\(16\), 7347-7352, 2010.](#)

1590 [Jones, P. D., & Moberg, A.: Hemispheric and large-scale surface air temperature variations: An](#)  
1591 [extensive revision and an update to 2001. \*Journal of Climate\*, 16\(2\), 206-223, 2003.](#)

1592 [Kane, E. S., Turetsky, M. R., Harden, J. W., McGuire, A. D., & Waddington, J. M.: Seasonal ice](#)  
1593 [and hydrologic controls on dissolved organic carbon and nitrogen concentrations in a boreal-rich](#)  
1594 [fen. \*Journal of Geophysical Research: Biogeosciences\*, 115\(G4\), 2010.](#)

1595 [Kaufman, D. S., Ager, T. A., Anderson, N. J., Anderson, P. M., Andrews, J. T., Bartlein, P. J., ...](#)  
1596 [& Dyke, A. S.: Holocene thermal maximum in the western Arctic \(0–180 W\). \*Quaternary\*](#)  
1597 [\*Science Reviews\*, 23\(5\), 529-560, 2004.](#)

1598 [Kaufman, D.S., Axford, Y.L., Henerson, A., McKay, N.P., Oswald, W.W., Saenger, C.,](#)  
1599 [Anderson, R.S., Bailey, H.L., Clegg, B., Gajewski, K., Hu, F.S., Jones, M.C., Massa, C.,](#)  
1600 [Routson, C.C., Werner, A., Wooller, M.J., Yu, Z.: Holocene climate changes in eastern Beringia](#)  
1601 [\(NW North America\) e a systemic review of multi-proxy evidence. \*Quaternary Science Reviews,\*](#)  
1602 [this volume. <http://dx.doi.org/10.1016/j.quascirev.2015.10.021>, 2016.](#)

1603 [Keller, J. K., & Bridgman, S. D.: Pathways of anaerobic carbon cycling across an ombrotrophic-](#)  
1604 [minerotrophic peatland gradient, 2007.](#)

1605 [Keller, J. K., & Takagi, K. K.: Solid-phase organic matter reduction regulates anaerobic](#)  
1606 [decomposition in bog soil. \*Ecosphere\*, 4\(5\), 1-12, 2013.](#)

1607 [Kimball, J. S., McDonald, K. C., Running, S. W., & Frolking, S. E.: Satellite radar remote](#)  
1608 [sensing of seasonal growing seasons for boreal and subalpine evergreen forests. \*Remote Sensing\*](#)  
1609 [of Environment, 90\(2\), 243-258, 2004.](#)

1610 [Kivinen, E., and P. Pakarinen.: Geographical distribution of peat resources and major peatland](#)  
1611 [complex types in the world. \*Annales Academiae Scientiarum Fennicae, Series A, Number 132,\*](#)  
1612 [1981.](#)

1613 [Kleinen, T., Brovkin, V., & Schuldt, R. J.: A dynamic model of wetland extent and peat](#)  
1614 [accumulation: results for the Holocene. \*Biogeosciences\*, 9\(1\), 235-248, 2012.](#)

1615 [Kuhry, P., & Vitt, D. H.: Fossil carbon/nitrogen ratios as a measure of peat](#)  
1616 [decomposition. \*Ecology\*, 77\(1\), 271-275, 1996.](#)

1617 [Linderholm, H. W.: Growing season changes in the last century. \*Agricultural and Forest\*](#)  
1618 [\*Meteorology\*, 137\(1\), 1-14, 2006.](#)

1619 [Loisel, J., Gallego-Sala, A. V., & Yu, Z.: Global-scale pattern of peatland \*Sphagnum\* growth](#)  
1620 [driven by photosynthetically active radiation and growing season length. \*Biogeosciences\*, 9\(7\),](#)  
1621 [2737-2746, 2012.](#)

1622 [Loisel, J., Yu, Z., Beilman, D. W., Camill, P., Alm, J., Amesbury, M. J., ... & Belyea, L. R.: A](#)  
1623 [database and synthesis of northern peatland soil properties and Holocene carbon and nitrogen](#)  
1624 [accumulation. \*the Holocene\*, 0959683614538073, 2014.](#)

1625 [Maltby, E., & Immirzi, P.: Carbon dynamics in peatlands and other wetland soils regional and](#)  
1626 [global perspectives. \*Chemosphere\*, 27\(6\), 999-1023, 1993.](#)

1627 [Manabe, S., & Wetherald, R. T.: On the distribution of climate change resulting from an increase](#)  
1628 [in CO<sub>2</sub> content of the atmosphere. \*Journal of the Atmospheric Sciences\*, 37\(1\), 99-118, 1980.](#)

1629 [Manabe, S., & Wetherald, R. T.: Reduction in summer soil wetness induced by an increase in](#)  
1630 [atmospheric carbon dioxide. \*Science\*, 232\(4750\), 626-628, 1986.](#)

1631 [Marcott, S. A., Shakun, J. D., Clark, P. U., & Mix, A. C.: A reconstruction of regional and global](#)  
1632 [temperature for the past 11,300 years. \*science\*, 339\(6124\), 1198-1201, 2013.](#)

1633 [Matthews, E., & Fung, I.: Methane emission from natural wetlands: Global distribution, area,](#)  
1634 [and environmental characteristics of sources. \*Global biogeochemical cycles\*, 1\(1\), 61-86, 1987.](#)

1635 [McGuire, A. D., & Hobbie, J. E.: Global climate change and the equilibrium responses of carbon](#)  
1636 [storage in arctic and subarctic regions. In \*Modeling the Arctic system: A workshop report on the\*](#)  
1637 [\*state of modeling in the Arctic System Science program\*, pp. 53-54, 1997.](#)

1638 [McGuire, A. D., Anderson, L. G., Christensen, T. R., Dallimore, S., Guo, L., Hayes, D. J., ... &](#)  
1639 [Roulet, N.: Sensitivity of the carbon cycle in the Arctic to climate change. \*Ecological\*](#)  
1640 [\*Monographs\*, 79\(4\), 523-555, 2009.](#)

1641 [McGuire, A. D., Melillo, J. M., Kicklighter, D. W., & Joyce, L. A.: Equilibrium responses of soil](#)  
1642 [carbon to climate change: empirical and process-based estimates. \*Journal of Biogeography\*, 785-](#)  
1643 [796, 1995.](#)

1644 [Melillo, J. M., Kicklighter, D. W., McGuire, A. D., Peterjohn, W. T., & Newkirk, K.: Global](#)  
1645 [change and its effects on soil organic carbon stocks. In Dahlem Conference Proceedings, John](#)  
1646 [Wiley and Sons, New York, John Wiley & Sons, Ltd., Chichester, pp. 175-189, 1995.](#)  
1647 [Mitchell, T. D., Carter, T. R., Jones, P. D., Hulme, M., & New, M.: A comprehensive set of](#)  
1648 [high-resolution grids of monthly climate for Europe and the globe: the observed record \(1901–](#)  
1649 [2000\) and 16 scenarios \(2001–2100\).Tyndall centre for climate change research working](#)  
1650 [paper, 55\(0\), 25, 2004.](#)

1651 [Moore, T. R., Bubier, J. L., Frolking, S. E., Lafleur, P. M., & Roulet, N. T.: Plant biomass and](#)  
1652 [production and CO<sub>2</sub> exchange in an ombrotrophic bog. \*Journal of Ecology\*, 90\(1\), 25-36, 2002.](#)

1653 [Nobrega, S., & Grogan, P.: Deeper snow enhances winter respiration from both plant-associated](#)  
1654 [and bulk soil carbon pools in birch hummock tundra. \*Ecosystems\*, 10\(3\), 419-431, 2007.](#)

1655 [Oechel, W. C., Hastings, S. J., Vourlitis, G., Jenkins, M., Riechers, G., & Grulke, N.: Recent](#)  
1656 [change of Arctic tundra ecosystems from a net carbon dioxide sink to a](#)  
1657 [source. \*Nature\*, 361\(6412\), 520-523, 1993.](#)

1658 [Oechel, W. C.: Nutrient and water flux in a small arctic watershed: an overview. \*Holarctic\*](#)  
1659 [\*Ecology\*, 229-237, 1989.](#)

1660 [Oksanen, P. O., Kuhry, P., & Alekseeva, R. N.: Holocene development of the Rogovaya river](#)  
1661 [peat plateau, European Russian Arctic. \*The Holocene\*, 11\(1\), 25-40, 2001.](#)

1662 [Peteet, D., Andreev, A., Bardeen, W., & Mistretta, F.: Long-term Arctic peatland dynamics,](#)  
1663 [vegetation and climate history of the Pur-Taz region, western Siberia. \*Boreas\*, 27\(2\), 115-126,](#)  
1664 [1998.](#)

1665 [Prentice, I. C., Cramer, W., Harrison, S. P., Leemans, R., Monserud, R. A., & Solomon, A. M.:](#)  
1666 [Special paper: a global biome model based on plant physiology and dominance, soil properties](#)  
1667 [and climate. \*Journal of biogeography\*, 117-134, 1992.](#)

1668 [Raich, J. W., Rastetter, E. B., Melillo, J. M., Kicklighter, D. W., Steudler, P. A., Peterson, B. J.,](#)  
1669 [... & Vorosmarty, C. J.: Potential net primary productivity in South America: application of a](#)  
1670 [global model. \*Ecological Applications\*, 1\(4\), 399-429, 1991.](#)

1671 [Renssen, H., Seppä, H., Heiri, O., Roche, D. M., Goosse, H., & Fichefet, T.: The spatial and](#)  
1672 [temporal complexity of the Holocene thermal maximum. \*Nature Geoscience\*, 2\(6\), 411-414,](#)  
1673 [2009.](#)

1674 [Roulet, N. T., Lafleur, P. M., Richard, P. J., Moore, T. R., Humphreys, E. R., & Bubier, J. I. L.](#)  
1675 [L.: Contemporary carbon balance and late Holocene carbon accumulation in a northern](#)  
1676 [peatland. \*Global Change Biology\*, 13\(2\), 397-411, 2007.](#)

1677 [Saarinen, T.: Biomass and production of two vascular plants in a boreal mesotrophic](#)  
1678 [fen. \*Canadian Journal of Botany\*, 74\(6\), 934-938, 1996.](#)

1679 [Schuur, E. A., Bockheim, J., Canadell, J. G., Euskirchen, E., Field, C. B., Goryachkin, S. V., ...](#)  
1680 [& Mazhitova, G.: Vulnerability of permafrost carbon to climate change: implications for the](#)  
1681 [global carbon cycle. \*BioScience\*, 58\(8\), 701-714, 2008.](#)

1682 [Sitch, S., Smith, B., Prentice, I. C., Arneth, A., Bondeau, A., Cramer, W., ... & Thonicke, K.:](#)  
1683 [Evaluation of ecosystem dynamics, plant geography and terrestrial carbon cycling in the LPJ](#)  
1684 [dynamic global vegetation model. \*Global Change Biology\*, 9\(2\), 161-185, 2003.](#)

1685 [Spahni, R., Joos, F., Stocker, B. D., Steinacher, M., & Yu, Z. C.: Transient simulations of the](#)  
1686 [carbon and nitrogen dynamics in northern peatlands: from the Last Glacial Maximum to the 21st](#)  
1687 [century. \*Climate of the Past\*, 9\(3\), 1287-1308, 2013.](#)

1688 [Stocker, B. D., Spahni, R., & Joos, F.: DYPTOP: a cost-efficient TOPMODEL implementation](#)  
1689 [to simulate sub-grid spatio-temporal dynamics of global wetlands and peatlands. \*Geoscientific\*](#)  
1690 [Model Development](#), 7(6), 3089-3110, 2014.

1691 [Stocker, B. D., Strassmann, K., & Joos, F.: Sensitivity of Holocene atmospheric CO<sub>2</sub> and the](#)  
1692 [modern carbon budget to early human land use: analyses with a process-based](#)  
1693 [model. \*Biogeosciences\*](#), 8(1), 69-88, 2011.

1694 [Tang, J., & Zhuang, Q.: A global sensitivity analysis and Bayesian inference framework for](#)  
1695 [improving the parameter estimation and prediction of a process-based Terrestrial Ecosystem](#)  
1696 [Model. \*Journal of Geophysical Research: Atmospheres\*](#), 114(D15), 2009.

1697 [Tang, J., & Zhuang, Q.: Equifinality in parameterization of process-based biogeochemistry](#)  
1698 [models: A significant uncertainty source to the estimation of regional carbon dynamics. \*Journal\*](#)  
1699 [of Geophysical Research: Biogeosciences](#), 113(G4), 2008.

1700 [Tang, J., Zhuang, Q., Shannon, R. D., & White, J. R.: Quantifying wetland methane emissions](#)  
1701 [with process-based models of different complexities. \*Biogeosciences\*](#), 7(11), 3817-3837, 2010.

1702 [Tarnocai, C., Canadell, J. G., Schuur, E. A. G., Kuhry, P., Mazhitova, G., & Zimov, S.: Soil](#)  
1703 [organic carbon pools in the northern circumpolar permafrost region. \*Global biogeochemical\*](#)  
1704 [cycles](#), 23(2), 2009.

1705 [Timm, O., & Timmermann, A.: Simulation of the Last 21 000 Years Using Accelerated](#)  
1706 [Transient Boundary Conditions\\*. \*Journal of Climate\*](#), 20(17), 4377-4401, 2007.

1707 [Tucker, C. J., Slayback, D. A., Pinzon, J. E., Los, S. O., Myneni, R. B., & Taylor, M. G.: Higher](#)  
1708 [northern latitude normalized difference vegetation index and growing season trends from 1982 to](#)  
1709 [1999. \*International journal of biometeorology\*](#), 45(4), 184-190, 2001.

1710 [Turetsky, M. R., Treat, C. C., Waldrop, M. P., Waddington, J. M., Harden, J. W., & McGuire, A.](#)  
1711 [D.: Short-term response of methane fluxes and methanogen activity to water table and soil](#)  
1712 [warming manipulations in an Alaskan peatland. \*Journal of Geophysical Research:\*](#)  
1713 [Biogeosciences](#), 113(G3), 2008.

1714 [Turunen, J., Tomppo, E., Tolonen, K., & Reinikainen, A.: Estimating carbon accumulation rates](#)  
1715 [of undrained mires in Finland—application to boreal and subarctic regions. \*The Holocene\*](#), 12(1),  
1716 69-80, 2002.

1717 [Vitt, D. H., Halsey, L. A., Bauer, I. E., & Campbell, C.: Spatial and temporal trends in carbon](#)  
1718 [storage of peatlands of continental western Canada through the Holocene. \*Canadian Journal of\*](#)  
1719 [Earth Sciences](#), 37(5), 683-693, 2000.

1720 [Wang, S., Zhuang, Q., Yu, Z., Bridgham, S., & Keller, J. K.: Quantifying peat carbon](#)  
1721 [accumulation in Alaska using a process-based biogeochemistry model, \*Journal of Geophysical\*](#)  
1722 [Research: Biogeosciences](#), 121, doi: 10.1002/2016JG003452, 2016.

1723 [XU-RI and PRENTICE, I. C.: Terrestrial nitrogen cycle simulation with a dynamic global](#)  
1724 [vegetation model. \*Global Change Biology\*](#), 14: 1745–1764. doi:10.1111/j.1365-  
1725 [2486.2008.01625.x, 2008.](#)

1726 [Yu, Z. C.: Northern peatland carbon stocks and dynamics: a review. \*Biogeosciences\*](#), 9(10),  
1727 [4071-4085, 2012.](#)



1728 [Yu, Z., Beilman, D. W., & Jones, M. C.: Sensitivity of northern peatland carbon dynamics to](#)  
1729 [Holocene climate change. Carbon cycling in northern peatlands, 55-69, 2009.](#)

1730 [Yu, Z., Loisel, J., Brosseau, D. P., Beilman, D. W., & Hunt, S. J.: Global peatland dynamics](#)  
1731 [since the Last Glacial Maximum. Geophysical Research Letters, 37\(13\), 2010.](#)

1732 [Zhuang, Q., McGuire, A. D., Melillo, J. M., Clein, J. S., Dargaville, R. J., Kicklighter, D. W., ...](#)  
1733 [& Hobbie, J. E.: Carbon cycling in extratropical terrestrial ecosystems of the Northern](#)  
1734 [Hemisphere during the 20th century: a modeling analysis of the influences of soil thermal](#)  
1735 [dynamics. Tellus B, 55\(3\), 751-776, 2003.](#)

1736 [Zhuang, Q., McGuire, A. D., O'Neill, K. P., Harden, J. W., Romanovsky, V. E., & Yarie, J.:](#)  
1737 [Modeling soil thermal and carbon dynamics of a fire chronosequence in interior Alaska. Journal](#)  
1738 [of Geophysical Research: Atmospheres, 107\(D1\), 2002.](#)

1739 [Zhuang, Q., Melillo, J. M., Kicklighter, D. W., Prinn, R. G., McGuire, A. D., Steudler, P. A., ...](#)  
1740 [& Hu, S.: Methane fluxes between terrestrial ecosystems and the atmosphere at northern high](#)  
1741 [latitudes during the past century: A retrospective analysis with a process-based biogeochemistry](#)  
1742 [model. Global Biogeochemical Cycles, 18\(3\), 2004.](#)

1743 [Zhuang, Q., Melillo, J. M., McGuire, A. D., Kicklighter, D. W., Prinn, R. G., Steudler, P. A., ...](#)  
1744 [& Hu, S.: Net emissions of CH<sub>4</sub> and CO<sub>2</sub> in Alaska: Implications for the region's greenhouse](#)  
1745 [gas budget. Ecological Applications, 17\(1\), 203-212, 2007.](#)

1746 [Zhuang, Q., Romanovsky, V. E., & McGuire, A. D.: Incorporation of a permafrost model into a](#)  
1747 [large-scale ecosystem model: Evaluation of temporal and spatial scaling issues in simulating soil](#)  
1748 [thermal dynamics. Journal of Geophysical Research: Atmospheres, 106\(D24\), 33649-33670,](#)  
1749 [2001.](#)

1750 [Zhuang, Q., Zhu, X., He, Y., Prigent, C., Melillo, J. M., McGuire, A. D., ... & Kicklighter, D.](#)  
1751 [W.: Influence of changes in wetland inundation extent on net fluxes of carbon dioxide and](#)  
1752 [methane in northern high latitudes from 1993 to 2004. Environmental Research Letters, 10\(9\),](#)  
1753 [095009, 2015.](#)

1754 [Zimov, S. A., Schuur, E. A., & Chapin III, F. S.: Permafrost and the global carbon](#)  
1755 [budget. Science\(Washington\), 312\(5780\), 1612-1613, 2006.](#)

1756 [Zoltai, S. C.: Permafrost distribution in peatlands of west-central Canada during the Holocene](#)  
1757 [warm period 6000 years BP. Géographie physique et Quaternaire, 49\(1\), 45-54, 1995.](#)

1758

1759

1760

1761

1762 ~~Table 1. Assignment of biomized fossil pollen data to the vegetation types in TEM (He et al.,~~  
 1763 ~~2014).~~

| <del>TEM upland vegetation</del>                        | <del>TEM peatland vegetation</del>          | <del>BIOMISE code</del>   |
|---|---|---------------------------|
| <del>Alpine tundra</del>                                |   | <del>CUSH DRYT PROS</del> |
| <del>Moist tundra</del>                                 | <del><i>Sphagnum</i> spp. open fen</del>    | <del>DWAR SHRU</del>      |
| <del>Boreal evergreen needleleaf and mixed forest</del> |   | <del>TAIG COCO CLMX</del> |
| <del>Boreal deciduous broadleaf forest</del>            | <del><i>Sphagnum</i> black spruce bog</del> | <del>COMX</del>           |
|   |   | <del>CLDE</del>           |

1764

1765

1766 ~~Table 2. Relations between peatland basal age and vegetation distribution~~

| <del>Peatland basal age</del> | <del>Vegetation types</del>                   | <del>Location</del>                                    |
|-------------------------------|---|--|
| <del>15–11 ka</del>           | <del>alpine tundra</del>                      | <del>south, northwestern, and southeastern coast</del> |
| <del>11–10 ka</del>           | <del>moist tundra</del>                       | <del>south, north, and southeastern coast</del>        |
|                               | <del>boreal evergreen needleleaf forest</del> | <del>east</del>  |
|                               | <del>boreal deciduous broadleaf forest</del>  | <del>east-central part</del>                           |
| <del>10–9 ka</del>            | <del>moist tundra</del>                       | <del>south and north coast</del>                       |
|                               | <del>boreal evergreen needleleaf forest</del> | <del>central part</del>                                |
|                               | <del>boreal deciduous broadleaf forest</del>  |  |
| <del>9–5 ka</del>             | <del>moist tundra</del>                       | <del>central part</del>                                |
|                               | <del>boreal evergreen needleleaf forest</del> |  |
| <del>5 ka–1900 AD</del>       | <del>moist tundra</del>                       | <del>west coast</del>                                  |
|                               | <del>boreal evergreen needleleaf forest</del> |  |

1767

1768

1769

1770

1771

1772

1773

1774

1775

1776

1777

1778 **Table 3. Description of sites and variables used for parameterizing the core carbon and nitrogen**  
 1779 **module (CNDM):**

| Site <sup>a</sup> | Vegetation   | Observed variables for CNDM parameterization  | References   |
|-------------------|--|---|--|
| APEXCON           | Moderate rich open fen with sedges ( <i>Carex</i> sp.), spiked rushes ( <i>Eleocharis</i> sp.), <i>Sphagnum</i> spp., and brown mosses (e.g., <i>Drepanocladus aduncus</i> ) | Mean annual aboveground NPP in 2009;<br>Mean annual belowground NPP in 2009;<br>Aboveground biomass in 2009 | Chivers et al. (2009)<br>Turetsky et al. (2008)<br>Kane et al. (2010)<br>Churchill et al. (2011) |
| APEXPER           | Peat plateau bog with black spruce ( <i>Picea mariana</i> ), <i>Sphagnum</i> spp., and feather mosses  |   |  |

1780  
 1781 <sup>a</sup>The Alaskan Peatland Experiment (APEX) site is adjacent to the Bonanza Creek Experimental Forest (BCEF) site,  
 1782 approximately 35 km southwest of Fairbanks, AK. The area is classified as continental boreal climate with a mean annual  
 1783 temperature of -2.9°C and annual precipitation of 269 mm, of which 30% is snow (Hinzman et al., 2006).

1784

1785

1786 **Table 4. Carbon pools and fluxes used for calibration of CMDM**

| Annual Carbon Fluxes or Pools <sup>a</sup> | <i>Sphagnum</i> Open Fen |            | <i>Sphagnum</i> Black Spruce Bog |            | References                                  |
|--|--------------------------|------------|----------------------------------|------------|---|
|  | Observation              | Simulation | Observation                      | Simulation |   |
| NPP  | 445±260                  | 410        | 433±107                          | 390        | Turetsky et al. (2008),<br>Churchill (2011) |
| Aboveground Vegetation Carbon              | 149-287                  |            | 423                              |            | Moore et al. (2002)                         |
| Belowground Vegetation Carbon              | 564                      |            | 658-1128                         |            | Zhuang et al. (2002)                        |
| Total Vegetation Carbon Density            | 713-851                  | 800        | 732-1551                         | 1300       | Farnocai et al. (2009)                      |
| Litter Fall Carbon Flux                    | 300                      | 333        | 300                              | 290        | Kuhry and Vitt (1996)                       |
| Methane Emission Flux                      | 19.5                     | 19.2       | 9.7                              | 12.8       |   |

1787

1788 <sup>a</sup>Units for annual net primary production (NPP) and litter fall carbon are g C m<sup>-2</sup> yr<sup>-1</sup>. Units for vegetation carbon density are  
 1789 g C m<sup>-2</sup>. Units for Methane emissions are g C — CH<sub>4</sub> m<sup>-2</sup> yr<sup>-1</sup>. The simulated total annual methane fluxes were compared with  
 1790 the observations at APEXCON in 2005 and SPRUCE in 2012. A ratio of 0.47 was used to convert vegetation biomass to carbon  
 1791 (Raich 1991).

1792

1793

1794

1795

1796

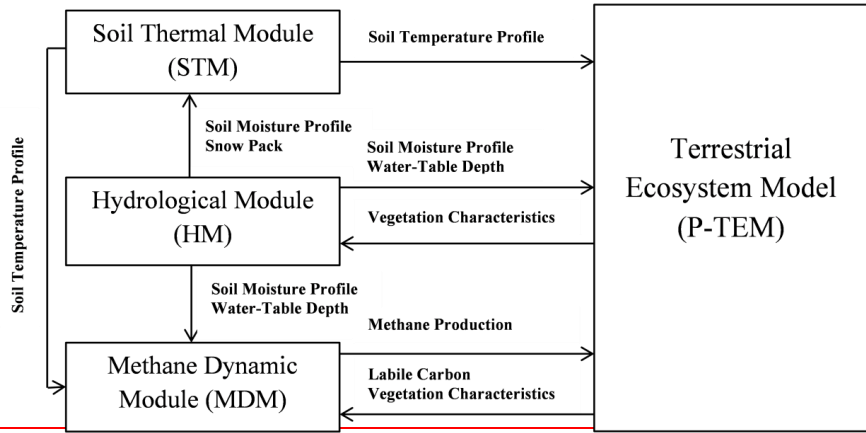
1797

1798

1799

1800

1801



1802

1803 **Figure 1. P-TEM (Peatland Terrestrial Ecosystem Model) modeling framework, including a soil**  
1804 **thermal module (STM), a hydrologic module (HM), a carbon/ nitrogen dynamic model (CNDM),**  
1805 **and a methane dynamics module (MDM) (Wang et al., 2016).**

1806

1807

1808

1809

1810

1811

1812

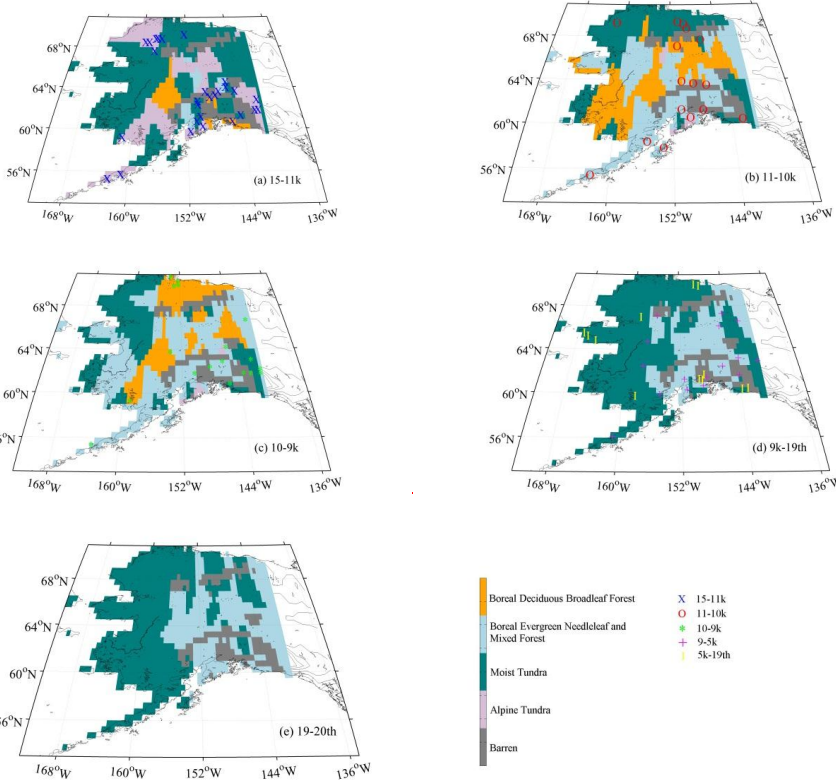
1813

1814

1815

1816

1817



1818

1819

1820

1821

1822

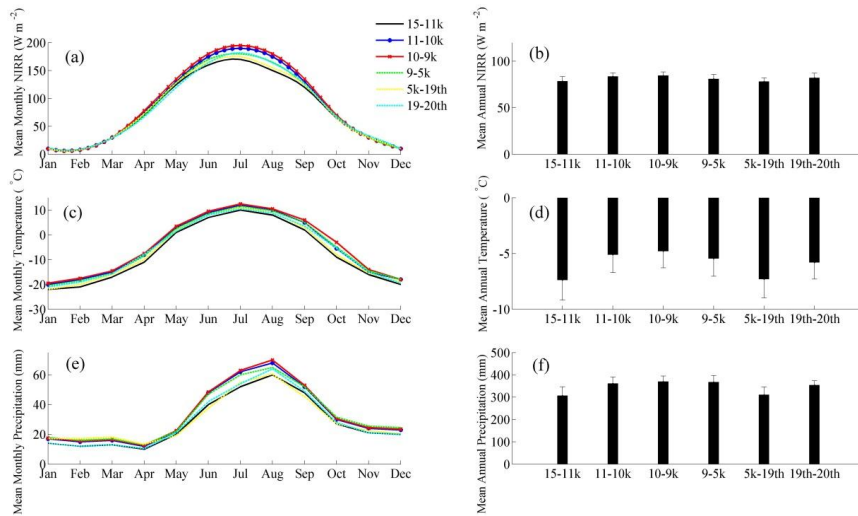
1823

1824

1825

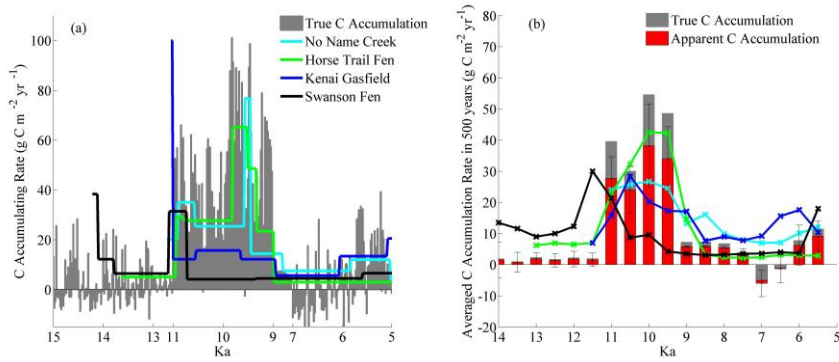
1826

Figure 2. Alaskan vegetation distribution maps reconstructed from fossil pollen data during (a) 15–11 ka, (b) 11–10 ka, (c) 10–9 ka, (d) 9 ka–1900 AD, and (e) 1900–2000 AD (He et al., 2014). Symbols represent the basal age of peat samples (n = 102) in Gorham et al. (2012). Barren refers to mountain range and large body areas which could not be interpolated.



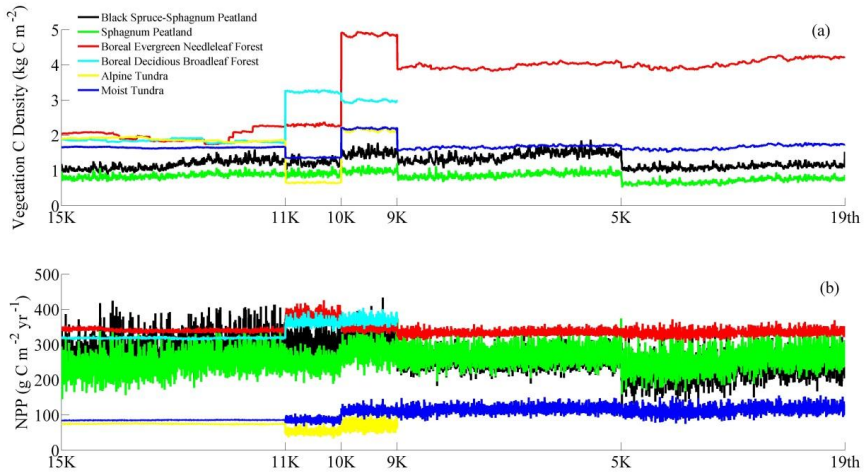
1827  
 1828 **Figure 3. Simulated Paleo-climate and other input data from 15 ka to 2000 AD, including (a)**  
 1829 **mean monthly and (b) mean annual net incoming solar radiation ( $W m^{-2}$ ), (c) mean**  
 1830 **monthly and (d) mean annual air temperature ( $^{\circ}C$ ), (e) mean monthly and (f) mean annual**  
 1831 **precipitation (mm) (Timm and Timmermann, 2007; He et al., 2014).**

1832  
 1833  
 1834  
 1835  
 1836  
 1837  
 1838



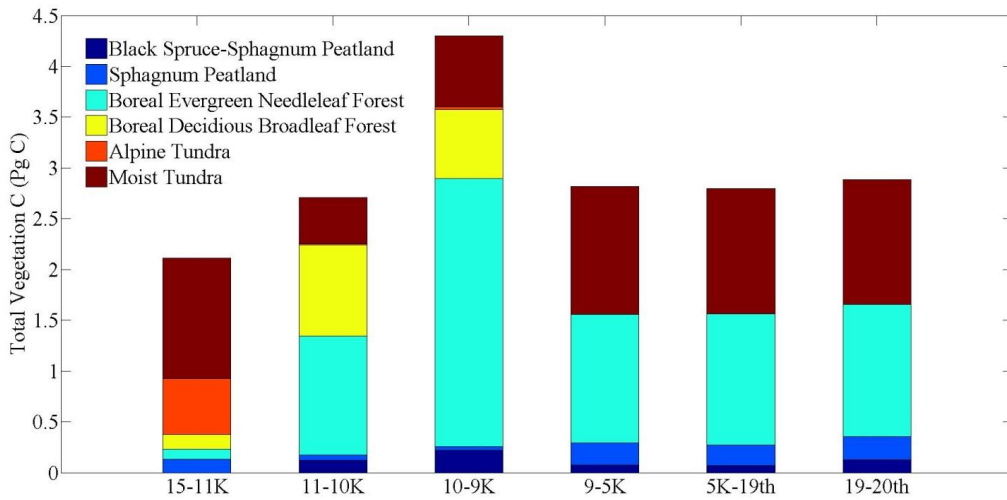
1839  
 1840 **Figure 4. Simulated and observed carbon accumulation rates from 15 ka to 5 ka in 20-yr bins (a)**  
 1841 **and 500-yr bins with standard deviation (b) for No Name Creek, Horse Trail Fen, Kenai Gasfield,**  
 1842 **and Swanson Fen. Peat core data were from Jones and Yu (2010).**

1843  
 1844  
 1845  
 1846  
 1847  
 1848  
 1849  
 1850  
 1851



1852  
1853 **Figure 5. Simulated (a) mean vegetation carbon density (kg C m<sup>-2</sup>) of different vegetation types**  
1854 **and (b) NPP (g C m<sup>-2</sup> yr<sup>-1</sup>).**

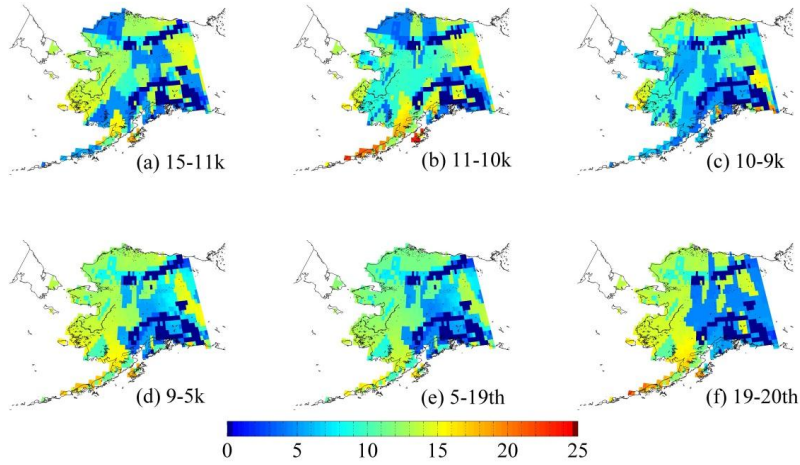
1855  
1856  
1857



1858  
1859 **Figure 6. Total C (Pg C) stored in vegetation of Alaska for different time periods.**

1860





1861  
 1862  
 1863  
 1864  
 1865  
 1866  
 1867  
 1868  
 1869

Figure 7. Non-peatland (mineral) SOC density ( $\text{kg C m}^{-2}$ ) (cumulative) during (a) 15–11 ka, (b) 11–10 ka, (c) 10–9 ka, (d) 9–5 ka, (e) 5 ka–1900 AD, and (f) 1900–2000 AD.

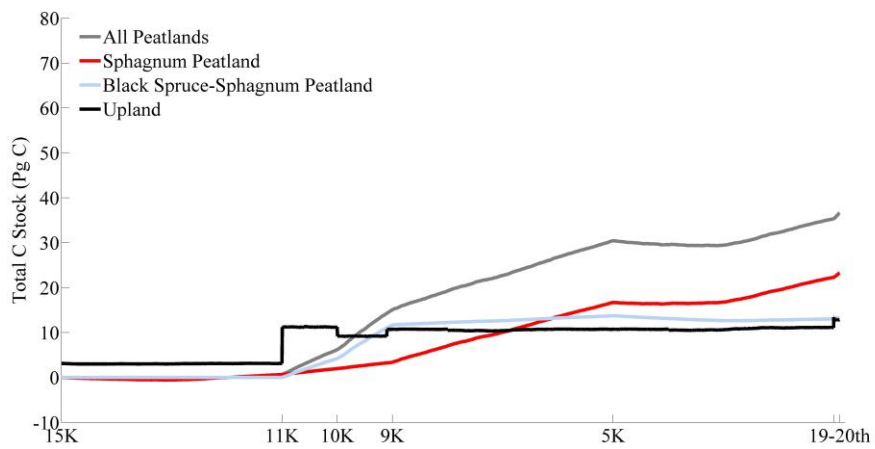
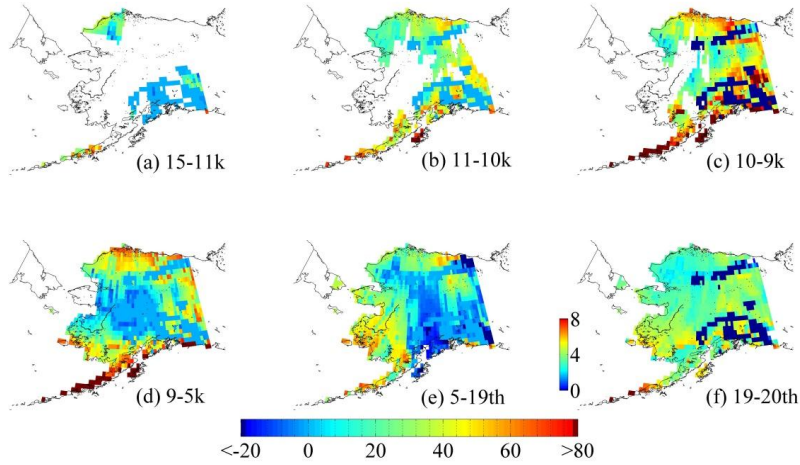


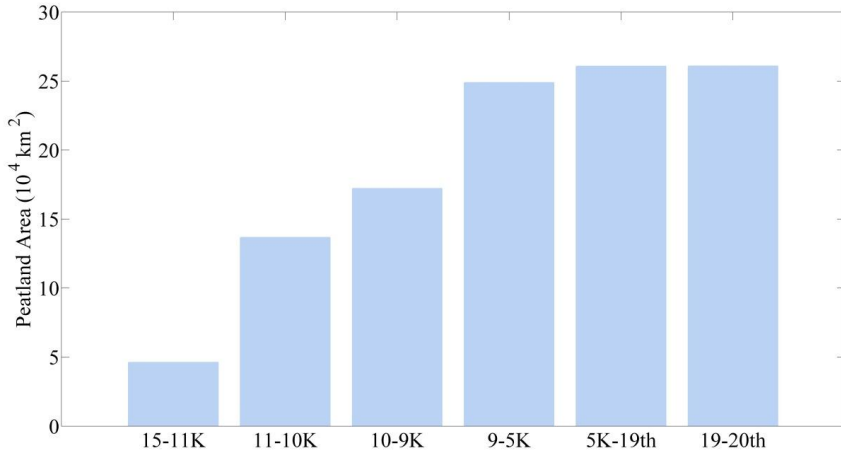
Figure 8. Total C stock accumulated from 15 ka to 2000 AD for all peatlands, *Sphagnum* open peatland, *Sphagnum* black spruce peatland, and upland soils.

1870  
 1871  
 1872  
 1873  
 1874  
 1875  
 1876  
 1877  
 1878  
 1879



1880  
 1881 **Figure 9. Peatland area expansion and peat soil C accumulation per 1000 years ( $\text{kg C m}^{-2} \text{kyr}^{-1}$ )**  
 1882 **during (a) 15–11 ka, (b) 11–10 ka, (c) 10–9 ka, (d) 9–5 ka, (e) 5 ka–1900 AD, and (f) 1900–2000**  
 1883 **AD. The amount of C represents the C accumulation as the difference between the peat C**  
 1884 **amount in the final year and the first year in each time slice.**

1885  
 1886  
 1887  
 1888  
 1889  
 1890  
 1891  
 1892  
 1893  
 1894  
 1895  
 1896  
 1897



1898  
1899  
1900  
1901  
1902

Figure 10. Peatland expansion area ( $10^4 \text{ km}^2$ ) in different time slices, the area of barren in the map is set to  $0 \text{ km}^2$ .

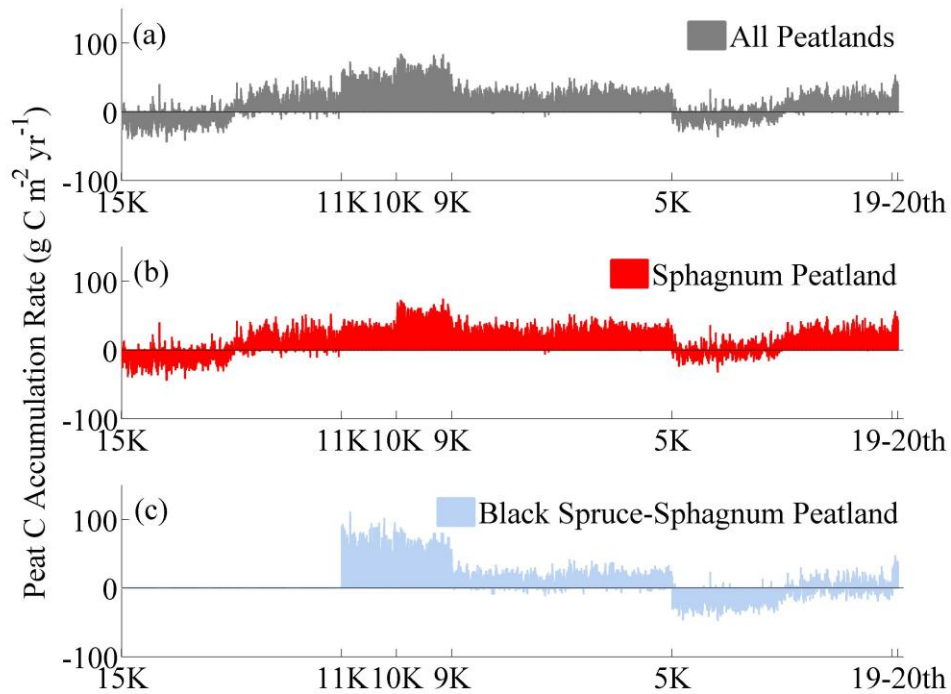
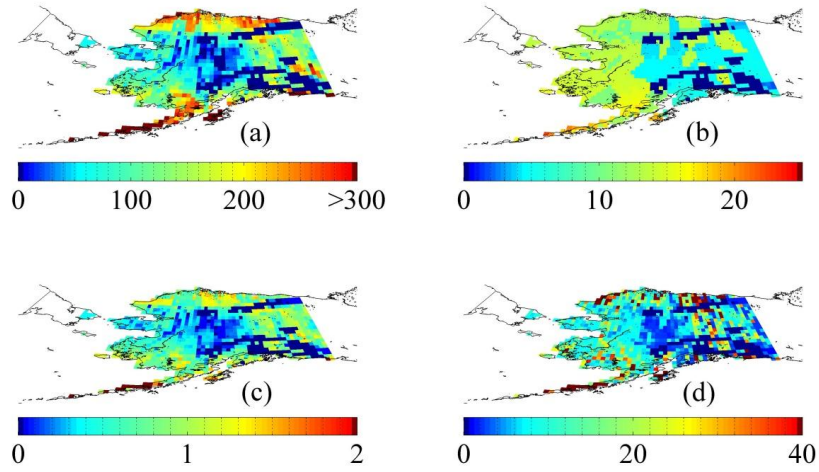


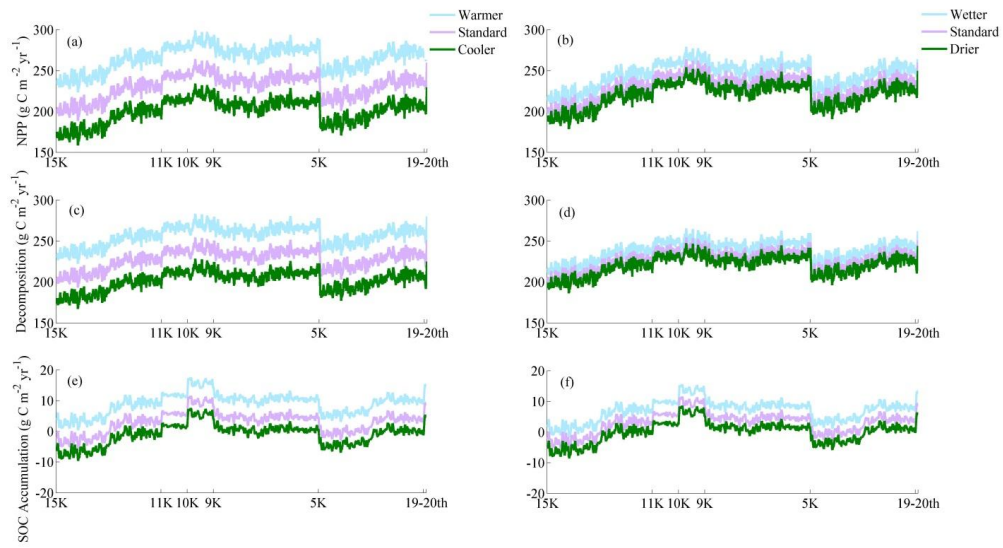
Figure 11. Peatland mean C accumulation rates from 15 ka to 2000 AD for (a) weighted average of all peatlands, (b) *Sphagnum* open peatland, and (c) *Sphagnum* black spruce peatland.

1903  
 1904  
 1905  
 1906  
 1907  
 1908  
 1909  
 1910  
 1911  
 1912  
 1913  
 1914



1915  
 1916 **Figure 12. The spatial distribution of (a) total peat SOC density ( $\text{kg C m}^{-2}$ ), (b) total mineral**  
 1917 **SOC density ( $\text{kg C m}^{-2}$ ), (c) total peat depth (m), and (d) weighted average of total (peatlands**  
 1918 **plus non-peatlands) SOC density ( $\text{kg C m}^{-2}$ ) in Alaska from 15 ka to 2000 AD.**

1919  
 1920  
 1921



1922

1923

1924

1925

Figure 13. Temperature and precipitation effects on (a)(b) annual NPP, (c)(d) annual SOC decomposition rate (aerobic plus anaerobic), and (e)(f) annual SOC accumulation rate of Alaska. A 10-year moving average was applied.

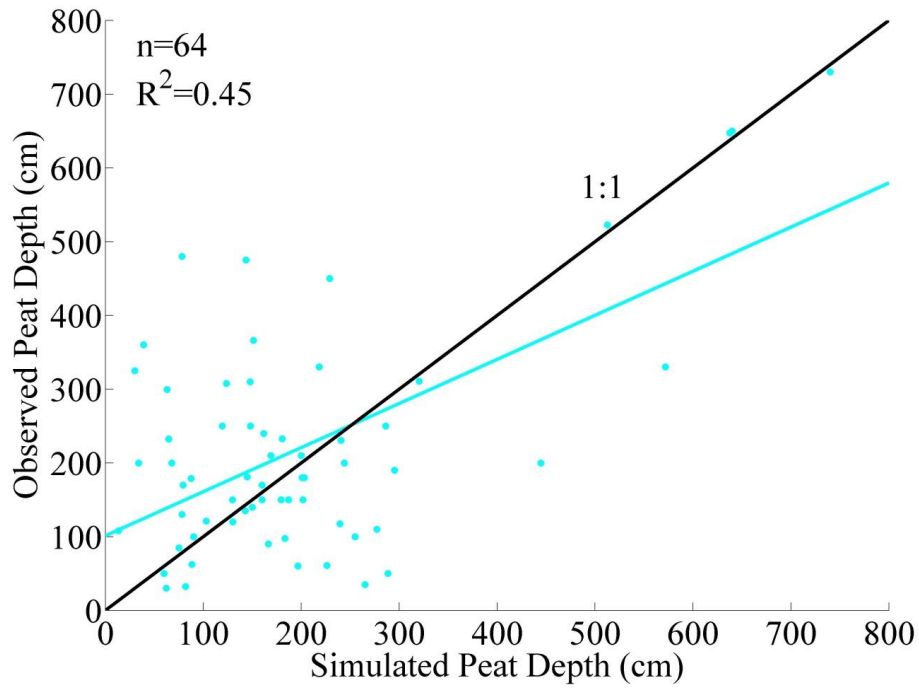


Figure 14. Field-based estimates and model simulations for peat depths in Alaska: The observed and simulated data are extracted from the same grids on the map. Linear regression line (cyan) is compared with the 1:1 line. The linear regression is significant ( $P < 0.001$ ,  $n = 64$ ) with  $R^2 = 0.45$ , slope = 0.65, and intercept = 101.05 cm. The observations of  $> 1000$  cm are treated as outliers.

1926  
 1927  
 1928  
 1929  
 1930  
 1931  
 1932  
 1933  
 1934  
 1935  
 1936  
 1937  
 1938  
 1939



1940 Table 1. Description of sites and variables used for parameterizing the core carbon and nitrogen  
 1941 module (CNDM).

| Site <sup>a</sup> | Vegetation   | Observed variables for CNDM parameterization   | References   |
|-------------------|--|--|--|
| <u>APEXCON</u>    | <u>Moderate rich open fen with sedges (<i>Carex</i> sp.), spiked rushes (<i>Eleocharis</i> sp.), <i>Sphagnum</i> spp., and brown mosses (e.g., <i>Drepanocladus aduncus</i>)</u> | <u>Mean annual aboveground NPP in 2009;</u><br><u>Mean annual belowground NPP in 2009;</u><br><u>Aboveground biomass in 2009</u> | <u>Chivers et al. (2009)</u><br><u>Turetsky et al. (2008)</u><br><u>Kane et al. (2010)</u><br><u>Churchill et al. (2011)</u> |
| <u>APEXPER</u>    | <u>Peat plateau bog with black spruce (<i>Picea mariana</i>), <i>Sphagnum</i> spp., and feather mosses</u>   |  |  |

1942  
 1943 <sup>a</sup>The Alaskan Peatland Experiment (APEX) site is adjacent to the Bonanza Creek Experimental Forest (BCEF) site,  
 1944 approximately 35 km southwest of Fairbanks, AK. The area is classified as continental boreal climate with a mean annual  
 1945 temperature of -2.9°C and annual precipitation of 269 mm, of which 30% is snow (Hinzman et al., 2006).

1946  
 1947

1948 Table 2. Carbon pools and fluxes used for calibration of CMDM

| Annual Carbon Fluxes or Pools <sup>a</sup> | <u><i>Sphagnum</i> Open Fen</u> |                   | <u><i>Sphagnum</i>-Black Spruce Bog</u> |                   | References  |
|--|---------------------------------|-------------------|---|-------------------|---|
|  | <u>Observation</u>              | <u>Simulation</u> | <u>Observation</u>                      | <u>Simulation</u> |   |
| <u>NPP</u>                                 | <u>445±260</u>                  | <u>410</u>        | <u>433±107</u>                          | <u>390</u>        | <u>Turetsky et al. (2008),</u><br><u>Churchill (2011)</u> |
| <u>Aboveground Vegetation Carbon</u>       | <u>149-287</u>                  |                   | <u>423</u>                              |                   | <u>Saarinen et al. (1996)</u>                             |
| <u>Belowground Vegetation Carbon</u>       | <u>347-669</u>                  |                   | <u>987</u>                              |                   | <u>Moore et al. (2002)</u>                                |
| <u>Total Vegetation Carbon Density</u>     | <u>496-856</u>                  | <u>800</u>        | <u>1410</u>                             | <u>1300</u>       | <u>Zhuang et al. (2002)</u>                               |
| <u>Litter Fall Carbon Flux</u>             | <u>300</u>                      | <u>333</u>        | <u>300</u>                              | <u>290</u>        | <u>Tarnocai et al. (2009)</u>                             |
| <u>Methane Emission Flux</u>               | <u>19.5</u>                     | <u>19.2</u>       | <u>9.7</u>                              | <u>12.8</u>       | <u>Kuhry and Vitt (1996)</u>                              |

1949  
 1950 <sup>a</sup> Units for annual net primary production (NPP) and litter fall carbon are g C m<sup>-2</sup> yr<sup>-1</sup>. Units for vegetation carbon density are  
 1951 g C m<sup>-2</sup>. Units for Methane emissions are g C – CH<sub>4</sub> m<sup>-2</sup> yr<sup>-1</sup>. The simulated total annual methane fluxes were compared with  
 1952 the observations at APEXCON in 2005 and SPRUCE in 2012. A ratio of 0.47 was used to convert vegetation biomass to carbon  
 1953 (Raich 1991).

1954  
 1955  
 1956  
 1957  
 1958  
 1959  
 1960  
 1961  
 1962

1963 Table 3. Assignment of biomized fossil pollen data to the vegetation types in TEM (He et al.,  
 1964 2014).

| <u>TEM upland vegetation</u>                        | <u>TEM peatland vegetation</u>          | <u>BIOMISE code</u>   |
|---|---|-----------------------|
| <u>Alpine tundra</u>                                |   | <u>CUSH DRYT PROS</u> |
| <u>Moist tundra</u>                                 | <u><i>Sphagnum</i> spp. open fen</u>    | <u>DWAR SHRU</u>      |
| <u>Boreal evergreen needleleaf and mixed forest</u> |   | <u>TAIG COCO CLMX</u> |
| <u>Boreal deciduous broadleaf forest</u>            | <u><i>Sphagnum</i>-black spruce bog</u> | <u>COMX</u>           |
|   |   | <u>CLDE</u>           |

1965

1966

1967 Table 4. Relations between peatland basal age and vegetation distribution

| <u>Peatland basal age</u> | <u>Vegetation types</u>  | <u>Location in Alaska</u>   |
|---------------------------|--|---|
| <u>15-11 ka</u>           | <u>alpine tundra</u>   | <u>south, northwestern, and southeastern coast</u>                      |
| <u>11-10 ka</u>           | <u>moist tundra</u><br><u>boreal evergreen needleleaf forest</u><br><u>boreal deciduous broadleaf forest</u> | <u>south, north, and southeastern coast</u><br><u>east central part</u> |
| <u>10-9 ka</u>            | <u>moist tundra</u><br><u>boreal evergreen needleleaf forest</u><br><u>boreal deciduous broadleaf forest</u> | <u>south and north coast</u><br><u>central part</u>                     |
| <u>9-5 ka</u>             | <u>moist tundra</u><br><u>boreal evergreen needleleaf forest</u>   | <u>central part</u>   |
| <u>5 ka-1900 AD</u>       | <u>moist tundra</u><br><u>boreal evergreen needleleaf forest</u>   | <u>west coast</u>   |

1968

1969

1970

1971

1972

1973

1974

1975

1976

1977

1978

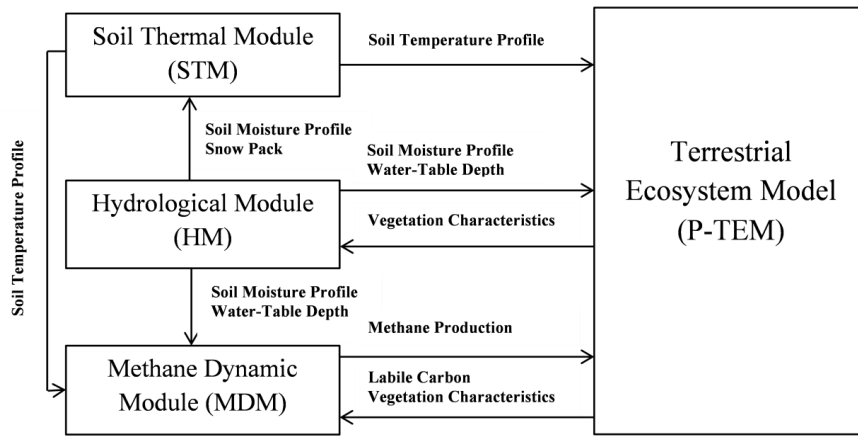
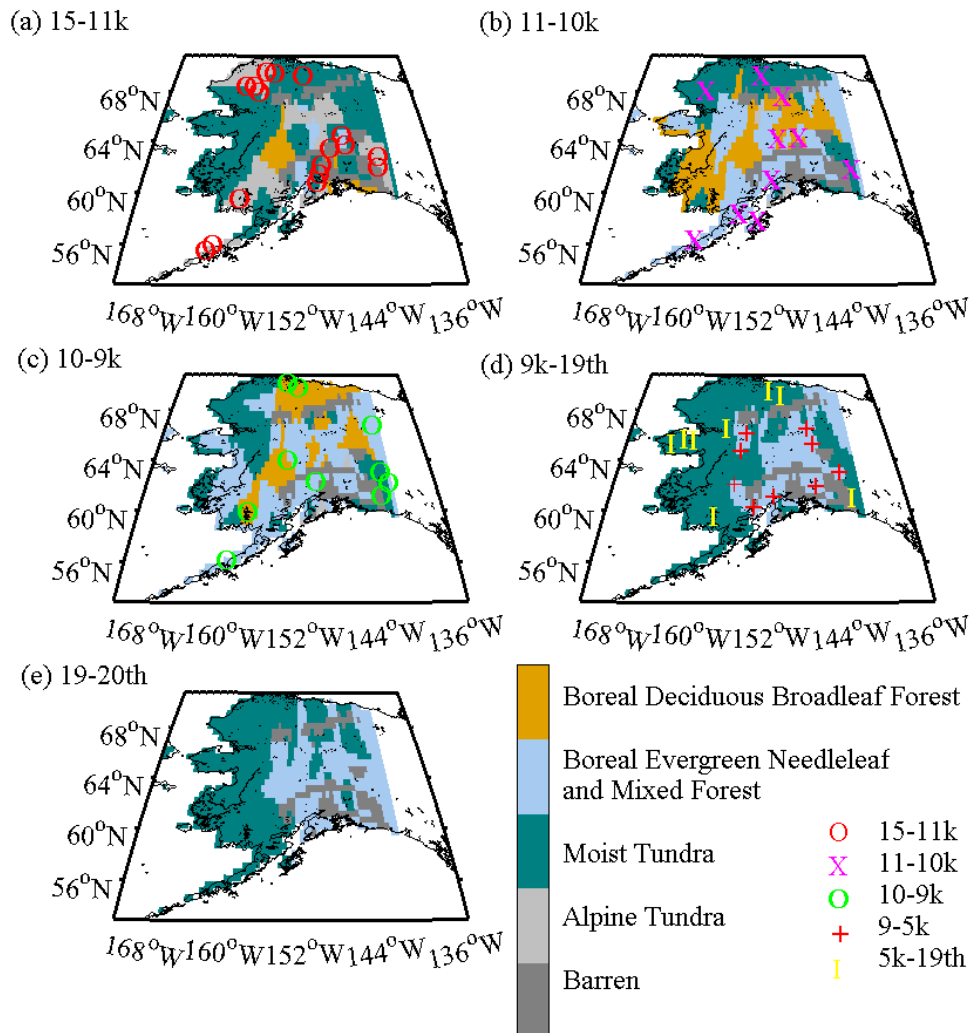


Figure 1. P-TEM (Peatland-Terrestrial Ecosystem Model) framework includes a soil thermal module (STM), a hydrologic module (HM), a carbon/ nitrogen dynamic model (CNDM), and a methane dynamics module (MDM) (Wang et al., 2016).

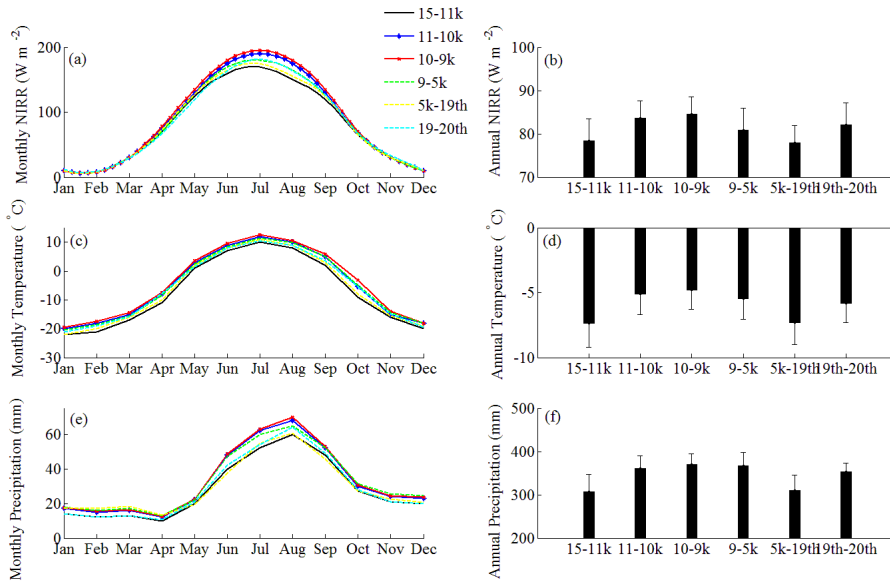
1979  
1980  
1981  
1982  
1983  
1984  
1985  
1986  
1987  
1988  
1989  
1990  
1991  
1992  
1993  
1994  
1995  
1996



1997  
 1998  
 1999  
 2000  
 2001  
 2002  
 2003  
 2004  
 2005

Figure 2. Alaskan vegetation distribution maps reconstructed from fossil pollen data during (a) 15-11 ka, (b) 11-10 ka, (c) 10-9 ka, (d) 9 ka -1900 AD, and (e) 1900-2000 AD (He et al., 2014). Symbols represent the basal age of peat samples (n = 102) in Gorham et al. (2012). Each symbol indicates 1-3 peat samples in the map. Peat samples with basal age 9-5k and 5k-19<sup>th</sup> are shown in map (d) as there is no change of vegetation distribution during 9k-19<sup>th</sup>. Barren refers to mountain range and large water body areas that can not be interpolated.

2006



2007

2008

2009

2010

2011

2012

2013

2014

2015

2016

2017

2018

Figure 3. Simulated Paleo-climate and other input data from 15 ka to 2000 AD: (a) mean monthly and (b) mean annual net incoming solar radiation ( $W m^{-2}$ ), (c) mean monthly and (d) mean annual air temperature ( $^{\circ}C$ ), (e) mean monthly, and (f) mean annual precipitation (mm) (Timm and Timmermann, 2007; He et al., 2014).

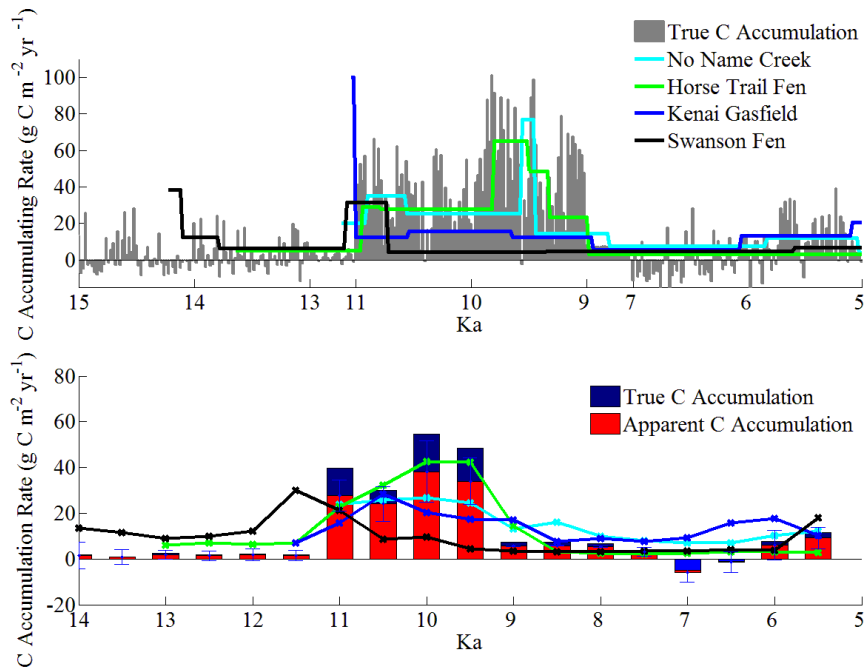
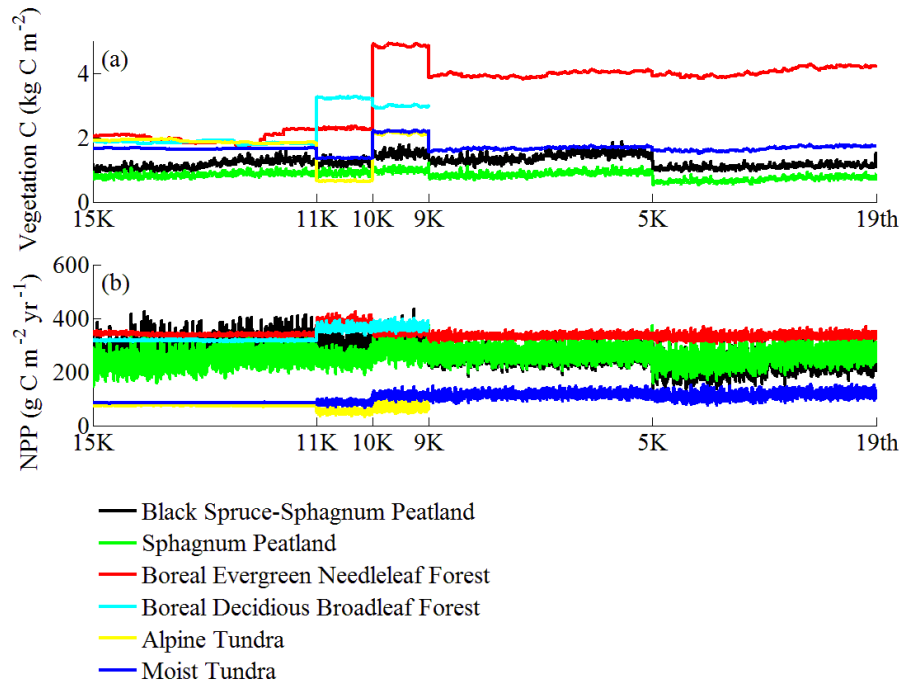


Figure 4. Simulated and observed carbon accumulation rates from 15 ka to 5 ka in 20-yr bins (a) and 500-yr bins with standard deviation (b) for No Name Creek, Horse Trail Fen, Kenai Gasfield, and Swanson Fen. Peat-core data were from Jones and Yu (2010).

2019  
 2020  
 2021  
 2022  
 2023  
 2024  
 2025  
 2026  
 2027  
 2028  
 2029  
 2030  
 2031



2032  
 2033  
 2034  
 2035  
 2036  
 2037

Figure 5. Simulated (a) mean vegetation carbon density (kg C m<sup>-2</sup>) of different vegetation types and (b) NPP (g C m<sup>-2</sup>yr<sup>-1</sup>).

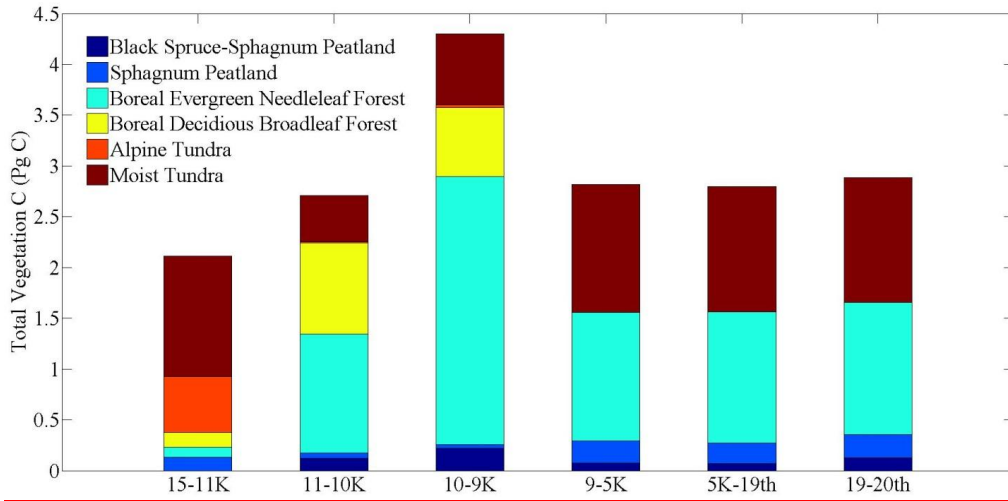
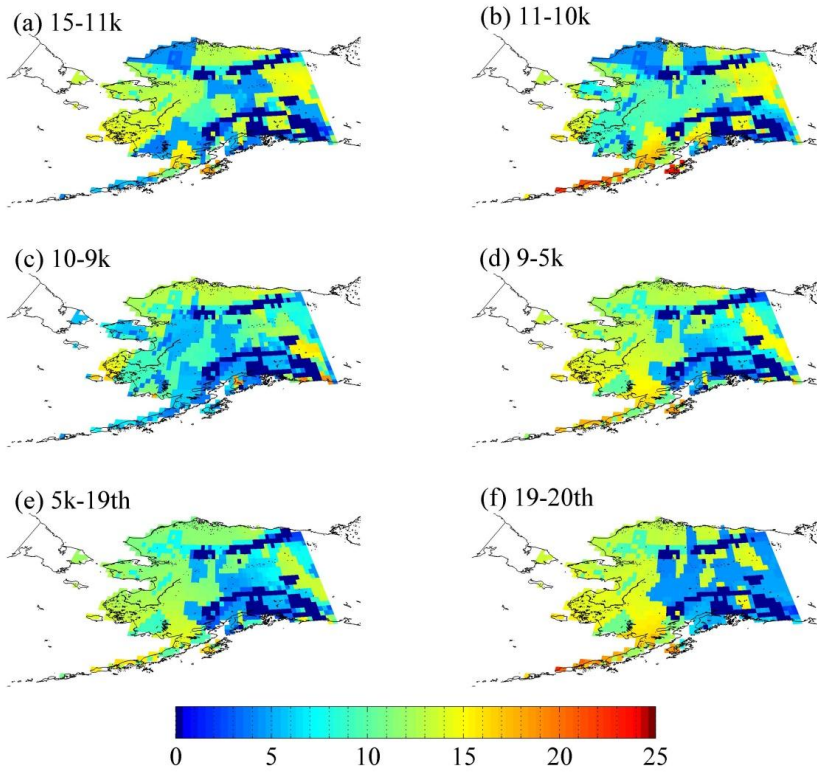


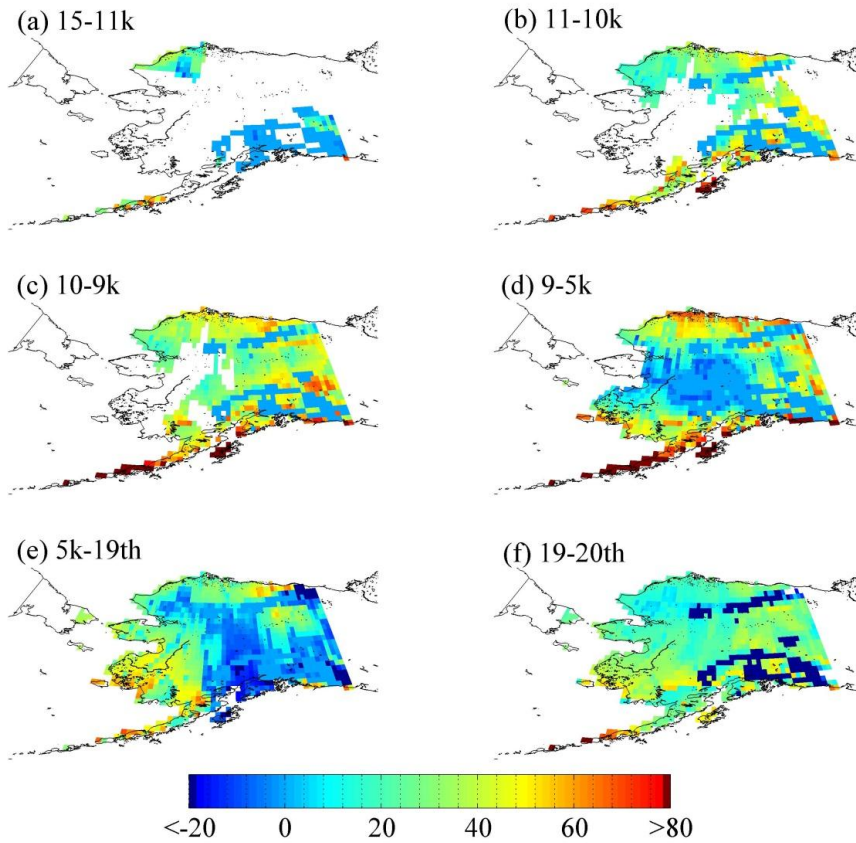
Figure 6. Total C (Pg C) stored in Alaskan vegetation for different time periods.

2038  
2039  
2040





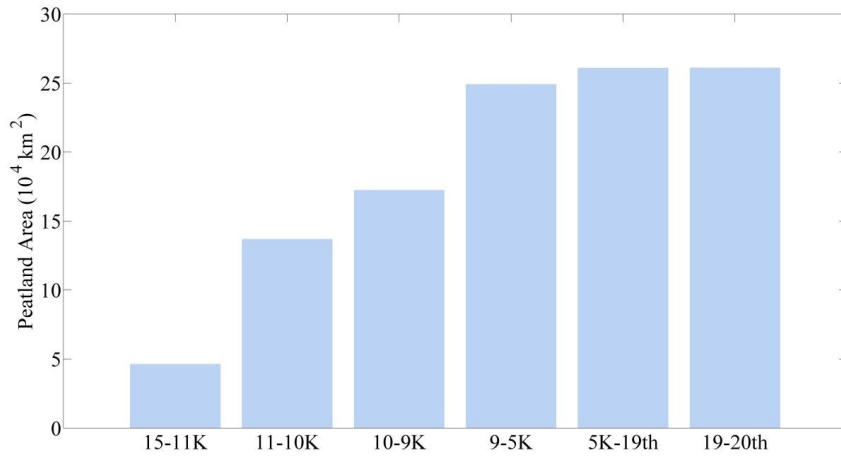
2041  
 2042 Figure 7. Average non-peatland (mineral) SOC density ( $\text{kg C m}^{-2}$ ) during (a) 15-11 ka, (b) 11-  
 2043 10 ka, (c) 10-9 ka, (d) 9-5 ka, (e) 5 ka -1900 AD, and (f) 1900-2000 AD. The period of 9k-19<sup>th</sup> in  
 2044 Figure 2d is separated into 9-5k and 5k-19<sup>th</sup>.  
 2045



2046  
 2047 Figure 8. Peatland area expansion and peat soil C accumulation per 1000 years ( $\text{kg C m}^{-2} \text{ kyr}^{-1}$ )  
 2048 during (a) 15-11 ka, (b) 11-10 ka, (c) 10-9 ka, (d) 9-5 ka, (e) 5 ka -1900 AD, and (f) 1900-2000  
 2049 AD. The amount of C represents the C accumulation as the difference between the peat C  
 2050 amount in the final year and the first year in each time slice. The period of 9k-19<sup>th</sup> in Figure 2d is  
 2051 separated into 9-5k and 5k-19<sup>th</sup>.

2052  
 2053  
 2054  
 2055  
 2056  
 2057

2058



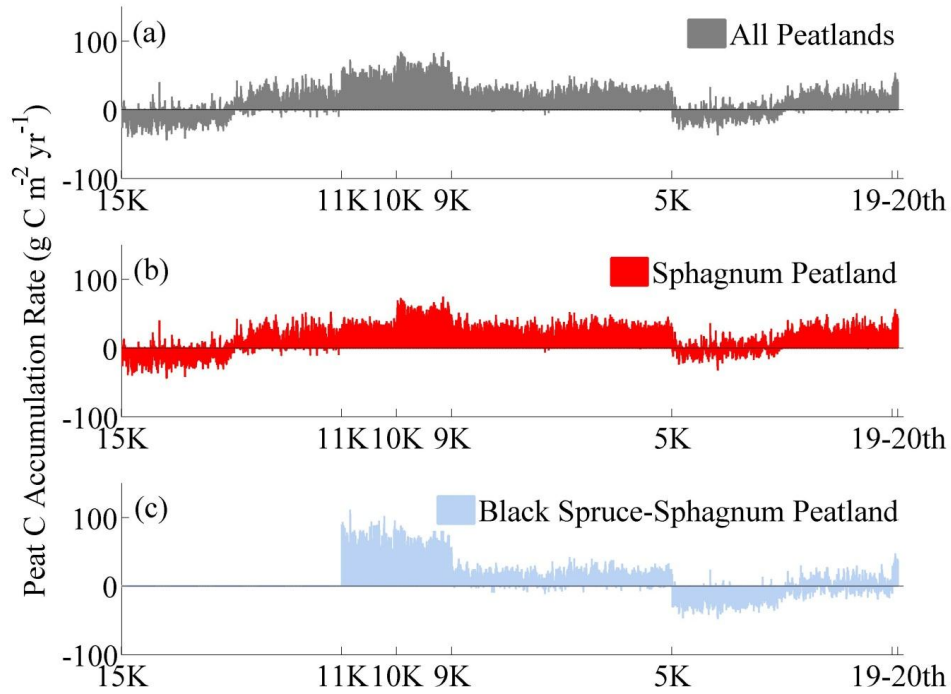
2059

2060

2061

2062

Figure 9. Peatland expansion area (10<sup>4</sup> km<sup>2</sup>) in different time slices, the area of barren in the map is set to 0 km<sup>2</sup>.

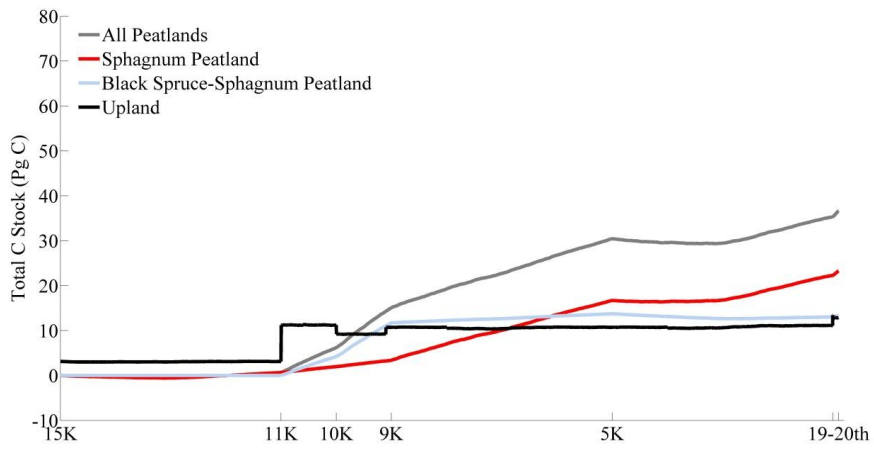


2063

2064 Figure 10. Peatland mean C accumulation rates from 15 ka to 2000 AD for (a) weighted average  
 2065 of all peatlands, (b) *Sphagnum* open peatlands, and (c) *Sphagnum*-black spruce peatlands.

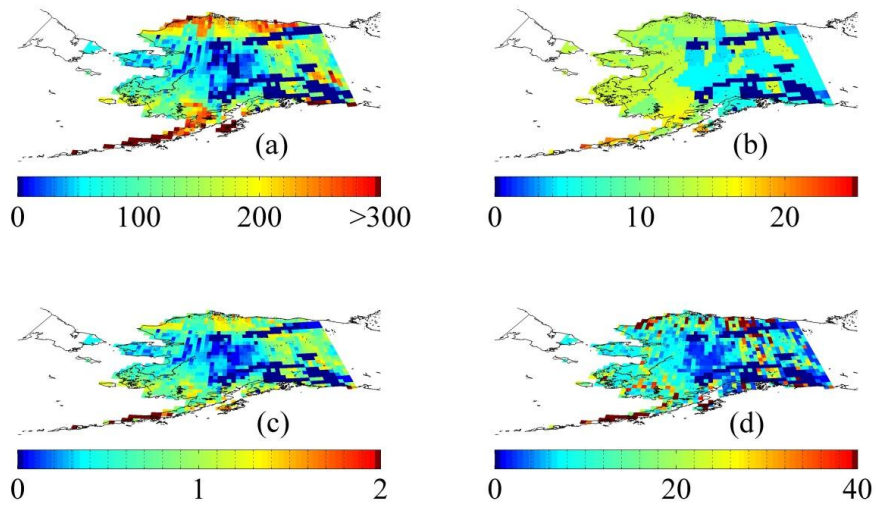
2066

2067



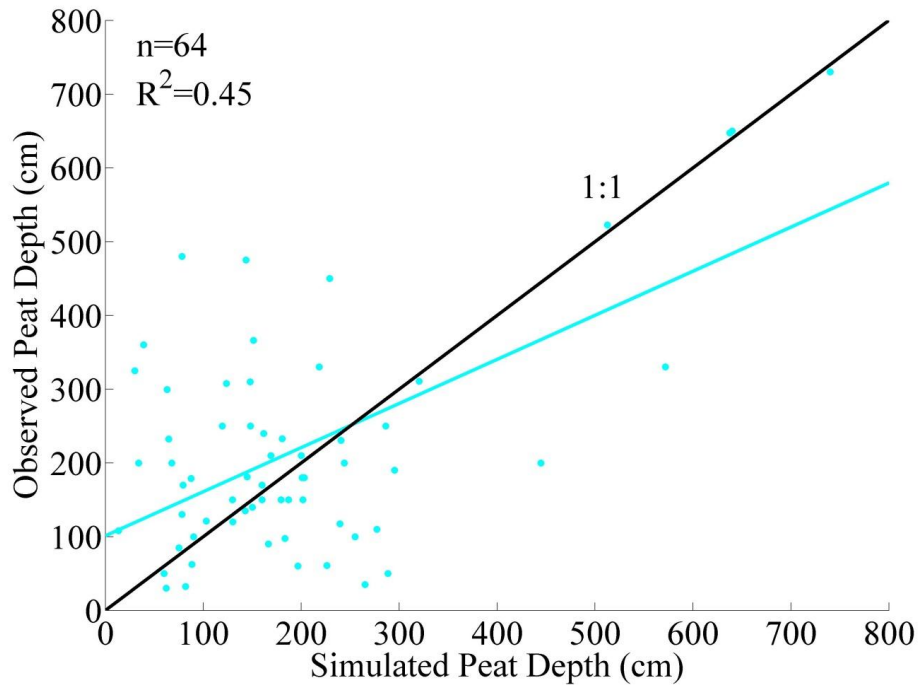
2068  
 2069  
 2070  
 2071  
 2072  
 2073  
 2074  
 2075  
 2076  
 2077  
 2078  
 2079  
 2080

Figure 11. Total C stock accumulated from 15 ka to 2000 AD for all peatlands, *Sphagnum* open peatlands, *Sphagnum*-black spruce peatlands, and upland soils.



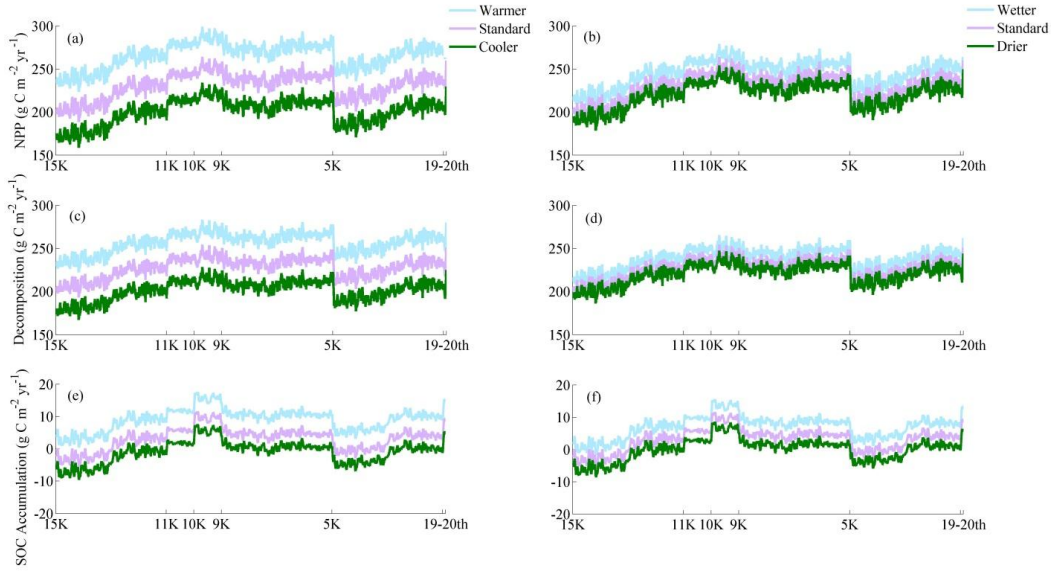
2081  
 2082  
 2083  
 2084

Figure 12. Spatial distribution of (a) total peat SOC density (kg C m<sup>-2</sup>), (b) total mineral SOC density (kg C m<sup>-2</sup>), (c) total peat depth (m), and (d) area-weighted total (peatlands plus non-peatlands) SOC density (kg C m<sup>-2</sup>) in Alaska from 15 ka to 2000 AD.



2085  
 2086  
 2087  
 2088  
 2089  
 2090  
 2091  
 2092  
 2093

Figure 13. Field-based estimates and model simulations for peat depths in Alaska: The observed and simulated data are extracted from the same grids on the map. Linear regression line (cyan) is compared with the 1:1 line. The linear regression is significant ( $P < 0.001$ ,  $n = 64$ ) with  $R^2 = 0.45$ , slope = 0.65, and intercept = 101.05 cm. The observations of >1000 cm are treated as outliers.



2094

2095 Figure 14. Temperature and precipitation effects on (a)(b) annual NPP, (c)(d) annual SOC  
 2096 decomposition rate (aerobic plus anaerobic), and (e)(f) annual SOC accumulation rate of Alaska.  
 2097 A 10-year moving average was applied.

2098

2099

2100

2101

2102

2103

2104

2105

2106

2107

2108

2109



2110